DETERMINATION OF PHYSICOCHEMICAL PARAMETERS AND REMEDIATION OF Pb (II) USING A COMPOSITE OF *MORINGA OLEIFERA* SEEDS AND KAOLIN CLAY IN BOREHOLE WATER WITHIN NAKURU EAST SUB COUNTY, KENYA

GEOFRY KIPRONO

A Thesis Submitted to the Graduate School in Partial Fulfillment of the Requirements for the Award of the Degree of Master in Chemistry of Chuka University

CHUKA UNIVERSITY

OCTOBER 2024

DECLARATION AND RECOMMENDATION

Declaration

This thesis is my original work and it has not been submitted for award of diploma or conferment of a degree in any other institution.

Signature_____ Date. 13/10/24

Geofry Kiprono
SM11/63282/23.

Recommendation

This thesis has been examined, passed and submitted with our approval as university supervisors.

Signature_____ Date. 14/10/24

Prof. Eric Njagi
Chuka University

Signature_____ Date. 14/10/24.

Dr. Zipporah Muthui
Chuka University

DEDICATION

This work is dedicated to my parents Mr. Joseph Siele and Selina Siele on whose constant support, encouragement and prayers that I really relied on for moral support during the study and even for their financial support.

ACKNOWLEDGEMENT

I would want to thank everyone who put in a great deal of effort to make this work possible. I sincerely thank Prof. Eric Njagi and Dr. Zipporah Muthui as my supervisors, for their commitment, support and encouragement. I would especially like to express my gratitude to the technical personnel in the Chuka University Chemistry Laboratory, Egerton University Safe Food Laboratory and Menengai laboratory where I carried out the research for their help. Thank you to the entire Joseph's family for your financial, moral and spiritual support to this far. I am grateful for the support from all these personnel when things got too much they were in for support. I would want to express my sincere gratitude to my fellow classmates for their support in helping me complete this Masters through their encouragements. I am most appreciative to God, who has made everything possible.

ABSTRACT

The contamination of borehole water in Nakuru East Sub County, primarily due to heavy metals and non-metals from natural origins and anthropogenic activities, poses significant health risks. Exposure to these contaminants, beyond the World Health Organization (WHO) and Kenya Bureau of Standards (KEBS) limits, can lead to various diseases and even death. Activities such as industrial processes, agriculture and waste disposal in the area contribute to the infiltration and leaching of toxic elements into borehole water. These toxic elements can enter the human body through ingestion, inhalation or dermal absorption. The Nakuru Water and Sanitation Service Company (NAWASSCO) operate 40 boreholes in the region; however, only 19 were functional during the sample collection, which took place in both dry and wet seasons. These boreholes supply water to Nakuru City and surrounding areas. This study aimed to determine the levels of physicochemical parameters and remediation of Pb (II) from these boreholes. Water samples were collected from six water fields: Kiundo (1 borehole), Kabatini (6 boreholes), Nairobi Road (6 boreholes), Baharini (4 boreholes), Madaraka (1 borehole) and Olbanita (1 borehole) during both seasons. The samples were analyzed for various parameters including Temperature, pH, Turbidity, Electrical Conductivity, Dissolved Oxygen, Fluoride, Lead (Pb), Cadmium (Cd) and Arsenic (As), with heavy metal concentrations measured using Flame Atomic Absorption Spectroscopy (FAAS). Results indicated that the temperature of the borehole water ranged from 23.8 to 26.4 ±0.2°C. Dissolved Oxygen levels were found to be below WHO acceptable limits in all samples. Turbidity levels ranged from 1.54 to 4.32 ±0.01 in the dry season and 0.36 to 9.30 ±0.02 in the wet season, with 36.8% of samples exceeding WHO limits in the dry season and all samples exceeding limits in the wet season. pH values were between 6.4 and 7.6 ±0.1 in the dry season and 7.0 to 7.7 ±0.2 in the wet season, mostly within WHO guidelines, except for a few boreholes that were slightly acidic. Electrical conductivity ranged from 392.0 to 823.1 ±0.1 mS/cm in the dry season and 186.7 to 350.6 ±0.2 mS/cm in the wet season; with all dry season samples above the WHO threshold of 400.0 mS/cm. Flouride had the same mean concentrations of 1.23mg/l for both the two seasons. Significant differences ($P \leq 0.05$) were noted between the physicochemical parameters and WHO standards. Correlations among parameters were observed, ranging from negative to positive ($p < 0.001$). Cd concentrations were below detection limits in all samples for both seasons, while Pb (II) levels exceeded the WHO limit of 0.01 mg/L in 31.6% of boreholes during the dry season and 42.1% in the wet season. Arsenic concentrations were above the WHO limit of 0.01 mg/L in both seasons. To address the contamination, a composite of *Moringa oleifera* seed powder obtained from Tharaka Nithi County and pure kaolin clay were used as an adsorbent for Pb (II). Characterization of the composite was conducted using Powder X-ray diffraction (XRD) and Fourier-transform infrared spectroscopy (FTIR). The adsorption study focused on Pb, revealing that the base-activated composite effectively adsorbed Pb at a dosage of 0.5 g. The adsorption data fit the Langmuir isotherm, Temkin, and Pseudo-Second-Order models. Thermodynamic studies yielded values of 25,340.57 J/mol for ΔH, 58.32 J/mol/K for ΔS and a decrease from 7.95 kJ/mol at 25°C to -3.71 kJ/mol at 225°C for ΔG. The adsorbate was effective at 83.77% in sample NR7.The results obtained indicated the urgent need for water treatment due to elevated levels of As (III) and Pb (II). The composite showed a positive effectiveness on the remediation of Pb (II), however further research should be carried out to investigate its effectives on other heavy metals remediation and outside the boreholes of the study area.

TABLE OF CONTENTS

LIST OF TABLES

LIST OF FIGURES

LIST OF ACRONYMS AND ABBREVIATIONS

ANOVA	Analysis of variance
CF	Contamination Factor
DMA	Dimethyl Arsenite
DO	Dissolved Oxygen
EARS	Eastern Africa Rift Valley System
EMCA	Environmental Management and Co-ordination Act
FAAS	Flame Atomic Absorption Spectrometry
FAO	Food and Agriculture Organization
FT-IT	Fourier Transform Infra-Red
IARC	International Agency for Research on Cancer
ICP-MS	Inductive Coupled Plasma Mass Spectrometry.
KEBS	Kenya Bureau of Standards
MMA	Monomethyl Arsenite
NAWASSCO	Nakuru Water and Sanitation Service Company
NEMA	National Environmental Management Authority
SEM	Scanning Electron Microscope
SPSS	Statistical Packages for Social Sciences
TDO	Total Dissolved Oxygen
US-EPA	United States Environmental Protection Agency
WHO	World Health Organization
WRMA	Water Resource Management Authority
XRD	X-Ray Diffraction

CHAPTER ONE
INTRODUCTION

1.1 Background Information

A vital component of all living organisms is water. For instance, about two thirds of the weight of an adult human is made up of water. Almost two billion people do not have access to clean drinking water globally (Wang *et al*., 2014). There are many unforeseeable dangers associated with ingesting tainted or hazardous water. The World Health Organization (WHO) states that consuming tainted water is a primary cause of diarrhea illnesses, which rank as the second greatest cause of death for children under five, killing over 760,000 of them each year (Omona *et al*., 2020). Groundwater is a major and important water source for domestic use in urban and rural areas. It is believed to be among the purest natural source of water (Kumar *et al*., 2010). A stable and dependable source of water must be available in order to support continued population expansion and development. About one-third of the world's population depends on groundwater for their water supply. In many developing countries, the main contributor to environmental degradation and pollution is dumping of industrial waste into water bodies. Wastes are mostly produced by home, industrial and agricultural operations. Numerous enterprises lack adequate facilities for disposing of toxic wastes that can damage human health. These liquid and solid forms of effluents enter the aquatic bodies (Tamasi *et al*, 2004).

As of 2023, approximately 2 billion people worldwide lacked access to safely managed drinking water, significantly impacting health and economic development (WHO, 2023). The ongoing effects of climate change and urbanization further exacerbate water scarcity and quality issues, particularly in low-income regions (UNICEF, 2023). To address these challenges, global initiatives are increasingly focusing on sustainable water management and infrastructure investments to ensure equitable access to clean water (World Bank, 2023).Groundwater basically comes from boreholes and wells. Up to 90% of rural settlers worldwide, particularly in Africa, receive their water from boreholes as one of the groundwater sources (Abally *et al*., 2012). The Kenyan Vision 2030 calls for using one of the safest sources of water to ensure that improved water sanitation is available and accessible to all Kenyans (Kumar *et al*., 2007). Heavy metals contaminate boreholes water in

colloidal, particulate and dissolved phases. This occurrence in boreholes can either be of natural origin, for instance, eroded minerals within sediments, leaching and infiltration of ore deposits or anthropogenic origin like solid wastes disposal, industrial and domestic effluents (Smith *et al.*, 2007).

The problem of water degradation and contamination has become a daily topic of discussion in developing and developed countries and therefore it calls for more research to find out a lasting solution for it (Emerton *et al*, 2010). This water degradation occurs through natural activities, industrial activities and mining operations, weathering of rocks, sedimentary aquifers and mobilization of naturally occurring heavy metals and in most cases, through agricultural activities. Heavy metals such as lead, arsenic and cadmium compounds are one of the contaminants of borehole water. Millions of people worldwide are at risk for health problems due to the usage of water with high fluoride concentrations as well, thus it's important to measure the concentration of fluoride and heavy metals in home water and figure out how to remove or lower their concentration (Aderemi *et al.*, 2021).

Contamination of boreholes in Nakuru East Sub-County has emerged as a significant public health concern, primarily attributed to factors such as improper waste disposal, agricultural runoff, and inadequate sanitation infrastructure. Studies indicated that the presence of nitrates and pathogens in groundwater is increasing, posing risks to local communities that rely on these boreholes for drinking water (Muthoni *et al*., 2022). Furthermore, research highlights the impact of urbanization and industrial activities on groundwater quality, exacerbating contamination levels (Ochieng *et al*., 2023). Efforts to mitigate these risks include implementing stricter regulatory frameworks and community awareness programs to promote sustainable water management practices (Kamau *et al*., 2024). Addressing these issues is crucial for safeguarding public health and ensuring access to safe drinking water in the region

Contamination of heavy metal in borehole water is a big challenge, especially in developing countries. In most regions, heavy metal contamination is significant. An estimated 140 million people in at least 70 countries have been drinking water containing heavy metals such as lead, cadmium and arsenic at levels above the World

Health Organization (WHO, 2021). If this continues at the same rate, it suggests that between 94 and 220 million people will be at risk of exposure to elevated heavy metal concentrations in groundwater in 2030 (Deng *et al*., 2024). Other research reports which indicate water deterioration in Kenya due to heavy metal compounds are those by (Kithiia *et al*., 2012; Bastia *et al.*, 2016). Kithiia also noted that pollution in rivers and boreholes were chiefly due to domestic waste, industrial wastes and agricultural activities. A study carried out by (Bhaskar *et al*., 2010) of Nairobi-Athi River system showed an increase in heavy metal levels due to agricultural activities. (Wang *et al.*, 2014) reports the same results within the study area.

The physical parameters of the groundwater, like temperature, electrical conductivity and pH, affect the function of human cells. An increase in water pH generally may increase the body's acidic condition when human beings take these waters, hence deactivating the functioning of the enzymes in the human body (Kithiia *et al*., 2012). Also, the presence of fluorides above the recommended level in water consumed by human beings may cause fluorosis. Critical data on the impacts of fluoride (F) in water systems along the Eastern Africa Rift Valley System (EARS) Nakuru City being one of them is needed for public health risk assessment and for the development of strategies for ameliorating its deleterious effects among the affected communities. Long-term fluorides overexposure causes dental and skeletal fluorosis, and leads to neurotoxicity, which impacts several important body functions. Investigating fluorides exposure pathways is of essence to inform and safeguard public health of the affected communities (Kumar *et al*., 2013).

Exposure to heavy metals, for example, cadmium, lead, and arsenic compounds above the recommended limit of WHO, have long-term effects on human beings, for instance, cancer, lung diseases, heart attack and kidney failures are associated with the above mentioned heavy metals. However, excess exposure to heavy metals results in toxicity. Heavy metals cause serious effects with varied symptoms depending on the nature and quantity of the metal ingested when humans use this water from the boreholes (Ali *et al.*, 2019). Arsenic, lead and cadmium form toxicity by forming complexes with protein, which modifies biological molecules to lose their ability to function properly, resulting in malfunctioning or death of cells (Nrior *et al*., 2022).

Also, numerous studies have demonstrated the negative impact of arsenic exposure on memory, cognitive development and intelligence (WHO, 2018). Lead poisoning causes various symptoms, including abnormal pain, which varies from person to person, while exposure time plays an important role (Ali *et al*, 2016). These heavy metals, like arsenic compounds, have been classified as carcinogenic to humans (IARC, 2024).

The origins of lead, cadmium and arsenic ions as hazardous materials and the justification for their removal from our environment have been explored in the current contribution. Because traditional removal techniques such as membrane filtration and ion exchange are costly, it is necessary to look for cost effective and environmental friendly materials. Based on the literature (Gadd *et al*., 2009) bio adsorption is the most cost-effective and environmentally responsible way to remove heavy metals from both boreholes and commercial wastewater. It is used as a substitute for traditional techniques in the elimination of hazardous heavy metals from industrial wastewater. It has a number of benefits, including high efficiency, low production of chemical and biological sludge, economic effectiveness, and their potential to recover metals through bio adsorption is regeneration (Abu-Dief *et al*., 2018).

Heavy metal waste can be treated using various techniques, including extraction, flocculation, precipitation, electrochemical, ion exchange, and adsorption. The most advantageous method is the adsorption method. Adsorbents generated from biomass can be used for adsorption. *Moringa oleifera* seeds and kaolin clay can be converted into bio adsorbents. The advantage of adsorptions over other methods is that it is cost effective, an environmental friendly and innovative natural biomaterial that are readily available. (Poulin *et al*., 2020). Adsorption is a significant phenomenon that underlies several highly significant industrial and environmental processes. There is no denying the importance of adsorption to water purification and environmental preservation. Furthermore, the initial stage of many catalytic reactions involves the adsorption of reactants onto the catalyst. Thus, a lot of work has gone into learning more about the various facets of the adsorption process. But before designing and using adsorption equipment, one must have a basic understanding of adsorption equilibrium and kinetics. To understand the adsorption equilibrium and kinetics,

several different isotherms and kinetics models have been devised namely Langumir and Freudlich, Pseudo-First order and Pseudo-Second order (Azizian *et al*,. 2021). Adsorption isotherms, or mathematical equations, can be used to realize the interpretation of adsorption equilibria. Additionally, rate equations for adsorption kinetics models are provided to describe the adsorption process's time dependency.

The carbonaceous solid known as "biochar," which is produced when biomass is pyrolyzed in an inert environment, has drawn a lot of interest due to its potential uses as a soil amendment or, when upgraded to activated carbon, as fuel cell and gas adsorbents, supercapacitor electrodes, and water treatment to get rid of a range of organic and inorganic pollutants (Kimetu *et al*., 2014). Biochar can now be modified in a number of ways to improve its ability to adsorb different types of contaminants from aquatic environments. Clay minerals exhibit great potential in industrial and petroleum engineering, as well as in agriculture, due to their unique layered structure, high specific surface area and ion exchange capacity. Among these clays, kaolin is perhaps the most studied due to its exchangeable cations, which have a strong ability to acquire electrons and perform well in adsorption between layers. Kaolin offers several benefits, including a large adsorption surface area, high porosity, high cation exchange capacity, and low cost. The adsorption capacity of kaolin clay may be increased by expanding its surface area and sorption site through modification of its structure (Istan *et al*., 2016).

Strong evidence has been provided by *Moringa oleifera* seeds to support their use as an efficient natural adsorbent in the water treatment process to improve the chemical and physical properties of groundwater, including conductivity, pH, hardness, turbidity, alkalinity, suspended solids and (Total Dissolved Solids) TDS (Semanka *et al*., 2022). All things considered, *Moringa oleifera* seeds offer a solid route for emphasizing their application as a potent substitute for artificial adsorbent in water purification (Nartey *et al*., 2011).

Moringa oleifera is a species that are found in dry lands like Machakos and parts of Tharaka Nithi due to its ability to do well in hot weather and low rainfall, and it has many nutritional and medicinal benefits derived from various parts of the plant

(Chakava *et al.*, 2014). The adsorption of metals using *Moringa oleifera* is limited to the adsorption surface. *Moringa oleifera* is a cationic polyelectrolyte of short-chain and low molecular weight. Heavy metals and solids with higher charges than *Moringa's* colloidal surface will remove a high percentage of metals compared to other plants (Makokha *et al.*, 2012).

The mechanism that brings about the adsorption of heavy metals in *Moringa oleifera* seeds is through the positive metal ions that form a bridge between the anionic polyelectrolyte and negatively charged proteins' functional groups on the colloidal particles' surface. Complexes are formed with *Moringa's* heavy metals and organic matter and other seeds, such as proteins. Due to its hydrophilic character, several hydrogen bonds are formed among polyelectrolyte and water molecules (Wang *et al.*, 2014). Polyelectrolyte coagulant aids consist of repeating units of small molecular weight forming molecules of colloidal sizes that carry an electrical charge or ionizable groups that provide bonding surfaces for the flocks. Adsorption describes the attachment of ions and molecules from seeds proteins using specific mechanisms (Owusu *et al*., 2008).

Researchers studied the use of local seeds to improve the quality of drinking water. They gave their analysis as follows, heavy metals cadmium, copper, chromium, lead and zinc were performed before and after treatment of water with local seed *Moringa Oleifera*, *Arachis hypogea* (peanuts), *Vignaunguiculata* (cowpeas), *vignamungo* (urad) and *Zea mays* (corn), and the results showed that *Moringa Oleifera* seeds are capable of absorbing the heavy metals tested compared to other seeds in some water samples. The percentage removal by *Moringa oleifera* seeds was 90% copper, 80% for lead, 60% for cadmium and 50% for zinc and chromium (Wang *et al.*, 2014).

However, these study aims at determining the levels of the physicochemical parameters of the boreholes used by NAWASSCO within Nakuru East Sub- County and to prepare composite a of *Moringa oleifera* seeds and kaolin clay as a cost efeective method of lowering the concentration of Pb (II) in boreholes water.

1.2 Statement of the Problem

Nakuru East Sub County, located within Nakuru County, Kenya, relies heavily on borehole water for domestic and industrial use due to inadequate surface water sources. Despite its importance, borehole water in Nakuru East Sub County faces significant quality challenges, which can have adverse effects on human health and the environment. In particular, heavy metal contamination is a significant concern. Lead (Pb), arsenic (As), and cadmium (Cd) are among the most harmful contaminants, posing severe health risks even at low concentrations. Sources of these contaminants include industrial activities, agricultural runoff, and improper waste disposal. Long-term exposure to these heavy metals can lead to serious health issues such as neurological damage, cancer, and kidney problems. The presence of these metals in borehole water necessitates effective monitoring and remediation strategies to protect public health. Current methods of heavy metal remediation face several limitations. Firstly, techniques such as chemical precipitation and ion exchange can be expensive and generate secondary waste and a complicating disposal. Bioremediation, while environmentally friendly, often depends on specific conditions and may not effectively remove all types of heavy metals, especially at higher concentrations. Additionally, physical methods like adsorption can be limited by the availability of suitable adsorbents and may require extensive processing to recover and reuse them. These challenges highlight the need for more efficient, cost-effective, and sustainable remediation technologies. *Moringa oleifera* seeds and kaolin clay have shown significant potential as effective adsorbents for removing heavy metals from water. *Moringa* seeds contain natural coagulants that can bind to heavy metals, while kaolin clay offers a large surface area for adsorption. Combining these materials could provide a low-cost, sustainable solution for water treatment in Nakuru East Sub County. This study aimed to explore the efficacy of this composite material in remediating heavy metal contamination in borehole water, contributing to safer and healthier water for the study area and other regions facing the same problem..

1.3 Objectives

1.3.1 Broad Objective

To determine the levels of physicochemical parameters and remediation of Pb (II) using a composite of *Moringa oleifera* seeds and kaolin clay in boreholes' water used by NAWASSCO within Nakuru East Sub County during dry and wet seasons.

1.3.2 Specific Objectives

i. To determine the levels of selected physicochemical parameters in boreholes' water used by NAWASSCO within Nakuru East Sub County during dry and wet season and compare with World Health Organization limits.
ii. To prepare a composite adsorbate of kaolin clay and *Moringa oleifera* seeds and characterize its structural and textual properties.
iii. To determine the efficiency, adsorption kinetics and isotherms of remediation of Pb (II) compounds in boreholes' water using the prepared composite adsorbent.

1.4 Research Questions

i. What are the levels of selected physicochemical parameters in boreholes' water used by NAWASSCO within Nakuru East Sub County during dry and wet seasons?
ii. What are the structural and textual properties of the prepared composite adsorbent of *Moringa oleifera* seeds and kaolin clay?
iii. What is the efficiency and kinetic model of the adsorbent on remediation of Pb (II) concentration on boreholes water?

1.5 Justification

Borehole water is essential for Nakuru East Sub County and Nakuru Town due to limited surface water supplies, serving various domestic, agricultural, and industrial purposes. To ensure the water's safety and sustainability, regular monitoring of physicochemical parameters such as turbidity, temperature, pH, dissolved oxygen (DO) and conductivity is crucial (Gereva *et al*., 2022). Heavy metals like lead, arsenic and cadmium pose significant health risks and can contaminate groundwater through industrial discharges, agricultural runoff, and improper waste disposal (Namungu *et*

al., 2021). The prevalence of industrial and agricultural activities in Nakuru East heightens the risk of contamination, emphasizing the need for effective remediation strategies beyond conventional treatment methods, which primarily target biological contaminants and turbidity but are inadequate for heavy metals (Mwiathi *et al*., 2022).

Research indicated that *Moringa oleifera* seeds and kaolin clay can serve as natural adsorbents for heavy metals, with *Moringa* seeds binding metals effectively and kaolin providing a large surface area for adsorption (Shields *et al*., 2015). This study aimed to evaluate the efficacy of combining *Moringa oleifera* seeds and kaolin clay to remediate heavy metal contamination in borehole water. By assessing both the physicochemical parameters and heavy metal remediation, the research will contribute to the sustainable management of borehole water resources in Nakuru East Sub County and other regions with similar problem providing valuable insights for NAWASSCO and other stakeholders. Utilizing locally available materials for water treatment not only aligns with environmental sustainability principles but also enhances public health and promotes sustainable development in Nakuru East Sub County and its environment.

CHAPTER TWO
LITERATURE REVIEW

2.1 Boreholes

2.1.1 Boreholes as one of the Groundwater Source

Water makes up around seventy-five percent of the earth's surface (Ikeme *et al*., 2014), making it a plentiful and vital component of the planet's environment. It can be found as surface water for instance lakes, streams, rivers, ponds, shallow aquifers, seas, ice caps, glaciers, etc., or it can accumulate as ground water, which can be found as well as springs, wells, and boreholes water (Ikeme *et al*., 2014). A great deal of research has been done in the literature and in theory to evaluate the quality and quantity of ground water supplies in both rural and urban settings. One important factor influencing a user's health is the quality of their drinking water. Periodic quality control measures are therefore required. But many groundwater supplies are not routinely subjected to quality monitoring measures. Around two billion people worldwide rely on groundwater as one of their primary water sources for their irrigation, industrial, and rural requirements (Dula *et al*., 2011). Many of the world's population, including the people of Kenya, depend on freshwater supplies from ponds, natural springs, boreholes, wells, and open wells. It is said to be purer than surface water since it often results from rainwater seeping into underground aquifers through the earth (Kumar *et al*., 2015). Numerous interactions involving complex chemical compounds, such as those involving amino acids, involve water. It is essential to many elements of domestic use, agriculture as well as industrial and manufacturing processes. Since life cannot survive without water, water is a crucial natural resource. Safe and dependable water sources are a necessary prerequisite for the development of a stable community. Water scarcity has historically caused serious conflict, migration, and adjustments to agricultural practices (Ikeme *et al*., 2014).

When pesticides, herbicides and fertilizers are used in agricultural operations, hazardous materials are created. These materials are then carried as effluents into borehole water sources, where they contaminate water bodies (Obi *et al*., 2019). In a similar vein, waste water from the textile industry contains organic dyes that introduce various ions into the water that can change its makeup. Water bodies are contaminated by oil spills, which also create a coating on the water's surface that

stifles oxygen flow. Aquatic species eventually die from anaerobic conditions as a result. The introduction of specific ions or compounds into borehole water during oil drilling operations frequently contaminates ground water supplies, which lowers the quality of the borehole water; poisonous ions are clearly present in contaminated surface and ground water. On the other hand, certain ions added to water bodies could mix with other substances to create insoluble substances that could cause major harm to the body when ingested (Olewe *et al*., 2015).

Unless it is contaminated, groundwater is thought to be naturally clean, flavorless, and odorless. Despite being regarded as safe, some groundwater sources can nonetheless become contaminated by physicochemical agents because of their shallow depth (Foster *et al*., 2012). The health of water users could be impacted if groundwater has excessive concentrations of certain ions and salts (Kumar *et al*., 2015). There are many ways to contaminate ground water; including using fertilizers in farming and sewer system effluent seeping through the ground to water-bearing rocks (Foster *et al.*, 2012). Water moves through the earth, dissolving minerals in rocks and accumulating suspended particles, especially from organic sources, which causes groundwater to become contaminated (Bhaumik *et al*., 2015).

A research carried out among the slum dwellers in Kaptembwa in Nakuru town, research paper showed that the proportion of households with access to adequate water in the study area of Kaptembwo location is quite low, far below the national average. The current water supply to the Kaptembwo location by NAWASSCO is 2,000m^3, while the present demand is estimated at 10,000m^3 (NAWASSCO, 2023), this indicated a big short fall. The current water distribution conditions in Kaptembwo are constrained due to several problems affecting large proportion of the households. The problems included low service coverage by the distribution system, intermittent mode of water supply, and long periods of cut-offs (Mokaya *et al*., 2016).

2.1.2 Boreholes Water Contamination

One of our time's most significant environmental challenges is groundwater poisoning, which is reportedly linked to many users' serious health conditions. Natural elements or anthropogenic actions that alter natural materials or introduce

contaminants into already contaminated borehole water (Smith *et al.*, 2018). In a study carried out in Nakuru City revealed that the effects of drinking borehole water crisis linked to climate variability and change in terms of prediction methods, frequency, and rate of change, quality and quantity are wider, deeper and more uncertain requiring immediate attention. The existing challenges limit sustainable development, effective long-term planning and management of the areas drinking borehole water resources (Keli *et al.*, 2019).

Many chemical pollutants have been found to have negative health impacts on people when they are exposed to them over time through drinking water. These encompass a range of substances, including certain insecticides, both organic and inorganic. Some of them harm human health or degrade the aesthetics of water. The World Health Organization (WHO) has proposed guideline values that establish thresholds for numerous pollutants found in potable water. Kenya has its own standards for drinking water quality that are compliant with global standards and principles. The WHO's legally enforceable drinking water quality specifications, which specify limitations for both physical and chemical parameters as well as other parameters, are the basis for the water standards (Saidu *et al*., 2021). Contamination of groundwater and the variety of pollutants affecting water supplies are among the most significant environmental challenges of our time. Although the inherent chemical quality of groundwater is generally good, difficulties with water use might arise from high quantities of various elements. The quality of groundwater can be significantly altered by intensively irrigated agricultural discharges into the groundwater. The groundwater consumers are seriously threatened by these human activities on the groundwater. It is not possible to restore the quality of groundwater once contamination has occurred by removing the pollutants from their sources. As a result, it becomes crucial to consistently check the quality of groundwater and to come up with strategies to safeguard it (Shigut *et al*., 2017).

A research carried out in Kakamega boreholes water which involved titrimetric and spectroscopic methods were used to determine the presence of heavy metals and important elements. The results of the analysis showed that the concentrations of arsenic (As) and mercury (Hg) ranged from 0.0103 to 0.0119 ± 0.00005 mg/L and

0.00256 to 0.0611 ± 0.00005 mg/L, respectively. The potassium and sodium concentrations varied from 2.53 to 4.08 ± 0.15 mg/L and 6.74 to 9.260 ± 0.2 mg/L, respectively. The levels of mercury, iron, lead, and arsenic in the Kakamega waters exceeded the globally recognized thresholds, despite the fact that the cadmium content was lower than what the World Health Organization advised. Thus, there is a public health issue with high concentration of heavy metals in the boreholes waters that needed quick attention (Chebet *et al*., 2020).

A research carried out in the Robe Town indicates that spring water sources and borehole water sources had different water quality. These distinctions were noted based on changes in the physico-chemical characteristics of spring and borehole water sources. It was discovered that the borehole water sources had the highest concentrations of TDS, EC, TH, Ca, and Mg and were slightly acidic (above the MPL). As a result, the three deep borehole groundwater sources were not as suitable for drinking water quality as the spring water sources. Furthermore, more actions needed to be made by the government and interested parties in order to enhance the towns water quality and provide the general population with safe, clean water that is devoid of health risks (Shigut *et al*., 2017).

A research carried out in Rubiri borehole analysis indicated that contamination of underground water for boreholes around geothermal producing areas. None of the seven sampled boreholes had optimum conditions for drinkable water. As such, they were all unfit for human consumption. In summary, the borehole at DCK had significantly higher fluoride values. The borehole at Florensis had significantly higher fluoride. More so, its maximum value for cadmium was beyond the permissible limit. The borehole at James Mange had significantly higher fluoride. The borehole at Jikaze was mildly acidic as its pH mean was below the lower range desirable for drinkable water. More so, the maximum value for sulphate was also high (Karanja *et al*., 2017). The Keekonyokie borehole had significantly higher means for fluoride and cadmium. Its minimum pH value recorded was also below the lower range desirable for drinkable water. The Maai Mahiu borehole had significantly higher sulphate values. For Rubiri borehole, it had significantly higher values for three parameters namely sulphates, fluorides and lead. None of the boreholes in the geothermal

producing areas could meet the optimum conditions for drinking water as set out by KEBS. Naivasha area had inadequate piped water as observed from the field. As such, there was heavy reliance on underground water as chief source of drinkable water (Karanja *et al*., 2017). Such a scenario could lead to health complications that could accumulate over time if not instantaneous. In the face of climate change, such underground resources are supposed to offer avenues for climate change mitigation and adaptation. Contamination of underground water is likely to stifle social progress which is a critical aspect of building climate resilience. By shutting this avenue for building resilience, climate change impacts are likely to be amplified hence curtailing the pathway towards robust sustainability envisioned in our national vision 2030 blue print. Inevitably, retarded social progress reverberates into economic systems thereby accelerating poverty and enhancing climate change vulnerability (Karanja *et al*., 2017).

2.1.3 Natural Substances

The types of geological components the water passes through as it travels to the aquifer determine the nature of the natural pollutants in groundwater. Water may be affected by the components of the rocks as it flows through the soils and rocks down to the aquifers and ends up containing a variety of minerals, some of which may be in high concentrations. The type of contaminants and their concentrations in the water determine how these natural contamination sources affect the groundwater quality. Although pollutants in water pose a risk to human health and life, their occurrence at levels below the allowable limit is considered harmless to human health (Smith *et al.*, 2007).

2.1.4 Anthropogenic Activities

The type of human activity in the area has an impact on the safety of the groundwater as well. For instance, agricultural activities can contaminate groundwater in a variety of ways. Common examples include fertilizer and pesticide spills while being handled, washing pesticide sprayers or other application equipment nearby shallow wells, and adding organic manure to the soil to mimic animal waste. Economic processes like manufacturing and transportation also contaminate groundwater by causing chemical leaks and spills that seep into the aquifers through leaching.

Domestic garbage is also a major worry because, when it is released close to wells, it may leak into the groundwater and contaminate it (Smith *et al.*, 2007).

2.2 Physicochemical parameters

2.2.1 Temperature

Any living thing's body metabolic processes are influenced by temperature (Smith *et al.*, 2007). Additionally, it is essential for regulating the solubility of gases in water (Reddy *et al*., 2014). According to (Kithure *et al*., 2021), the permitted range is 28–320C. Water that effluents have contaminated becomes hotter and has less dissolved oxygen (Smith *et al.*, 2007).

2.2.2 pH

The term pH is widely used to describe how strongly an acidic or alkaline state exists in a solution. This gauges how much hydrogen potential there is in water (Smith *et al.*, 2007) and it is a sign that water is undergoing chemical change (Gichumbi *et al*., 2013). According to (Kithure *et al*., 2021), the acceptable range is 6.5–8.5. Low pH values indicate acidic water, which can result in gastrointestinal issues like hyperacidity and ulcers in humans (Popoola *et al*., 2019) and corrode with the natural rocks within the aquifer, increasing contaminants in water. Higher pH values indicate productive water (Smith *et al.*, 2007), which results in a bitter taste of the water (Rane *et al*., 2021). On research done in Njoro and Mau Narok parts of Nakuru county to establish the acidity of the soil on to varieties of potatoes (Shangi and Destiny) with application of DAP fertilizers indicated that the soil pH before addition of this fertilizers was ranging between 5.0 – 6.0, Soil acidity in these areas was attributed to constant use of chemical fertilizers, mostly DAP, which supply H^+ ions whose accumulation in soil will acidify the soils in the long run (Muthoni *et al.*, 2009). A researched carried out in Ethiopia found out that three out of the six sampled boreholes indicates that the level of pH was higher than the recommended level and this was linked to human activities like fertilizer use and sewage disposal on the research area's agricultural grounds. The weathering of plagioclase feldspar in sediments is linked to the overall increase in pH in sedimentary terrain. This is facilitated by atmospheric carbon dioxide that has been dissolved, which releases calcium and sodium and gradually raises the pH and alkalinity of the groundwater.

Because the water from the borehole groundwater sources is acidic, it can very readily erode the water piping. A metallic or sour taste in the water can also be an aesthetic issue caused by damaged metal pipes brought on by acidic pH levels (Shigut *et al*., 2017).

2.2.3 Electrical Conductivity

The conducting capacity of water is represented by EC. Total dissolved solids (TDS) are measured by EC, which is based on the ionic strength of the solution. The ionic strength of the solution rises as the concentration of dissolved solids does. The ionic species present in the water significantly impact its conductivity, which is a measure of its capacity to conduct electricity. The mobility of the ions at a specific temperature affects both the anion and cation concentrations in water (Nirmala *et al*., 2012). It is a salinity indicator that significantly impacts water flavor and reveals the presence of dissolved ions. High ionizable salt concentrations in water cause high electrical conductivity, inhibiting plant seed germination and lowering crop yields (Frisbie *et al*., 2022). The acceptable limit for electrical conductivity, according to (Kithure *et al*., 2021), is 1400 Scm^{-l}.

2.2.4 Turbidity.

One of the key physical characteristics of water quality is turbidity, which indicates the presence of suspended particulates in the water and gives a body of water its muddy or turbid appearance. The presence of silt and other suspended materials in the water is the cause. It degrades water quality by changing the color of the water and encouraging microbial growth (Zeitoun *et al*., 2013). According to studies, turbidity is mostly brought on by silt deposition into the aquifer and is higher during the wet seasons and lower during the dry ones (Vimercati *et al*., 2016). (Kithure *et al*., 2021), states that a turbidity limit of 5 NTU is acceptable. A research carried out to compare the turbidity of borehole water and the springer water showed that every sample examined was confirmed to be within the WHO-recommended ranges of 1–5 NTU. According to the results, the spring water source was somewhat less turbid than the water from the borehole groundwater source. This modest turbidity suggests that non-soluble metal oxides and inorganic particle debris might be present. Drinking water

with a high turbidity level could be harmful to your health since it can shield harmful germs from the actions of disinfectants.

2.2.5 Fluoride ions

Fluoride crystals made of fluorspar and phosphorite are found naturally in rocks. Weathering rocks, phosphates fertilizers, and leaching from untreated sewage are all sources of fluoride in groundwater (Kumar *et al*., 2013). The (Kithure *et al*., 2021), accepted norm for fluoride level in water is 1.5mg/l; fluorosis of the teeth, dental fluorosis, and skeletal fluorosis are all harmful to human health at levels over this level (Struthers *et al*., 2021). The halogen that is the most prevalent in sedimentary rock types is fluorine. Because it is very soluble, fluorine is liberated as the fluoride ion during weathering. Fluoride forms powerful complexes with other ions in solution, particularly calcium, aluminum, iron, and phosphate (Gichumbi *et al*., 2012).

Additionally, fluoride adsorbs to the surfaces of minerals such as gibbsite, kaolinite, halloysite, and recently precipitated amorphous minerals. The application of phosphate fertilizer and the use of insecticides are examples of anthropogenic sources of fluoride (Sambu *et al*., 2012). Mammals require fluorine as a micronutrient because it helps to build the apatite matrix that makes up their skeletal tissues and teeth. The ideal fluoride concentration for drinking water is 1 mg/l. Low amounts may worsen dental health, while high levels may impair kidneys, nerves, and muscles and cause skeletal and dental diseases (Struthers *et al*., 2021).

On a reaserch carried out on boreholes within Nakuru County the correlations imply that the primary mechanisms for fluoride release and concentration in borehole may be evaporative enrichment and mineral disintegration. According to spatial analysis, fluoride concentrations were determined by the locations of aquifers rather than by their type. The Bahati and Mau escarpments of the rift were home to low-fluoride aquifers, while the fluoride hot zone was situated on the rift level, which had high-fluoride aquifers (Gevera *et al*., 2018)

2.2.6 Total Dissolved Oxygen

Total Dissolved Oxygen (TDO) heavily depends on the presence of biological activity, salinity, turbulence and also waters temperature density relationship also plays a significant role (Akkoyunlu *et al*., 2012). TDO is a good indicator of the health of water ecosystem since the oxygen present is by plants and animals for respiration and by the aerobic bacterial which consume oxygen during decomposition process (Areerachakul *et al*., 2013).

2.2.7 Factors Affecting Mobility of Heavy Metals in Water

The most important factors which affect their mobility of heavy metals are pH, sorbent nature, presence and concentration of organic and inorganic ligands. The pH is a good indicator of the quality and the productivity of soils (Zhang *et al.*, 2008). It should be considered as one of the most important factors in the control of the absorption, mobility of metallic elements in the soil solution. A high pH contributes to a decrease of heavy metal mobility by the formation of precipitates, by increasing the number of adsorption sites and decreasing the competition of H^+ for adsorption. As water circulate in the hydrosphere (sediments, soils and aquifers) before it percolates underground it acquires it intrinsic chemical composition through heterogeneous reaction (Yamengo *et al.*, 2019). These results from biological activity, water- solid interaction, water air exchange and adventive and dispersive transport, hence chemical composition of water varies with space. Anthropogenic activities like industry, mining, agriculture, transportation and urbanization lead to significance variation with time in the water composition (Yamengo *et al.*, 2019).

Heavy metals cation tends to adsorb or dissolve from solids as pH decreases, as pH increases, they adsorb or precipitate, but only up to a certain level after which they again solubilized. A number of heavy metals that is from transitional metals and metalloids occur as oxyanions. Their solubility pattern is the opposite to the one of cation, they tend to adsorb and precipitate more as pH decreases. On his research it showed that arsenic, copper, lead, and mercury are generally more soluble (or "dissolvable") at a lower pH (Smoke *et al.*, 2022). Weathering of sedimentary rocks and the erosion of the earth's surface are the major sources of dissolved solids in water. Other types of dissolved solids may originate in rain. The types of dissolved

ions in water are mainly related to the mineral assemblage of the underlying or surrounding rock. The solubility and rate of dissolution of minerals is high where the climate is warm and wet. The pH also affects the rate of weathering reactions such that a decrease in pH increases the weathering rates and increase in pH decreases the weathering rates. Dissolved carbon dioxide, the presence of organic acids and the extent of weathering determines the pH of weathering solutions.

2.2.8 Lead

Lead (Pb (II)) is one of the most common heavy metals widely used for industrial activities. The WHO, the European Union (EU), the US Environmental Protection Agency (USEPA), and Guidelines for Canadian Drinking Water Quality set the permissible level of Pb (II) in drinking water as 0.01, 0.01, 0.015, and 0.01 mg/L, respectively (Awual, 2019). Lead is the most important toxic heavy element in the environment. Due to its important physicochemical properties, its use can be retraced to historical times. Globally it is an abundantly distributed, important, yet dangerous environmental chemical. Its important properties like softness, malleability, ductility, poor conductibility and resistance to corrosion seem to make it difficult to give up its use. Due to its non-biodegradable nature and continuous use, its concentration accumulates in the environment with increasing hazards. Human exposure to lead and its compounds occurs mostly in lead-related occupations with various sources like leaded gasoline, industrial processes such as smelting lead and its combustion, pottery, boat building, lead-based painting, lead-containing pipes, and battery recycling (Srivastava *et al.*, 2017). On a research done in Naivasha boreholes it was that neither chromium nor cadmium were present. The outcomes were then contrasted with the WHO's drinking water recommendations and the East African Standard. The analysis revealed that while the other indicators were within the WHO guidelines, the levels of lead, fluoride, chlorine, and total suspended solids were higher. None of the sampled borehole water was appropriate for consumption, according to the WHO drinking water guidelines and the East African Standard. As a result, some remediation was required before the water could be safely consumed (Egbo *et al*., 2023).

2.2.9 Cadmium

According to (Wang *et al*. 2006), cadmium can be found as natural ores in rocks and soils and a by-product of zinc refining. As a by-product of smelting lead and zinc ores, cadmium is a soft, ductile metal. Greenockite, or CdS, is a mineral that is also present in chalophile. Cadmium in the environment can also come from volcanic eruptions. Although there are high concentrations of cadmium in the air near zinc smelters, naturally occurring amounts are estimated to be around 2 n/m^3.According to (Ramesh *et al.*, 2007), cadmium leached into groundwater when it came into touch with soil that discharges from the mining, paints, electroplating, petrochemical, plastics, and fertilizer sectors had contaminated. In his research, only three of the tested samples from various sites showed the presence of Cd, with a minimum value of 0.001 mg/L and a maximum concentration of 0.0025 mg/L. Even though Cd concentrations were below the WHO permitted range (0.003 mg/L), epidemiological studies have indicated that long-term exposure to Cd may cause kidney damage, lung cancer, high blood pressure, and bone defect.

In a research done in river Molo about determination of heavy metals (Ni, Cd, Cu, As and Pb), it was discovered that water from Nakuru County, the concentrations of lead (Pb) were from 0.06 to 10.24 mgkg-1, Cd was between 0.04-0.57 mgkg-1, Ni was between 0.29 and 30.24 mgkg-1, and zinc was between 0.1 and 91.58 mgkg-1. Pb and Cd concentrations exceeded other international norms as well as the World Health Organization's (WHO) maximum allowable levels (Muneer *et al*., 2012).

2.2.10 Arsenic

Arsenic element is a metalloid with an atomic mass 74.9 (Struthers *et al*., 2021). It is relatively abundant (20%) in the earth`s crust, and its compounds exist naturally in inorganic and organic forms, with the inorganic forms being toxic (Singh *et al*., 2015) (Struthers *et al*., 2021). Arsenic occurs in over 200 minerals, 60% being arsenates, 20% sulfosalts and sulphides. Arsenide, arsenites, alloys, oxides, and polymorphs comprise the remaining 20%. High concentration of arsenic minerals is found in areas with transition metals, with; arsenopyrite (FeAsS) being the most abundant (Smedley *et al*., 2002). It exists in nature in several oxidation states (-3, 0, +3 and +5), but the most common one is with oxidation +3 and +5 and in many organic and inorganic

forms. Inorganic arsenic can react with oxygen and Sulphur to provide inorganic derivatives and carbon and hydrogen to yield organic compounds (Seyfferth *et al.*, 2014). In a research carried out from Nairobi boreholes shows that As concentration was above the WHO recommended level in water from ten boreholes (16%) during the dry season and four boreholes (6%) during the wet season (Kiplangat *et al*., 2021).

Around the world, some areas are contaminated with arsenic, and several significant exposures have been discovered in places like Asia and America (Deng *et al*., 2024). Intensive arsenic research has been done on the level of exposure, spread, occurrence, and health impacts in groundwater in the United States, India, Bangladesh, and other developed nations (Steinmaus *et al*., 2005). According to studies by (Ali *et al.* 2019), groundwater contamination in several nations is higher than the WHO-recommended level of 0.01 mg/L. According to (Ali *et al*., 2019), the biggest reports came from Asia, with 32 nations and Europe, with 31 countries. Twenty (20) and eleven (11) countries are in Africa.

Regarding abundance in the earth's crust, arsenic comes in at number 20. It is typically stated that there are 1.5–2.0 ppm of arsenic in the earth's continental crust. Arsenic is present in sulfide deposits in high concentrations as the native element or alloys (four minerals), arsenide (27 minerals), sulphides (13 minerals), sulfosalts (arsenic-containing sulfides with other metals, 65 minerals), and oxidation products of those above (two oxides, 11 arsenates, 116 arsenates, and 7 silicates) (Brahman *et al*., 2014).

Arsenic can be found in several minerals, including sulphides, arsenates, arsenites, and elemental arsenic (Verma *et al*., 2018). Rocks are also a significant source of arsenic availability on the earth's surface (Brahman *et al*., 2014). Agricultural activities, industrial wastes, weathering of metamorphic and aquifer rock, and the development of reductive conditions at pH values near 7 cause the desorption of arsenic from mineral oxide (Rezaie *et al*., 2014). High arsenic levels in arid or semi-arid environments are created by high evaporative groundwater conditions, aided by the area's dry climate and high pH values of more than 7 (Thundiyil *et al*., 2007).

In many nations, including Sri Lanka, phosphate has been widely utilized as fertilizer. However, arsenic content has been found in Triple Super Phosphate (TSP) and Glyphosate (a pesticide), despite only being present in trace amounts in organic matter (Jayasumana *et al*., 2015). To reduce arsenic buildup, it has been advised to utilize organic fertilizers such as chicken litter and calf dung (Mitra *et al*., 2017). This happens as a result of the organic matter's (OM) capacity to combine with arsenic to form an arsenic-containing compound, also known as organic fertilizer (Mitra *et al*., 2017).

According to reports, the concentration of arsenic decreases as one approaches the earth's crust, suggesting that most of the arsenic is introduced through human activities on the planet's surface (Jayasumana *et al*., 2015). The availability of arsenic in the environment has been significantly impacted by using arsenic-based chemicals in livestock dip to treat pests like ticks and fleas on animals (Chen *et al*., 2014). Wastes from swimming pools and bathing places are discharged into agricultural land and water, which may have caused arsenic levels to rise there (Fransisca *et al*., 2015).

After exposure to arsenic, the liver goes through a methylation process of detoxification. As a result of this process, arsenate and arsenite are converted into monomethyl arsenic acid (MMAs (V)), monomethylarsonous acid (MMAs (III)), dimethylarsinic acid (DMAs(V)), dimethylarsinous acid (MMAs (III)), and trimethyl arsine oxide (TMAsO (V)). Only DMAs (V) and MMAs (V) are excreted through this process, but MMAs (III), which are thought to be more hazardous than inorganic arsenic, are not (Jaishankar *et al*., 2014).

2.3 Composite preparation and characterization

2.3.1 Methods of preparation

The composite preparation of *Moringa oleifera* seeds and kaolin clay has gained attention in materials science and environmental applications due to the synergistic benefits derived from their combined properties. *Moringa oleifera,* often referred to as the "miracle tree," contains various bioactive compounds such as proteins, vitamins, and phenolics, which exhibit flocculating and adsorptive properties (Hassan *et al*., 2021). When *Moringa* seeds are processed, typically through methods such as grinding and sieving, they yield a natural coagulant that can effectively remove

contaminants from water. Meanwhile, kaolin clay, a naturally occurring aluminosilicate mineral, is widely used in environmental remediation due to its high surface area and ion-exchange capacity (Zhao *et al*., 2020). The integration of these two materials can enhance the overall efficacy of pollutant removal processes.

The preparation of a composite material from *Moringa oleifera* seeds and kaolin clay often involves physical blending or chemical modification. Studies have demonstrated that by combining *Moringa* seed extract with kaolin, it is possible to achieve a composite that improves the mechanical properties and adsorption capabilities of the resulting material (Akanbi *et al*., 2022). For instance, the addition of *Moringa* seed extract to kaolin can lead to a more porous structure, enhancing the adsorption sites available for contaminants. This can be particularly useful in applications such as wastewater treatment, where the composite can effectively reduce turbidity and remove heavy metals (Zhao *et al*., 2020).

In practical applications, the *Moringa*- kaolin composite shows promise not only in environmental remediation but also in agricultural settings as a natural soil conditioner. The bioactive compounds from *Moringa* can enhance soil fertility, while the kaolin helps improve soil structure and moisture retention (Bashir *et al*., 2023). This dual functionality illustrates the potential for these composites to contribute to sustainable practices in both water purification and agriculture. Further research into optimizing the ratio of *Moringa* to kaolin and understanding the mechanisms behind their interactions will be crucial for developing efficient applications in these fields.

2.3.2 FT-IR

Fourier Transform Infrared Spectroscopy (FTIR) is a powerful analytical technique used to characterize materials, including composites, by identifying their molecular composition and functional groups. This method operates by measuring the absorption of infrared light by a sample, which causes molecular vibrations that correspond to specific chemical bonds. FTIR is particularly useful for analyzing organic compounds and can provide insight into the interactions between components in a composite material (Gonzalez *et al*., 2020). For instance, the presence of characteristic peaks in the FTIR spectrum can indicate the functional groups derived

from each component, allowing researchers to confirm successful incorporation of materials such as *Moringa oleifera* and kaolin clay into a composite.

In the context of composites, FTIR can elucidate the nature of chemical interactions occurring at the interfaces of different materials. When *Moringa oleifera* seed extract is combined with kaolin clay, FTIR can reveal shifts or changes in the absorption bands that signify interactions such as hydrogen bonding or van der Waals forces (Akanbi *et al*., 2022). For example, the broadening or shifting of peaks associated with hydroxyl groups may suggest hydrogen bonding between the bioactive compounds in *Moringa* and the silicate structure of kaolin, indicating enhanced compatibility and potential synergistic effects. Such insights are crucial for optimizing the composite's performance in applications such as water purification and soil enhancement.

Moreover, FTIR is valuable for monitoring the stability and degradation of composites over time. By performing FTIR analysis at various stages of composite development or after exposure to environmental conditions, researchers can assess how the material's properties change. For instance, the emergence of new peaks or changes in intensity can indicate chemical degradation or the formation of new compounds, which may affect the composite's effectiveness (Bashir et al., 2023). This capability makes FTIR an essential tool for evaluating the long-term viability of composites, ensuring that they remain functional in their intended applications.

2.3.3 Powder XRD

Powder X-ray Diffraction (PXRD) is a crucial technique for characterizing the structural properties of composite materials. This method involves the diffraction of X-rays by the crystalline phases within a powder sample, providing valuable information about the material’s crystalline structure, phase composition, and degree of crystallinity. PXRD is particularly effective in analyzing complex composites, such as those made from *Moringa oleifera* seeds and kaolin clay, as it can differentiate between various crystalline and amorphous phases present in the sample (Mishra *et al*., 2021). The resulting diffraction patterns can reveal the presence of specific

minerals and the arrangement of atoms within the composite, offering insights into how these components interact at the microscopic level.

The interpretation of PXRD data allows researchers to identify distinct peaks corresponding to different phases in a composite material. For example, the diffraction patterns of kaolin clay typically exhibit well-defined peaks due to its layered silicate structure, while *Moringa oleifera* seeds may show less pronounced features due to their more amorphous nature (Gonzalez *et al*., 2022). By analyzing the positions and intensities of these peaks, researchers can determine the crystallographic parameters, such as lattice parameters and unit cell dimensions, which are essential for understanding the physical properties of the composite. Additionally, the presence of new peaks or changes in existing peaks can indicate successful incorporation of *Moringa* components into the kaolin matrix, suggesting interactions that could enhance the composite's functionality.

Moreover, PXRD can provide insights into the degree of crystallinity within a composite, which is critical for applications where mechanical strength and stability are paramount. The ratio of crystalline to amorphous content can significantly affect the material's properties, such as its mechanical strength, thermal stability, and chemical resistance (Bashir *et al*., 2023). For instance, a higher degree of crystallinity in the kaolin phase may contribute to improved mechanical properties of the composite, which can be crucial for applications in construction or environmental remediation. Therefore, PXRD serves not only as a characterization tool but also as a predictive method for understanding how structural characteristics relate to the overall performance of the composite material.

Finally, the versatility of PXRD extends to the assessment of phase transitions and thermal stability in composites. By subjecting the material to varying conditions such as temperature or humidity and performing PXRD analysis before and after treatment, researchers can track changes in the crystalline structure. This is particularly relevant in the study of biocomposites like those made from *Moringa oleifera* and kaolin, where environmental factors may influence material properties (Mishra *et al*., 2021). Understanding these changes can inform the design of more durable and effective

composite materials for specific applications, enhancing their utility in fields ranging from environmental science to materials engineering.

2.4 Adsorption

2.4.1 Chemistry of *Moringa oleifera* Seeds and Kaolin clay

Heavy metals in natural waters have become increasingly severe, industries and farming activities are considered to be the main sources of pollution. Removal of heavy metals is very important and necessary before discharge into the environment. Chemical coagulation and precipitation, including flocculation and sedimentation, are employed to remove heavy metals in wastewater. Zinc, cadmium, manganese and magnesium are heavy metals used in the initial synthetic wastewater in the experiment carried out by (Oduro *et al*., 2008). Because of its excellent climatic adaptability and capacity to grow in dry soils, the perennial foliaged tree *Moringa oleifera* Lamarck (family Moringaceae) is planted extensively (Okuda *et al*., 2001). Because practically all components of this plant can be used for industrial, medical, and food purposes, it is regarded as one of the most useful trees in the world (Khalafalla *et al*., 2010). *Moringa oleifera* has been employed in several underdeveloped nations to avoid protein-energy malnutrition, particularly in young children and pregnant women (Oduro *et at*., 2008).

Nowadays, plant proteins are seen more as adaptable functional ingredients than as basic nutrients. Consumer demand is the primary force behind this progression toward functionality. The primary criterion for accepting and using proteins in food systems is their functional characteristics. The functional qualities of proteins are influenced by their physicochemical and structural characteristics, including surface hydrophobicity, ligand binding, secondary structure, molecular flexibility, and structure stability (Mune *et al*., 2016) (Grasso *et al*., 2022). Therefore, this work investigated the effects of oil concentration and pH on the emulsifying and foaming capabilities of *Moringa olifeira* seed and leaf flour. Other factors were secondary structure, surface hydrophobicity, water and fat-holding capacities, and solubility (Grasso *et al*., 2022).

Promotion and development of *Moringa oleifera* as a natural coagulant offers many diverse advantages to many countries of the developing world; sustainable, appropriate, effective and robust water treatment, effective enhancement of particular water treatment processes, decreased reliance on the importation and distribution of treatment chemicals, the creation of a new cash crop for farmers and employment opportunities. *Moringa oleifera* seed oil was extracted by using ethanol. The finding was as follows, *Moringa oleifera* seed cake oil yielded 12.78%, *Moringa oleifera* seed cake reduced the bacterial growth for the groundwater samples. Turbidity value was removed up to 85-94 % after the treatment and dissolved oxygen was significantly improved. There is no change in the pH value but a slight alteration of certain water parameters such as conductivity, salinity and total dissolved solids (Mune *et al*., 2016). However, *Moringa oleifera* seed cakes successfully removed the heavy metals from the water. The iron (Fe) was completely removed, whereas the copper (Cu) and cadmium (Cd) were successfully reduced up to 98 %. Lead (Pb) reduction has also been achieved by up to 78.1 %. Overall, 1 % of *Moringa oleifera* seed cake was enough to remove heavy metals from all samples (Mune *et al*., 2016).

In every nation, the use of natural resources to remove heavy metals is starting to raise concerns. Rapid industrialization has led to an excessive discharge of heavy metals into the environment, which is a major global concern. All forms of life are greatly impacted by heavy metal ions. The presence of heavy metals in surface and ground water presents a contaminating issue because they are found in both natural and industrial waste water (Wang *et al*., 2006). Wastes containing various heavy metals can be produced by a wide range of businesses and released into the environment. The production of pigments, batteries, tanneries, mining, smelting, and metal plating are the primary sources of heavy metal pollution. A class of metals having densities greater than 5 g/cm³, atomic numbers larger than 20, and low concentrations of toxicity or poisoning are all considered "heavy metals". “Chromium (Cr), manganese (Mn), cobalt (Co), copper (Cu), zinc (Zn), molybdenum (Mo), mercury (Hg), nickel (Ni), tin (Sn), lead (Pb), cadmium (Cd), antimony (Sb), are the principal elements that are classified as heavy metals. There are types of heavy metals that need to be taken into consideration: precious metals like hazardous metals (Hg, Cr, Pb, Zn, Cu, Ni, Cd, As, Co, Sn (Wang *et al*., 2006).

As a naturally occurring scavenger of pollutants, clay plays a vital function in the environment by absorbing cations and anions via adsorption, ion exchange, or both. As a result, its surface has exchangeable cations and anions including Pb^{2+}, As^{3+}, Cd^{2+}, Ca^{2+}, $Mg^{2+,}$ H^{+}, NH^{4+}, Na^{+}, SO_4^{2-}, Cl^{-}, and NO^{3-} that can be swapped out for other ions comparatively without changing the mineral structure of clay. Clays are ideal adsorbent materials because of their huge specific surface area, layered structure, high cation exchange capacity (CEC), mechanical and chemical stability, and other characteristics (Nwosu *et al*., 2018). Bronsted and Lewis type of acidity in clays have also boosted to considerable extent the adsorption capacity of clay minerals. When hydrated exchangeable metal cations on the surface split apart, leaving behind H^{+} ions, this causes the formation of Bronsted acidity. Bronsted acidity may develop if there is a net negative charge on the surface because Al^{3+} may replace Si in some tetrahedral locations, and H_3O^{+} cations will balance the resulting charge (Nwosu *et al*., 2018). Trivalent cations, usually Al^{3+}, that are exposed at the borders of natural water can absorb anions, cations, and nonionic and polar pollutants. It can also result from the breakage of Si–O–Al bonds or from the dihydroxylation of certain Bronsted acid sites. Pollutants can be held through H-bonding, Van der Waals interactions, or hydrophobic bonding arising from either strong or weak interactions occasionally, making it difficult to remove the contaminants that saturate the clay surface through the processes of ion exchange, coordination, or ion-dipole interactions. The clay mineral's numerous structural and physical characteristics influence the strength of the interactions (Nwosu *et al*., 2018).

2.4.2 Adsorption Isotherms and Kinetics

Pseudo first order equation; The Langergren pseudo-first-order kinetic model and the McKay pseudo-second-order model are used to examine the transient behavior of the batch sorption process at various starting concentrations. The adsorption kinetics has been largely predicted using Lagergren's pseudo-first-order kinetic model (Struthers *et al*., 2021). The pseudo-first-order model composite adsorption kinetics is provided by:

$$d_{qt} / d_t = k_1 / (q_e - q_t) \quad \text{...}(1)$$

Where K_1 denotes the adsorption rate constant (min^{-1}) and q and q_e represent the amount of composite adsorbed (mg/g^{-1}) at any time t and at equilibrium time,

respectively. When Equation (1) is integrated with regard to the boundary conditions q = 0 at t = 0 and q = q at t = t, it takes on the form shown in Equation (2);

$$\text{Log}\,(q_e - q_t) = \log q_e - (k_1/2.303) \quad \ldots\ldots (2)$$

Thus the rate constant K_1 (min^{-1}) can be calculated from the plot of log (q_e-q) vs time t. The values of q_e (amount adsorbed at equilibrium) and k_1(rate constant) are determined from the linear plot of $\log(q_e - q_t)$ vs t (Shin *et al*., 2021).

The kinetic data can then be subjected to additional analysis through the utilization of a pseudo-second-order connection that was created and represented by Equation (3):

$$d_{qt}/d_t = k_2(q_e - q_t)^2 \quad \ldots\ldots (3)$$

Where K_2 is the pseudo-second-order rate constant in ($g/mg^{-1}/min^{-1}$), and q_e and q denote the amount of composite adsorbed (mg/g^{-1}) at equilibrium and each time t.

Adsorption is a significant phenomenon that underlies several highly significant industrial and environmental processes. There is no denying the importance of adsorption to water purification and environmental preservation. Furthermore, the initial stage of many catalytic reactions involves the adsorption of reactants onto the catalyst. Thus, a lot of work has gone into learning more about the various facets of the adsorption process. But before designing and using adsorption equipment, one must have a basic understanding of adsorption equilibrium and kinetics. To understand the adsorption equilibrium and kinetics, several different isotherms and kinetics models have been devised (Azizian *et al.*, 2011). Adsorption isotherms, or mathematical equations, can be used to realize the interpretation of adsorption equilibria. Additionally, rate equations for adsorption kinetics models are provided to describe the adsorption process's time dependency.

Langmuir isotherm is among the earliest theories to explain the phenomena of adsorption. The following presumptions and kinetics arguments served as the foundation for the development of the Langmuir theory: Adsorption takes happen on sites that are energetically equivalent. Only one adsorbate may be loaded at a time at each adsorption site, and the bonding energy between the adsorbent and the adsorbate must be strong enough to prevent the adsorbed species from being displaced.

Furthermore, there is no repulsive force or attraction between the adsorbed species (Azizan *et al*., 2011). Probably the most well-known and frequently used equation to describe the adsorption equilibrium is the Langmuir isotherm. Nevertheless, the Langmuir isotherm's underlying assumptions are rarely found in actual systems. Therefore, the goal of multiple investigations was to modify the Langmuir isotherm. This section will cover several of these modifications. The constant and the adsorption's coverage independence are two of the Langmuir isotherm's most implausible assumptions (Mudhoo *et al*., 2023). Langmuir equation follows Equation (4) (Limousin *et al*., 2007),

$$qe = (q_{max} K_L C_e)/(1+K_L Ce) \quad \text{.....(4)}$$

Typically, the Freundlich adsorption isotherm is used to calculate the equilibrium connection between the concentration of adsorbate remains in the solution and the amount of adsorbate removed per unit weight of carbon. An effective way to explain adsorption processes is via the Freundlich adsorption isotherm. It is often given as an empirical formula with minimal theoretical support (Azizan *et al*., 2011). Although the Freundlich equation is primarily empirical, data description can occasionally be accomplished using it. This is because a variety of adsorbate concentrations can be effectively described by the equation, which describes the non-linear adsorption process. Its ease of use stems from its mathematical simplicity and its capacity to explain the adsorption process on energetically heterogeneous surface adsorption sites (Gupta *et al*., 2021). The Freundlich isotherm accurately demonstrates the relationship between adsorption and pressures at low pressures, but it is unable to forecast the amount of adsorption at high pressures. The equations follow Equation (5) (Wang *et al*., 2020),

$$\log q_e = \log K_F + (1/n) \log C_e \quad \text{.....(5)}$$

The Temkin isotherm model is used in adsorption studies to describe how adsorbates interact with adsorbents. It assumes that the heat of adsorption of all the molecules in the layer decreases linearly with coverage due to adsorbent-adsorbate interactions (Gupta *et al*., 2021). Temkim equation is given by Equation (6):

$$q_e = B \ln(AC_e) \quad \text{.....(6)}$$

Where: q_e is the amount of adsorbate adsorbed per unit mass of adsorbent (mg/g), C_e is the equilibrium concentration of the adsorbate (mg/L), A is the Temkin isotherm constant (L/g) and B is a constant related to the heat of adsorption (J/mol) (Shin *et al*., 2021). Plotting and analysis, $q_e$versus ln (Ce). The slope of the plot gives B. The intercept of the plot gives B ln(A) (Wang *et al*., 2020).

2.4.3 Adsorption Thermodynamics.

Adsorption thermodynamics involves studying the energy changes that occur during the adsorption process. Key thermodynamic parameters include Gibbs free energy (ΔG), enthalpy (ΔH), and entropy (ΔS) changes. These parameters help determine the feasibility, heat exchange, and randomness of the adsorption process. Understanding adsorption thermodynamics is crucial for designing efficient adsorbents and optimizing processes in water treatment, pollution control, and chemical separation (Wang *et al*., 2020). Gibbs free energy (ΔG); $\Delta G=\Delta H-T\Delta S$, indicates the spontaneity of the adsorption process. A negative value suggests a spontaneous process. Enthalpy (ΔH) provides insights into the heat exchange during adsorption. A positive value indicates an endothermic process, while a negative value indicates an exothermic process. Entropy (ΔS) measures the disorder or randomness at the solid-liquid interface during adsorption. A positive value suggests increased randomness (Gim *et al*., 2023).

CHAPTER THREE
METHODOLOGY

3.1 Study Areas

This research was carried out in Nakuru East Sub County, within Nakuru County, Kenya. Nakuru East Sub County (Figure 1) lies on latitude 0º18´ 11" S and longitude 36º31´18" E. Nakuru East has an altitude of 1850 M, annual average rainfall of 762 mm and an average temperature of 23ºC. The study area has two rainy seasons; the long rains occur between April and August, with a rainfall peak in April while the short rain occurs between October to December, with a rainfall peak in November (Keli *et al*., 2021). The study area has a population of 570 674 and an area of 548.2 km^2 (Mwangi *et al*., 2024).

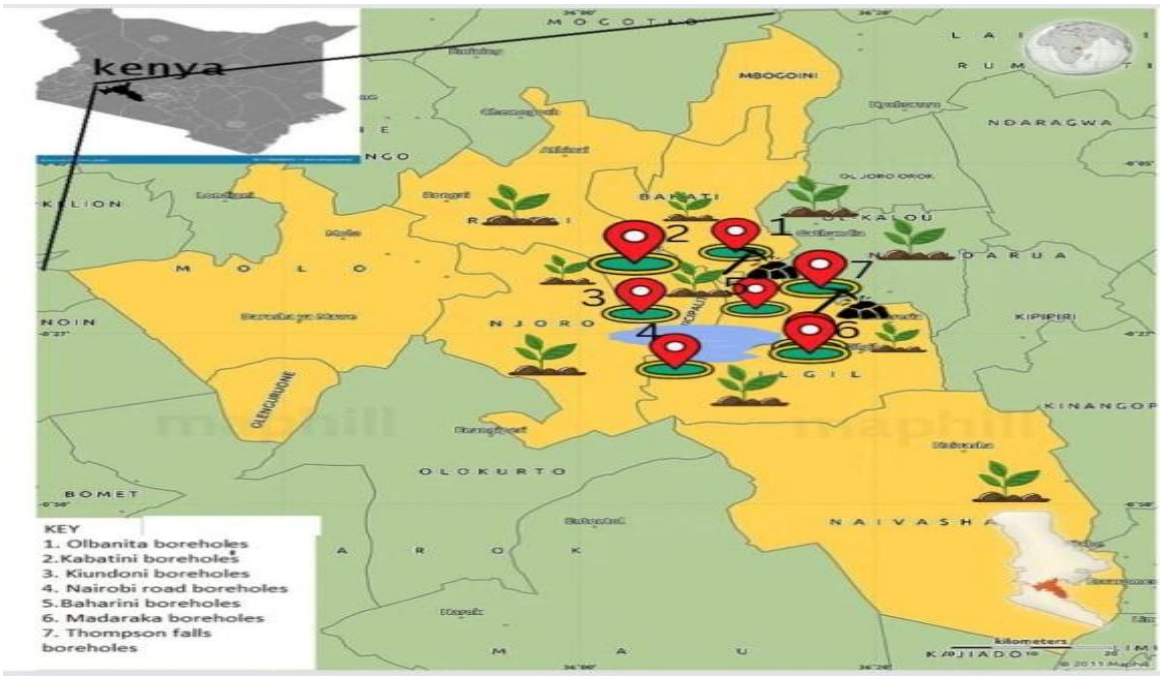

Figure 1: A Map of Nakuru East Sub County, Nakuru County

The main agricultural activities include subsistence and commercial production of maize, beans, Irish potatoes and wheat (Otieno *et al*., 2021). Several industries are located in the area including Menengai Oil Refineries Limited, Pixers Printers Nakuru and Mega Paper and Boards Limited (Mburu *et al*., 2017). A part of Nakuru city including the central business district and several residential areas (Kaptembwo, Pipeline, Section 58 and Free Area) are located within the study area. Nakuru East Sub County lies on the Gregory Rift Valley, which is in an unstable geological zone

characterized by frequent local geological faulting (Keli *et al*., 2021). The area is mainly composed of volcanic rocks of Tertiary-Quaternary age overlain by recent sediments (Keli *et al*., 2021). Most parts of the study area have loamy clay soil (Maskall *et al*., 1989).

Water for commercial and domestic use in Nakuru County is supplied by Nakuru Water and Sanitation Services Company Limited (NAWASSCO). NAWASSCO sources a significant portion of its water from boreholes located in the study area at Kiundo, Kabatini, Madaraka, Nairobi Road, Baharini and Olbanita (NAWASSCO, 2024).

The *Moringa Oleifera* seeds were collected at a commercial farm located at Chogoria area (0.228^{o} S, 37.63^{o} E) of Tharaka-Nithi County. Chogoria is located on the eastern side of Mount Kenya, on the upper ecological zone (the highlands) of Tharaka Nithi County (Kaua, 2021). The area has an annual average temperature of 23^{o}C and annual rainfall precipitation of approximately 1,702 mm (Kaua, 2021). The area has a bimodal rainfall pattern with the long rains falling between March and May and short rains between October and December (Kaua, 2021). The area is largely agricultural with mixed subsistence farming of maize, green grams and bananas and commercial production of tea (Kaua, 2021).

3.2 Research Design

The purposive sampling design was used to collect water samples from boreholes in the study area. NAWASSCO sources water from twenty-six boreholes in the study area (NAWASSCO, 2024). The twenty-six boreholes are located at Kiundo (1), Kabatini (8), Nairobi Road (3), Baharini (5), Madaraka (1) and Olbanita (8). Water samples were collected from the nineteen boreholes that were functional during the period of study. The nineteen boreholes were located at Kiundo (1), Kabatini (6), Nairobi Road (6), Baharini (4), Madaraka (1) and Olbanita (1). Water samples were collected from the boreholes during both the wet and the dry season. The experimental design was used for adsorption studies. The initial concentration of the selected heavy metals was taken as the dependent variable while dosage, temperature, pH, concentration, rotation and contact time were the independent variables.

3.3 Collection of Samples

3.3.1 Collection of Water Samples

Samples were collected from the nineteen functional boreholes located at six sites within the study area. The six sites were designated as follows: Kiundo (KI), Kabatini (KA), Nairobi Road (NR), Baharini (B), Madaraka (MA) and Olbanita (OL). Nineteen samples were collected during the dry season (January, 2024) when the average daily precipitation was 5 mm. The samples were labelled B3, B6, B7, B8, KA1, KA2, KA3, KA5, KA7, KA10, KI1, MA1, NR1, NR2, NR3, NR4, NR5, NR7 and OL1. Another nineteen samples were collected from the same working boreholes in April, 2023 during the wet season, when the average daily precipitation was 80 mm. These samples were labelled as follows: B3, B6, B7, B8, KA1, KA2, KA3, KA5, KA7, KA10, KI1, MA1, NR1, NR2, NR3, NR4, NR5, NR7 and OL1. Each borehole was sampled in triplicate with an interval of 10 min during the dry and wet season. Thus, a total of 114 grab samples were collected for the study. Samples were collected in the morning (6:00 am to 9:00 am) using 500 ml polyethylene bottles. The bottles were rinsed three times with the respective borehole water before collection. The pH, temperature and turbidity of the samples were measured in the field during sample collection. The pH and temperature were measured using a HI 2211 meter (HANNA instruments) while the turbidity was measured using a Lp 2000 turbidity meter (HANNA instruments). Samples were placed in a cooler box, transported to Chuka University Chemistry Laboratory and stored at 4^{o}C prior to analysis. Samples for elemental analysis were acidified using nitric acid to avoid precipitation of the metal ions.

3.3.2 Collection of *Moringa oleifera* Seeds

Dry seeds of *Moringa oleifera* were collected from Chogoria area in Tharaka Nithi County on 15^{th} of February, 2024. The seeds were placed in clean and dry polyethylene bottles, transported to Chuka University Chemistry Laboratory and stored at 4^{o}C to prevent biodegradation.

3.4 Analysis of Fluoride

The concentration of fluoride ions in the water samples was determined using an Ion Selective Electrode (ISE) fluoride meter (Model FL700, Extech Instruments).

Standards of 0.1 ppm, 1 ppm and 10 ppm were prepared using standard solutions of potassium fluoride and deionized water. The total ionic strength adjustment buffer (TISAB) solution was used to adjust the ionic strength and pH. Water samples were first filtered to prevent electrode fouling and then an equal amount of TISAB solution was added to each sample. The concentration of fluoride ions in each sample was then measured in triplicate (Wesley *et al*., 2023).

3.5 Analysis of Heavy Metals

3.5.1 Chemicals and Reagents

Chemicals of analytical grade were purchased from Sigma-Aldrich and used without further purification. The chemicals included HCl (65%), HNO_3 (95%), $NaBH_4$ (≥98.0%), NaOH solution, H_2SO_4 (95%), KCl (99.0-100.5%), $Pb(NO_3)_2$ (99.999%), $CdSO_4.8H_2O$ (98.0-102%) and $AsNO_3$.

3.5.2 Digestion of Water Samples

A composite water sample was prepared from the three triplicate grab samples collected from each borehole. A 45 ml composite sample was prepared by mixing 15 ml from each grab sample. The composite sample was acidified with 5 ml of concentrated HNO_3, heated on a hot plate to reduce the volume to 30 ml and cooled to ambient temperature. The sample was then filtered using 0.45 µm filter paper and the final volume adjusted to 40 ml.

3.5.3 Preparation of Standards and Stock Solutions

Stock solutions (1.0 L) of 1000 ppm were prepared using 1.6 g of $Pb(NO_3)_2$, 6.8 g $CdSO_4.8H_2O$ and 1.5 g $AsNO_3$. Working solutions of 2 ppm, 4 ppm, 6 ppm, 8 ppm and 10 ppm were prepared by serial dilution of the stock solutions. Deionized water and ultrapure water were used in all experiments.

3.5.4 Elemental Analysis

The concentration of lead, cadmium and arsenic in the water samples was determined by the standard calibration method using a Flame Atomic Absorption Spectrometer (Shimadzu AA-7000; Egerton University Safe Food Laboratory). The spectrometer was equipped with a Shimadzu ASC-7000 autosampler. The concentrations of the

blanks, standards and samples were determined in triplicate. The concentration of arsenic in the water samples was determined using Hydride Generation-Flame Atomic Absorption Spectrometry (HVG-FAAS). The water samples were acidified with HCl and reduced by $NaBH_4$ (Aga *et al*., 2014). The resultant arsenic hydride vapors were swept into a heated quartz cell by argon gas and analyzed in the flame of an air-acetylene burner of the atomic absorption spectrometer.

3.6 Preparation of Composite Adsorbent

Moringa oleifera seeds were washed with deionized water to remove dust and dried in an oven at a temperature of 50ºC for 24 h. The dried seeds were ground into a fine powder and sieved through a 105 μm mesh screen. The *Moringa oleifera* seed powder (MOSP) was transferred into a crucible and heated on a hotplate for 20 min. The sample was then carbonized using a Ceramic Fiber Muffle Furnace (MC5-12, Biobase). The carbonized sample was cooled and stored in a cool dry environment. Kaolin clay was purchased from Protist Lab Africa Limited, ground into powder using a mortar and pestle and then sieved through a 105 μm mesh screen.

The carbonized *Moringa oleifera* seed powder was mixed with the kaolin clay in the ratio of 1:1 to prepare the composite adsorbent. The raw composite was prepared using 25 g of carbonized *Moringa oleifera* seed powder and 25 g of kaolin clay. The mixture was dispersed and homogenized in 200 ml of ultrapure water using a magnetic stirrer. The homogenized mixture was filtered using 105 μm filters, dried in an oven for 12 h and cooled to obtain the raw composite. The same procedure was used to prepare acid and base activated composites. The acid activated composite was prepared by stirring the carbonized seed powder and kaolin clay in 200 ml of 0.1 M H_2SO_4 solution for 30 min. The composite was then filtered, washed with water until the pH was between 6.5 and 7.0 and dried in an oven for 4 h at 105ºC. The same procedure was used to prepare the base activated composite using 0.1 M NaOH solution. The obtained composites were then converted into fine powder and stored in sealed jars (Gao *et al*., 2021).

3.7 Characterization of the Composites

3.7.1 FT-IR Analysis

The FT-IR spectra of the samples were obtained using a Shimadzu IRAffinity-1S Fourier transform infrared (FT-IR) spectrophotometer (Chuka University). Powdered samples were mixed with KBr in the ratio of 1:100. The mixture was then homogenized and pressed into thin, transparent pellets (i.e. KBr Pellets) at 800 KPa using a hand operated press machine. The FT-IR spectra were then obtained in the range of 400-4000 cm^{-1}.

3.7.2 Powder XRD Analysis

The structural properties of Kaolin clay, the carbonized *Moringa oleifera* sample and the composites were investigated using powder x-ray diffraction (Rigaku MiniFlex 600, Rigaku Corporation, Geothermal Development Company Limited, Kenya). Powdered samples were loaded into glass sample holders and analyzed using Cu-Kα x-ray radiation (λ =1.5418 Å) with a beam voltage of 45 kV and a current of 40 mA. Scans were performed in continuous mode at a rate of 2^o per minute in the 2θ range of $0\text{-}90^o$. The x-ray diffraction (XRD) patterns were analyzed using the International Centre for Diffraction Data (ICDD) crystallographic database.

3.8 Batch Sorption Experiments

Batch adsorption experiments were conducted at ambient temperature in 100 ml propylene bottles containing 20 ml of 10 ppm Pb (II) ions prepared from the standard solution as per section 3.5.3. The three composite samples (raw, acid and base activated composites) were independently grounded into powder and sieved through a 105 μm mesh screen. The requisite amount was accurately weighed, placed in a 100 ml bottle and 20 ml of 8 ppm Pb (II) solution was added. The resultant mixture was equilibrated for 30 min on an orbital shaker operated at 500 rpm. The mixture was then filtered using a 0.45 μm pore size filter. The concentration of Pb (II) in the filtrate was determined by the standard calibration method using a Shimadzu GFA-7000A Flame Atomic Absorption Spectrophotometer. The amount of Pb (II) ions adsorbed per unit mass was calculated as:

$$Q_e = \frac{(C_i - C_e)V}{m} \quad \text{.....(7)}$$

Where C_i and C_e are the initial and equilibrium concentrations (ppm), *m* is the mass of the adsorbent (g) and *V* is the volume of the solution (mL).

The percentages of Pb (II) ions removed by the composite were calculated using the following equation:

$$\% \text{ Removal} = = \frac{C_{0\_}C_e}{C_0} \times 100 \ldots\ldots\ldots\ldots\ldots\ldots\ldots\ldots\ldots\ldots\ldots\ldots (8)$$

Where C_o, C_e are the original and final concentration of Pb (II) respectively.

The effects of several parameters on the adsorption process were determined by varying the amount of adsorbent (0.5, 1.0 and 1.5 g), initial concentration of adsorbate (2, 4, 6, 8 and 10 ppm), contact time (10, 20, 30, 40 and 50 min), rate of agitation (100, 200, 300, 400 and 500 rpm), temperature (25, 75, 125, 175 and 225^oC), presence of As^{2+} ions (2, 4, 6, 8 and 10 ppm) and pH (2-12). The pH of the solution was adjusted from 2 to 12 using 0.1M HCl and 0.1M NaOH. The optimized conditions were then applied to a standard solution of Pb^{2+} ions and a water sample from the study area.

3.9 Data Analysis

All experiments were conducted in triplicate and the results analyzed using mean. The data analysis for the physicochemical parameters of different boreholes in Nakuru East, Kenya was conducted using one-way analysis of variance (ANOVA) in R Studio version 4.3.2. The analysis utilized different packages including stats, goeveg, and DescTools. The dependent variables were the specific measurements of physico-chemical parameters analyzed (e.g., pH, temperature, Pb, Cd, As, fluoride), while the independent variable was the boreholes represented by the sample identifiers. Fisher's Least Significant Difference (LSD) test was applied following the ANOVA to identify specific pairs of boreholes with significant differences in parameter values at an alpha level of 0.05, with adjustments made using the Bonferroni method. In addition to ANOVA, correlation analyses were performed to explore relationships among the measured physico-chemical parameters. Pearson's correlation coefficients were calculated using the R correlation plot package.

Freundlich, Langmuir and Temkin adsorption isotherm models were used to describe the phenomenon governing the retention, release or mobility of pollutants from wastewater to base activated solid at constant temperature. In addition, the constants characterized by adsorption isotherm equations were computed to determine the surface properties and the effective of the base activated composites for the different pollutants. Kinetic data were analyzed using pseudo-first-order and pseudo-second-order model. These models were necessary in describing the nature of adsorbent surface (homogenous or heterogeneous), the rate limiting step and reversibility of the equilibrium between adsorbent and water samples. Thermodynamic parameters such as the standard free energy (ΔG^o), enthalpy change (ΔH^o) and entropy change (ΔS^o) were also determined.

3.10 Ethical Considerations

The study was approved by the Scientific Ethics Research Committee of Chuka University, Appendix 11. A research permit was obtained from the National Commission for Science, Technology and Innovation (NACOSTI), Appendix 12. All original sources were duly acknowledged and accurately cited to avoid plagiarism. Permission to collect water samples was granted by NAWASSCO, Appendix 10. The findings of the study will be disseminated to the local community, policymakers and other stakeholders in the water sector.

CHAPTER FOUR
RESULTS AND DISCUSSION

4.1 Physicochemical Properties of Water Samples

4.1.1 Physicochemical Properties of Water during the Dry Season

The values of physicochemical parameters of the borehole water during the dry season are given in Tables 1 and 2. The turbidity of the water samples ranged from 1.54 to 4.32 NTU, with an average of 2.30 NTU. The turbidity of all samples were below the maximum allowable value of 25 NTU set by the Kenya Bureau of Standards (KEBS) for natural portable water (KEBS, 2015) and 5 NTU set by the World Health Organization (WHO) for drinking water (WHO, 2022). Water from the boreholes (except for NR2 and OL1; >4 NTU) is therefore aesthetically appealing and suitable for disinfection using conventional technologies (WHO, 2022). Several studies have reported comparable NTU values and attributed the low turbidity to effective filtration of particulates from groundwater by geological formations (Fadiran *et al*., 2008; Orebiyi *et al*., 2010).

Table 1: Physicochemical parameters of borehole water during the dry season

BH	Turbidity (NTU)	pH	EC (µs/cm)	Temp (°C)	DO (mg/L)	Fluoride (mg/L)
B3	1.98±0.02	6.4±0.1	287.6±0.4	25.5±0.2	3.08±0.01	2.01±0.06
B6	1.57±0.10	6.3±0.0	316.4±0.4	25.5±0.2	2.73±0.02	2.02±0.02
B7	2.37±0.00	6.6±0.0	247.3±0.3	26.4±0.2	2.93±0.02	1.98±0.02
B8	1.80±0.08	6.5±0.1	313.2±0.8	26.2±0.2	3.24±0.00	1.86±0.01
KA1	1.92±0.07	6.4±0.0	186.7±0.5	25.5±0.1	2.90±0.11	1.11±0.00
KA10	2.27±0.02	6.5±0.1	198.7±0.6	25.5±0.2	3.13±0.01	1.43±0.01
KA2	1.54±0.02	6.5±0.1	194.9±0.6	25.6±0.1	2.95±0.10	1.41±0.01
KA3	1.64±0.00	6.4±0.1	195.7±0.6	25.6±0.5	3.44±0.01	0.82±0.01
KA5	1.94±0.01	7.2±0.0	195.9±0.3	25.3±0.2	2.72±0.01	1.21±0.00
KA7	2.75±0.06	6.5±0.0	200.3±0.3	26.0±0.1	2.03±0.00	0.89±0.01
KI1	2.45±0.10	6.4±0.1	300.6±0.5	25.7±0.1	1.97±0.27	1.73±0.04
MA1	2.81±0.02	7.3±0.1	209.1±0.5	25.2±0.1	3.15±0.02	1.23±0.01
NR1	1.95±0.00	7.6±0.1	298.4±0.4	25.1±0.1	2.91±0.17	1.15±0.00
NR2	4.32±0.04	7.3±0.1	345.3±0.8	24.6±0.1	2.31±0.04	0.79±0.01
NR3	1.78±0.01	6.5±0.1	324.9±0.8	25.5±0.2	3.21±0.03	0.68±0.03
NR4	1.75±0.00	7.2±0.2	338.6±0.3	24.9±0.2	2.66±0.01	0.65±0.06
NR5	2.40±0.01	7.2±0.1	338.1±0.2	25.3±0.1	3.19±0.03	0.68±0.01
NR7	2.26±0.01	7.4±0.0	349.7±0.5	25.0±0.1	2.61±0.03	1.30±0.01
OL1	4.11±0.10	6.6±0.0	350.6±0.1	26.2±0.1	0.60±0.04	0.48±0.02
Mean	2.30	6.8	273.3	25.5	2.72	1.23
SD	0.77	0.44	64.3	0.5	0.65	0.50

BH = Borehole; EC = Electrical Conductivity; DO = Dissolved Oxygen; SD = Standard Deviation

The pH of the water samples ranged between 6.3 and 7.6 with an average pH of 6.8. The pH of all samples was within the pH values of 5.5-9.5 set by KEBS for natural

portable water (KEBS, 2015). The pH values of the water samples are also within the WHO guideline of 6.5 to 8.5 except for KA1, KI1, KA3, B3 and B6 (WHO, 2022). The pH values suggest that borehole water in the study area is slightly acidic to neutral. The pH values are also slightly lower than those obtained in similar studies in Nakuru area (Madadi *et al*., 2017; Keli *et al*., 2019; Keli *et al*., 2021).

The electrical conductivity of the water samples ranged between 186.7 to 350.6 µs/cm with a mean of 273.3 µs/cm. The conductivity of all samples were significantly lower than the maximum conductivity limit of 2500 µs/cm set by KEBS for natural portable water (KEBS, 2015). The electrical conductivities were also below the maximum value of 400 µS/cm set by the World Health Organization (WHO, 2022). Conductivity of water is influenced by the concentration of dissolved salts and minerals. The observed levels suggested moderate mineralization, typical for groundwater in many regions. Several studies have reported higher conductivity in groundwater during dry seasons due to reduced dilution effect of precipitation and increased mineral dissolution (Zhang *et al.,* 2008).

The temperature of the water samples ranged from 24.6°C to 26.4°C with an average of 25.5°C. The temperatures of all samples were within permissible limit of WHO (WHO, 2022). Groundwater temperature is generally stable and reflects the ambient temperature of the region. Thus, the temperatures of groundwater are within the ambient temperatures of the region (Keli *et al*., 2021). The concentration of dissolved oxygen (DO) in the water samples ranged from 0.60 to 3.44 mg/L with an average of 2.72 mg/L. The concentrations of DO in all of the samples were below the WHO acceptable limit of 7–14 mg/L (WHO, 2022). In contrast, research by Ahmed *et al*. (2022) reported higher average DO levels of around 4.0 mg/L in boreholes.

The concentration of fluoride in the water samples ranged from 0.48 to 2.02 mg/L with a mean concentration of 1.23 mg/L. The concentration of fluoride in fourteen boreholes was below the maximum allowable limit of 1.5 mg/L established by KEBS and WHO for drinking water (KEBS, 2015; WHO, 2022). The concentrations of fluoride in four boreholes (B3, B6, B7, B8) located in Baharini area and one borehole (KI1) located in Kiundo area were above the maximum allowable limit. Low

concentrations of fluoride in drinking water are essential for proper formation of teeth and bones and for prevention of tooth decay (WHO, 2004). However, high concentrations of fluoride in drinking water can cause adverse health effects including dental fluorosis (1.5-2.0 mg/L), skeletal fluorosis (3–6 mg/L) and crippling fluorosis (> 10 mg/L) (WHO, 2004; Malago *et al*., 2017). The concentrations of fluoride in the five mentioned boreholes are therefore within the range that causes dental fluorosis.

High concentrations of fluoride in groundwater have been reported in several regions of the Kenyan Great Rift Valley (Nair *et al*., 1984; Olaka *et al*., 2016; Gevera & Mouri, 2018; Keli *et al*., 2019; Keli *et al*., 2021; Mwiathi *et al*., 2022). The high concentrations have been attributed to weathering and dissolution of fluorine bearing minerals (e.g. fluorite, fluorapatite, cryolite and villiaumite) in volcanic rocks (Khan *et al*., 2016; Olaka *et al*., 2016; Mwiathi *et al*., 2022).

The concentrations of heavy metals in borehole waters are shown in Table 2. The concentration of lead in the water samples ranged from below the detection limit (BDL) to 1.6 mg/L. The concentration of lead in the water samples was BDL in eleven boreholes. The concentration of lead in eight boreholes was higher than the maximum limit of 0.01 mg/L set by KEBS and WHO for drinking water (KEBS, 2015; WHO, 2022). Thus, 31.6% of the sampled boreholes had lead concentrations higher than the maximum allowable concentration. Lead is a highly toxic element that can cause several adverse health effects including developmental, learning and cardiovascular disorders, renal diseases, and digestive problems (Mandal *et al*., 2022). One probable source of lead in the groundwater is the dissolution of lead bearing minerals in volcanic rocks that are abundant in the East Africa rift system (Rango *et al*. 2010; Malago *et al*., 2020; Olaka *et al*., 2022).

Table 2: Concentration of heavy metals in borehole water during the dry season

Borehole	Lead (mg/L)	Cadmium (mg/L)	Arsenic (mg/L)
NR1	BDL	BDL	1.0475±0.0017
NR2	BDL	BDL	1.1298±0.0027
NR3	BDL	BDL	1.0790±0.0011
NR4	BDL	BDL	1.2130±0.0011
NR5	BDL	BDL	1.2130±0.0010
NR7	1.7496±0.0136	BDL	1.2209±0.0011
KA2	BDL	BDL	1.2446±0.0003
KA3	1.2000±0.0093	BDL	1.0554±0.0020
KA5	BDL	BDL	1.1342±0.0042
MA1	BDL	BDL	1.2446±0.0001
KI1	BDL	BDL	1.2366±0.0018
OL1	BDL	BDL	1.2761±0.0012
KA7	0.3930±0.0038	BDL	1.3154±0.0012
KA10	BDL	BDL	1.2682±0.0011
KA11	0.0264 ±0.0006	BDL	1.2682±0.0016
B3	0.2610±0.0022	BDL	1.3234±0.0004
B6	0.2757±0.0025	BDL	1.1736±0.0020
B7	1.6322±0.0125	BDL	1.2761±0.0015
B8	0.2537±0.0029	BDL	1.4101±0.0021
Mean	0.1480	-	1.0717
SD	0.3814	-	0.1530

BDL = Below Detection Limit

The concentration of cadmium in all samples was below the detection limit during the dry season. Thus, the concentration of cadmium was below the maximum acceptable concentration of 0.003 mg/L established by KEBS and 0.005 mg/L set by WHO for drinking water (KEBS, 2015; WHO, 2022). These results are in agreement with those of a study by Madadi and co-workers for borehole water within Nakuru area (Madadi *et al*., 2017). However, these results are in variant with several studies that found low concentrations of cadmium in groundwater from the study area (Keli *et al*., 2019; Keli *et al*., 2022).

The concentration of arsenic in the water samples ranged from 0.81 to 1.33 mg/L with an average of 1.07 mg/L. Arsenic concentrations in all samples were above the maximum acceptable concentration of 0.01 mg/L set by KEBS and WHO for drinking water (KEBS, 2015; WHO, 2022). Chronic exposure to arsenic can cause several adverse health effects including dermal, cardiovascular, reproductive, gastrointestinal and renal disorders (Mandal and Suzuki, 2002; Ng *et al*., 2003). Potential sources of groundwater arsenic in the study area include leaching from arsenic bearing minerals in tuffs, rhyolites, andesites and other volcanic rocks (Barringer and Reilly, 2013).

4.1.2 Physicochemical Properties of Water during the Wet Season

The physicochemical parameters for the wet season are shown on Tables 3 and 4. As shown in Table 3, the average turbidity was 2.06 NTU and values ranged from 0.36 to 9.30 NTU. Samples from NR1 and OL1 boreholes had their concentrations above the WHO and KEBS permissible limits, while the rest of the samples were below the recommended maximum concentration of 5 NTU (KEBS, 2015; WHO, 2022). Turbidity was significantly higher compared to the dry season. Increased turbidity during the wet season can be attributed to surface run-off carrying more particulates into the groundwater (Islam *et al*., 2021). Borehole NR1 had the highest turbidity of 9.30 NTU, suggesting substantial sediment infiltration during the wet season (Islam *et al*., 2021).

Table 3: Physicochemical parameters of borehole water during the wet season

BH	Turbidity (NTU)	pH	EC (µs/cm)	Temp (°C)	DO (mg/L)	Fluoride (mg/L)
B3	0.5670±0.06	7.045±0.02	659.000±0.16	24.2±0.10	6.0511±0.01	2.1133±0.14
B6	0.8020±0.01	7.053±0.02	714.111±0.06	24.0±0.10	3.9922±0.01	1.0933±0.01
B7	1.6880±0.00	7.021±0.01	681.567±0.11	24.3±0.10	3.3022±0.01	0.7867±0.01
B8	0.3600±0.04	7.028±0.02	676.233±0.23	24.2±0.10	3.7200±0.01	0.7700±0.04
KA1	1.4544±0.01	6.810±0.02	416.567±0.02	24.1±0.10	4.0967±0.02	0.8133±0.02
KA10	1.7740±0.03	6.833±0.04	400.867±0.02	24.1±0.10	3.1667±0.01	1.2367±0.01
KA2	1.2156±0.02	7.086±0.04	469.667±0.94	24.3±0.10	3.9167±0.03	1.5233±0.02
KA3	0.8389±0.01	7.121±0.02	533.633±0.07	24.3±0.10	4.0855±0.03	0.9333±0.02
KA5	2.0900±0.01	7.008±0.06	404.667±0.08	24.2±0.10	3.1067±0.01	1.3467±0.02
KA7	3.1545±0.02	6.768±0.06	555.333±0.14	24.2±0.10	3.7778±0.04	1.4767±0.01
KI1	1.3611±0.01	7.299±0.02	809.433±0.17	23.8±0.10	4.0022±0.02	1.8800±0.02
MA1	3.0500±0.02	7.090±0.01	410.433±0.16	24.2±0.10	3.5511±0.01	0.6067±0.01
NR1	9.3033±0.05	7.616±0.05	408.889±0.18	23.9±0.10	4.4333±0.01	0.9200±0.01
NR2	0.5433±0.01	7.459±0.03	810.000±0.14	24.2±0.10	3.8467±0.01	1.2733±0.01
NR3	0.6856±0.02	7.275±0.02	823.133±0.02	24.2±0.10	4.5967±0.01	1.6533±0.02
NR4	0.9150±0.02	7.384±0.01	822.567±0.46	24.3±0.10	3.8011±0.01	2.1367±0.01
NR5	0.3890±0.01	7.219±0.02	817.111±0.21	24.2±0.10	4.1078±0.01	2.1633±0.05
NR7	0.5378±0.01	7.339±0.01	811.567±0.21	24.1±0.10	3.8723±0.01	1.9800±0.00
OL1	8.3470±0.03	7.282±0.01	392.000±0.06	24.0±0.10	4.6567±0.04	1.9333±0.01
Mean	2.06	7.14	611.41	24.15	4.00	1.23
SD	0.5	0.22	175.79	0.14	0.65	0.13

BH = Borehole; EC = Electrical Conductivity; DO = Dissolved Oxygen; SD = Standard Deviation

The pH levels during the wet season ranged from 6.8 to 7.6 had an average pH of 7.14. The values were slightly higher than those obtained during the dry season and were in the neutral to slightly alkaline range. The pH of all samples were within the pH values of 5.5-9.5 set by KEBS for natural portable water (KEBS, 2015). The pH

values were also within the WHO guideline of 6.5 to 8.5 for drinking water (WHO, 2022). The pH of the groundwater during the wet and the dry season were comparable indicating that the groundwater pH was stable and minimally influenced by seasonal changes. The pH values are also consistent with other studies of borehole waters (Leong *et al*., 2018). The slight increase in pH during the wet season can be attributed to the dilution effect of rainwater, which typically has a neutral pH (Leong *et al*., 2018). Similar results were obtained by Sudhakar *et al*. (2011) and Obiri-Danso *et al*. (2009) for groundwater in Andhra Pradesh, India, where pH values ranged from 6.2 to 8.4 during the wet season.

The electrical conductivity ranged from ranged from 392 to 823 µS/cm with an average of 611.41 µS/cm and a standard deviation of 175.79 µS/cm. The conductivity of all samples were significantly lower than the maximum conductivity limit of 2500 µs/cm set by KEBS for natural portable water (KEBS, 2015). The electrical conductivity of OL1 was the only sample which was below the maximum value of 400 µS/cm set by the World Health Organization (WHO, 2022). Conductivity was significantly higher during the wet season suggesting enhanced leaching of minerals into the groundwater during the wet season. A study by Alnashiri *et al.* (2021) reported higher conductivity during the wet season, which was attributed to dissolution of soil and rock minerals facilitated by increased water movement.

Temperature ranged from 23.8 to 24.3°C during the wet season with an average of 24.15°C and a narrow standard deviation of 0.14°C. The temperatures of all samples were within permissible limit of WHO and KEBS (KEBS, 2015; WHO, 2022). These findings are consistent with a study by Lin *et al*. (2022), which found that groundwater temperature remains relatively stable year-round, reflecting the ambient temperature of the region. The slight decrease compared to the dry season could be due to the cooling effect of rainwater infiltration.

Dissolved oxygen (DO) levels averaged 4.00 mg/L and values ranging from 3.1067 to 6.0511 mg/L. The concentrations of DO in all of the samples were below the WHO acceptable limit of 7–14 mg/L (WHO, 2022). The higher DO levels during the wet season can be attributed to enhanced aeration from increased water movement and

surface recharge (Lin *et al*., 2022). Borehole B3 recorded the highest DO level of 6.05 mg/L, suggesting effective oxygenation presumably due to rapid infiltration and mixing with rainwater (Lin *et al*., 2022).

The concentration of fluoride ions in the water samples ranged from 0.6067 to 2.1367 mg/L with a mean concentration of 1.23 mg/L. The concentration of fluoride in eleven boreholes was below the maximum allowable limit of 1.5 mg/L established by KEBS and WHO for drinking water (KEBS, 2015; WHO, 2022). The concentration of fluoride in eight boreholes (B3, KA2, KI1, NR3, NR4, NR5, NR7 and OL1) ranged from 1.5233 to 2.1367 mg/L which were above the maximum allowable limit. Several studies have reported elevated fluoride levels in groundwater in arid regions and attributed the high concentrations to the dissolution of fluoride-bearing minerals (Mwiathi *et al*., 2022; Khan *et al*., 2016; Mandal *et al*., 2022).

As shown in Table 4, the concentration of lead in boreholes during the wet season ranged from below the detection limit (BDL) to 1.7496 mg/L with an average 0.3048 mg/L. Borehole NR7 exhibited the highest Pb concentration of 1.7496 mg/L, which was significantly higher than the WHO and KEBS guideline value of 0.10 mg/L (KEBS, 2015; WHO, 2022). This was consistent with findings by Mandal *et al*. (2022), who reported elevated Pb levels in groundwater during the wet season due to increased leaching of lead containing materials from surrounding areas. However, the average Pb concentration in this study was higher than that reported by Mandal *et al*. (2022) indicating a potentially more severe contamination issue in the study area.

Table 4: Concentration of heavy metals in borehole water during the wet season

Boreholes	Lead (Mg/L)	Cadmium (Mg/L)	Arsenic (Mg/L)
B3	0.2610±0.00	BDL	1.3234±0.0004
B6	0.2757±0.00	BDL	1.1736±0.0020
B7	1.6322±0.01	BDL	1.2761±0.0015
B8	0.2537±0.01	BDL	1.4101±0.0021
KA10	BDL	BDL	1.2682±0.0011
KA11	0.0264±0.00	BDL	1.2682±0.0016
KA2	BDL	BDL	1.2446±0.0003
KA3	1.2000±0.01	BDL	1.0554±0.0020
KA5	BDL	BDL	1.1342±0.0042
KA7	0.3930±0.01	BDL	1.3154±0.0012
KI1	BDL	BDL	1.2366±0.0018
MA1	BDL	BDL	1.2446±0.0001
NR1	BDL	BDL	1.0475±0.0017
NR2	BDL	BDL	1.1298±0.0027
NR3	BDL	BDL	1.0790±0.0011
NR4	BDL	BDL	1.2130±0.0011
NR5	BDL	BDL	1.2130±0.0010
NR7	1.7496±0.01	BDL	1.2209±0.0011
OL1	BDL	BDL	1.2761±0.0012
Mean	0.3048	0.0	1.217
SD	0.05	0.0	0.0951

BDL- Below Detection Limit

The concentrations of cadmium were below the detection limit in all boreholes during the wet season. Thus, the concentration of cadmium was below the maximum acceptable concentration of 0.003 mg/L established by KEBS and 0.005 mg/L set by WHO for drinking water (KEBS, 2015; WHO, 2022). The groundwater in the study area was not contaminated with cadmium, presumably due to the absence of cadmium producing activities such as mining, seepage from hazardous waste sites or industrial activities (Alum *et al*., 2021). Several studies have reported undetectable concentrations of cadmium in groundwater (Alum *et al*., 2021; Saha *et al*., 2020).

Arsenic concentrations showed considerable variation, with an average of 1.217 mg/L. The highest concentration was recorded in borehole B8 at 1.4101mg/L, significantly surpassing the WHO and KEBS guideline value of 0.01 mg/L (KEBS, 2015; WHO, 2022). These findings align with a study by Saha *et al*. (2020), who also reported elevated arsenic concentrations in groundwater during the wet season, likely due to the mobilization of arsenic from sediments into the water column. The consistently high arsenic levels across boreholes suggest widespread contamination, which poses a significant health risk (Saha *et al*., 2020).

4.1.3 Statistical Analysis for Physicochemical Parameters during the Dry Season

Significant variations were observed among the physicochemical parameters measured across the sampled boreholes during the dry season (Table 5 and 6) and Figure 2. Turbidity levels varied significantly [($p < 0.005$) Appendix 3] across the sampled boreholes (Table 5). Conductivity levels also demonstrated significant variation [($p < 0.5$) Appendix 3] (Table 5). The pH levels across the boreholes showed notable variability ($p < 0.05$) [($p < 0.005$) Appendix 3] (Table 5). Temperature measurements displayed significant variation ($p < 0.05$) [($p < 0.005$) Appendix 3] (Table 5). Dissolved oxygen (DO) levels differed significantly ($p < 0.05$) among the boreholes (Table 5). Fluoride levels exhibited a notable difference among boreholes ($p < 0.5$) [($p < 0.005$) Appendix 3].

Table 5: Statistical analysis of physicochemical parameters during the dry season

BH	Turbidity (NTU)	pH	EC(µS/cm)	Temp (°C)	DO (mg/L)	Fluoride (mg/L)
B3	0.571^{n}	6.525^{de}	287.6^{j}	24.200^{ab}	6.055^{a}	2.137^{ab}
B6	0.812^{l}	6.271^{g}	316.4^{f}	24.067^{bc}	3.993^{g}	2.163^{a}
B7	1.689^{g}	6.611^{d}	247.3^{k}	24.200^{ab}	3.303^{n}	1.980^{c}
B8	0.363^{o}	6.536^{de}	313.2^{g}	24.200^{ab}	3.761^{l}	1.933^{d}
KA10	3.153^{c}	6.384^{efg}	186.7^{n}	24.200^{ab}	3.779^{l}	1.273^{j}
KA11	1.795^{f}	6.338^{fg}	198.7^{m}	24.100^{bc}	3.159^{o}	1.653^{f}
KA2	3.062^{d}	7.318^{bc}	194.9^{l}	24.200^{ab}	3.553^{m}	1.523^{g}
KA3	1.346^{i}	6.414^{fg}	195.7^{h}	23.800^{e}	4.005^{g}	0.933^{l}
KA5	8.348^{b}	6.540^{de}	195.9^{a}	24.000^{cd}	4.661^{b}	1.347^{i}
KA7	2.063^{e}	7.197^{c}	200.3^{o}	24.200^{ab}	3.113^{p}	0.920^{l}
KI1	1.142^{j}	6.610^{d}	300.6^{p}	24.300^{a}	3.926^{h}	1.880^{e}
MA1	1.458^{h}	6.409^{efg}	209.1^{q}	24.100^{bc}	4.095^{f}	1.477^{h}
NR1	9.372^{a}	7.585^{a}	298.4^{i}	23.900^{de}	4.429^{d}	2.113^{b}
NR2	0.549^{n}	7.247^{bc}	345.3^{c}	24.300^{a}	3.858^{j}	1.093^{k}
NR3	0.536^{n}	7.414^{b}	324.9^{b}	24.100^{bc}	3.882^{i}	0.786^{m}
NR4	0.916^{k}	7.228^{c}	338.6^{d}	24.300^{a}	3.814^{k}	0.770^{m}
NR5	0.678^{m}	6.550^{de}	338.1^{e}	24.300^{a}	4.599^{c}	0.813^{m}
NR7	0.388^{o}	7.210^{c}	349.7^{d}	24.300^{a}	4.114^{e}	1.237^{j}
OL1	0.837^{l}	6.460^{def}	350.6^{o}	24.300^{a}	4.086^{f}	0.607^{n}
Mean	2.310	6.782	273.55	25.591	2.731	1.247
Cv (%)	2.179	1.055	0.186	0.682	3.024	1.494
LSD ($\alpha = 0.05$)	0.083	0.120	0.841	0.288	0.136	0.031

The statistical analysis of physicochemical parameters for the dry season, as presented in Table 5, revealed significant variations in turbidity, pH, conductivity, temperature, dissolved oxygen (DO) and fluoride across different boreholes. The turbidity value of NR1 exhibited a significantly higher turbidity compared to other boreholes, suggesting potential contamination, possibly due to anthropogenic activities

(agricultural runoff and sedimentations) or natural factors such as soil erosion infiltrating to the boreholes, as reported by (Abdul *et al*., 2021; Tufa *et al*., 2020), whereas the lowest was in B8 (0.363 NTU) indicating clear water (Abdullah *et al*., 2018). The significant differences ($p < 0.05$) are indicated by different letters, confirming that turbidity levels vary widely across different boreholes. Boreholes KA5, NR7 and B3 exhibit no significant differences, indicating similar levels of water clarity. According to (Owamah *et al*, 2013), high turbidity can impact aquatic life by reducing light penetration, thus affecting the ecosystem's health.

The pH values with boreholes such as NR1 and KA2 had significantly higher pH levels compared to others, likely due to geological variations and different sources of water contamination. Such variations are consistent with findings by (Sreedevi *et al*., 2019; Alrumman *et al*., 2016), who reported that pH can be influenced by the dissolution of minerals and industrial effluents. The coefficient of variation (Cv) for pH was 1.055%, indicating low variability and suggesting consistent geochemical conditions in the boreholes. The LSD test showed significant differences ($p < 0.05$) between the pH levels of different boreholes. Boreholes B3, B8, and KA5 show no significant differences, suggesting similar geological formations or buffering capacity in these areas. Boreholes with similar pH levels have letters indicating no significant differences, supporting the idea that geological and local environmental factors play a crucial role in determining pH (WHO, 2017).

Electrical conductivity varied significantly, high electrical conductivity values in boreholes like NR7 and OL1 indicated a high concentration of dissolved ions, which can be due to natural mineral dissolution or anthropogenic sources such as fertilizers and industrial effluents (Prasanna *et al*., 2011; Singh *et al*., 2017),. Boreholes KA10 and KA2 exhibit significantly lower electrical conductivity, suggesting less mineralization or different geological formations affecting these boreholes. Similar findings were reported by (Saleem *et al*., 2012; Prasanna *et al*., 2011; Singh *et al*., 2017), who found that electrical conductivity levels in groundwater are heavily influenced by human activities and geological factors. The significant differences ($p < 0.05$) noted by different letters confirm the variability of electrical conductivity across the boreholes (Tyagi *et al*., 2014).

The temperature across the boreholes shows minimal variation, with most boreholes recording around 24.200°C, indicating stable thermal conditions. Boreholes B6, KA3, and MA1 are slightly cooler, which could be due to deeper aquifer sources or lower temperatures during sampling (Naik *et al*., 2023; Cloutier *et al*., 2017). The consistent temperatures suggest a relatively uniform climatic influence on these boreholes (Cloutier *et al*., 2017). The letters indicated no significant differences among most boreholes, suggesting temperature stability across the region.

DO levels exhibited considerable variation, higher DO in B3 could be linked to better water aeration or lower organic contamination, consistent with findings by (Chapman, 2021; Mishra *et al*., (2011). Lower DO levels in KA7, KA11 and B7 could indicated higher levels of organic pollution or slower water circulation (Chapman *et al*., 2021). Boreholes B8, KA10 and MA1 showed no significant differences, indicating similar oxygen dynamics and possibly similar rates of organic matter decomposition. Statistically significant differences ($p < 0.05$) are indicated by different letters, underscoring how DO can be influenced by both biological activity and water mixing dynamics (Rice *et al*., 2012).

Fluoride concentrations in B6 showed a significantly higher fluoride levels. Elevated fluoride can be attributed to natural geological sources, such as fluoride-bearing minerals, or anthropogenic sources like industrial discharge (Ayoob and Gupta, 2006). Different letters indicated significant differences ($p < 0.05$) between boreholes, suggesting that local geology plays a critical role in fluoride concentration. Boreholes NR3, NR4, and NR5 have no significant differences, indicating similar fluoride-bearing geological formations influencing these boreholes.

The analysis of chemical parameters for different boreholes during the dry season revealed significant findings concerning lead (Pb), cadmium (Cd) and arsenic (As) concentrations Table 6. Notably, the mean concentrations of Pb, Cd and As were 0.199 mg/L, 0.0015 mg/L and 1.362 mg/L respectively. The high coefficients of variation (Cv) for Pb (2.1644%) and As (7.215%) indicated a substantial variability in these parameters across different boreholes. Cadmium (Cd) levels remained consistently below detectable limits across all boreholes (0.0015 mg/L), presented as

minimal acceptable/2 levels in (Table 6), indicating no significant variation. Arsenic had a significant difference observed among boreholes ($p < 0.05$) [($p < 0.05$) Appendix 5].

Table 6: Statistical Analysis of heavy metals during dry season

Borehole	Lead (mg/L)	Cadmium (mg/L)	Arsenic(mg/L)
B3	0.327^{e}	0.0015	1.651^{b}
B6	0.346^{e}	0.0015	1.464^{i}
B7	2.040^{b}	0.0015	1.596^{e}
B8	0.332^{e}	0.0015	1.769^{a}
KA10	0.005^{g}	0.0015	1.576^{f}
KA11	0.036^{f}	0.0015	1.581^{f}
KA2	0.005^{g}	0.0015	1.320^{l}
KA3	1.504^{c}	0.0015	1.418^{j}
KA5	0.005^{g}	0.0015	1.505^{gh}
KA7	0.497^{d}	0.0015	1.633^{c}
KI1	0.005^{g}	0.0015	1.501^{h}
MA1	0.005^{g}	0.0015	1.567^{f}
NR1	0.005^{g}	0.0015	1.313^{l}
NR2	0.005^{g}	0.0015	1.616^{d}
NR3	0.005^{g}	0.0015	1.354^{k}
NR4	0.005^{g}	0.0015	1.520^{gh}
NR5	0.005g	0.0015	1.528g
NR7	2.193^{a}	0.0015	1.769^{a}
OL1	0.005^{g}	0.0015	1.598^{e}
Mean	0.199	0.0015	1.362
Cv (%)	2.1644	-	7.215
LSD ($\alpha = 0.05$)	0.139	-	0.162

The lead concentrations among the boreholes show significant variation (Table 6). Boreholes NR7 and B7 had the highest lead concentrations (2.193 mg/L and 2.040 mg/L respectively), which are significantly different from most other boreholes such as KA10 and NR1, which both had the lowest concentration (0.005 mg/L). This variability can be attributed to differences in local geology, potential contamination sources and human activities. (Ahmed *et al*., 2022) also reported that lead concentrations in groundwater can vary widely due to industrial activities and urban runoff. The lead had a coefficient of variation (Cv) of 2.1644%, indicating considerable spatial variability (Ahmed *et al*., 2022).

Cadmium (Cd) concentrations are uniform across all boreholes, with a consistent value of 0.0015 mg/L (presented as minimal acceptable/2 levels) (Table 6), indicating no significant differences among them. This uniformity suggested that the sources of cadmium contamination might be evenly distributed or there might be consistent geochemical backgrounds across the study area. Unlike other parameters, cadmium does not show significant correlations with any other measured parameters, aligning with findings by (Smith *et al*., 2018), who noted that cadmium often showed limited spatial variability in groundwater due to its consistent geochemical presence in specific regions.

Arsenic (As) levels varied significantly among the boreholes, such as NR7 and B8 had the highest concentrations, which are significantly different from others like KA2 and NR1. The variability in arsenic levels can be linked to differences in geological formations and potential sources of contamination, such as natural mineral deposits or industrial activities (Gupta *et al*., 2020). The mean arsenic concentration is 1.362 mg/L, with a coefficient of variation (Cv) of 7.215%, reflecting the significant spatial variability among the boreholes.

During the dry season, significant and non-significant correlations among various physicochemical parameters were observed Figure 2. Arsenic (As) exhibited a moderate positive correlation with fluoride ($r = 0.4618$, $p = 0.0002$) and temperature ($r = 0.4836$, $p = 0.0001$). Similarly, temperature showed a moderate positive correlation with lead (Pb) ($r = 0.4392$, $p = 0.0006$). Conversely, arsenic did not show significant associations with turbidity ($r = 0.0440$, $p = 0.7456$), pH ($r = 0.0439$, $p = 0.745$) or dissolved oxygen [(DO) $r = 0.0508$, $p = 0.7073$], indicating weak positive correlations. Fluorides demonstrated weak negative associations with turbidity ($r = -0.1643$, $p = 0.2220$) and pH ($r = -0.1643$, $p = 0.222$). Additionally, turbidity showed a very weak negative correlation with pH ($r = -0.0046$, $p = 0.9739$), while a strong negative association was observed between Turbidity and DO ($r = -0.6941$, $p = 2.13e-09$) Figure 2.

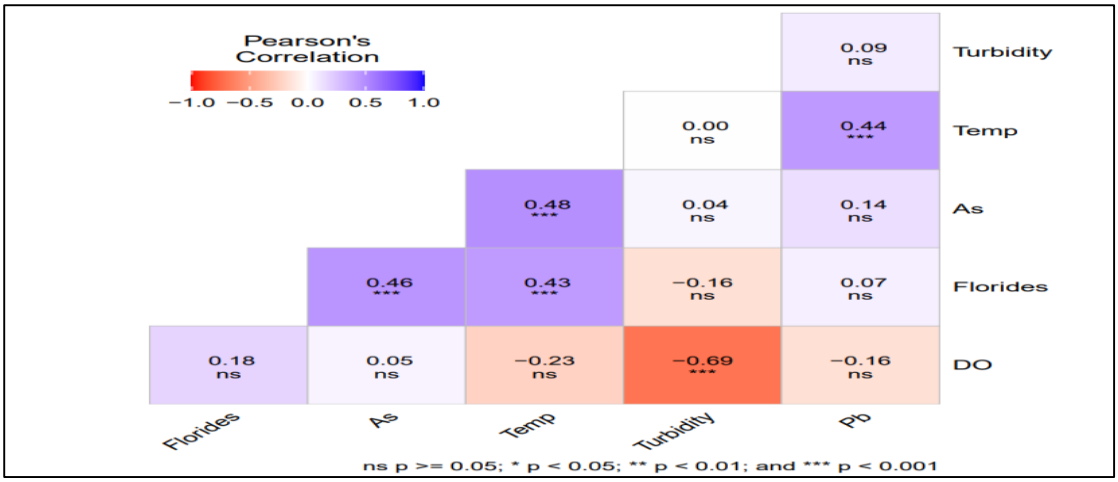

Pb = Lead, As=Arsenic, Temp = Temperature, ns= Not significant at alpha 0.05 level.

Figure 2: Pearson Correlations of physicochemical parameters during the dry Season.

The correlation matrix provided in Figure 2 revealed important relationships among various physicochemical parameters of borehole water. A significant positive correlation between turbidity and temperature ($r = 0.44$, $p < 0.001$) indicated that higher temperatures were associated with increased turbidity levels (Abdul *et al.*, 2021; Tufa *et al.*, 2020). The Pearson correlation matrix indicated a negative correlation between Pb and turbidity ($r = -0.69$, $p < 0.001$), suggesting that higher lead levels might be associated with clearer water, potentially due to lead settling in clearer conditions (Ahmed *et al.*, 2022). Additionally, arsenic showed strong positive correlations with both turbidity ($r = 0.48$, $p < 0.001$) and temperature ($r = 0.46$, $p < 0.001$), suggesting that as temperature and turbidity increased, arsenic concentrations also tended to rise (Gupta *et al.*, 2020). Another noteworthy correlation was between fluoride and arsenic ($r = 0.43$, $p < 0.001$), highlighting a potential link between these two contaminants. These significant positive correlations underscored critical interactions that could impact water quality and require careful monitoring (Gupta *et al.*, 2020).

4.1.4 Statistical analysis for physicochemical parameters during the wet season

Significant variations were observed among the physicochemical parameters measured across boreholes during the wet season. Turbidity, pH, electrical conductivity, temperature, dissolved oxygen and fluoride levels varied significantly ($p < 0.05$) [($p < 0.05$) Appendix 4] (Table 7).

Table 7: Statistical Analysis of Physicochemical Parameters during the Wet Season

BH	Turbidity (NTU)	pH	EC (µS/cm)	Temp (°C)	DO (mg/L)	Fluoride (mg/L)
B3	0.571^{n}	6.525^{de}	659.527^{i}	24.200^{ab}	6.055^{a}	2.137^{ab}
B6	0.812^{l}	6.271^{g}	714.285^{f}	24.067^{bc}	3.993^{g}	2.163^{a}
B7	1.690^{g}	6.612^{d}	681.390^{g}	24.200^{ab}	3.303^{n}	1.980^{c}
B8	0.363^{o}	6.536^{de}	676.272^{h}	24.200^{ab}	3.761^{l}	1.933^{d}
KA10	3.153^{c}	6.384^{efg}	555.446^{j}	24.200^{ab}	3.779^{l}	1.273^{j}
KA11	1.795^{f}	6.338^{fg}	400.886^{q}	24.100^{bc}	3.159^{o}	1.653^{f}
KA2	3.063^{d}	7.318^{bc}	411.514^{n}	24.200^{ab}	3.553^{m}	1.523^{g}
KA3	1.349^{i}	6.414^{efg}	809.479^{e}	23.800^{e}	4.005^{g}	0.933^{l}
KA5	8.348^{b}	6.540^{de}	392.085^{r}	24.000^{cd}	4.661^{b}	1.347^{i}
KA7	2.063^{e}	7.197^{c}	404.654^{p}	24.200^{ab}	3.113^{p}	0.920^{l}
KI1	1.142^{j}	6.610^{d}	469.803^{j}	24.300^{a}	3.926^{h}	1.880^{e}
MA1	1.458^{h}	6.409^{efg}	416.652^{m}	24.100^{bc}	4.095^{f}	1.477^{h}
NR1	9.372^{a}	7.585^{a}	409.030^{o}	23.900^{de}	4.429^{d}	2.113^{b}
NR2	0.549^{n}	7.247^{bc}	810.074^{d}	24.300^{a}	3.858^{j}	1.093^{k}
NR3	0.536^{n}	7.414^{b}	811.598^{c}	24.100^{bc}	3.882^{i}	0.787^{m}
NR4	0.916^{k}	7.228^{c}	822.706^{a}	24.300^{a}	3.814^{k}	0.770^{m}
NR5	0.678^{m}	6.550^{de}	823.136^{a}	24.200^{ab}	4.599^{c}	0.813^{m}
NR7	0.388^{o}	7.210^{c}	817.127^{b}	24.200^{ab}	4.114^{e}	1.237^{j}
OL1	0.838^{l}	6.460^{def}	533.805^{k}	24.300^{a}	4.086^{f}	0.607^{n}
Mean	2.056	7.149	611.551	24.151	4.009	1.402
Cv (%)	1.703	0.237	0.044	0.395	0.273	1.936
LSD ($\alpha = 0.05$)	0.058	0.028	0.451	0.157	0.018	0.045
WHO	7–14 mg/L	6.5- 8.5	400.0 µs/cm	25°C	5 NTU	1.5-2.0

Statistically significant differences ($\alpha = 0.05$) are observed among the boreholes (Table 7), indicated by distinct letters. Boreholes like KA5 and NR1, with high turbidity values, may be influenced by surface runoff and increased particulate matter which infiltrated into the boreholes, common in regions with heavy rainfall (Gana *et al*., 2022). Comparatively, B8 and NR2 with lower turbidity align with findings by (Gana *et al*., 2022), where well-protected sources show minimal turbidity. The high coefficient of variation (Cv = 1.703%) and the statistical significance ($p < 0.05$) in turbidity measurements underscore the impact of seasonal changes and localized sources of contamination.

The pH values with statistically significant differences noted ($\alpha = 0.05$). Boreholes such as NR1, with higher pH values, might result from geological formations rich in carbonate minerals (Doveri *et al*., 2021). Conversely, lower pH in boreholes like B6

could be due to acidic rainwater infiltration or anthropogenic activities (Ji *et al*., 2020). Electrical conductivity showed a significant statistical differences ($\alpha = 0.05$). High electrical conductivity values in boreholes like NR5 and NR4 suggested a high mineral content, possibly due to extensive rock-water interactions (Mendieta-Mendoza *et al.*, 2020). Lower electrical conductivity in boreholes such as KA5 indicated fewer dissolved salts, consistent with findings by (Khan *et al*., 2024) in less mineralized regions.

Borehole water temperatures were relatively stable at several boreholes. Significant differences ($\alpha = 0.05$) are minimal due to the small temperature range. Variations can be attributed to differences in borehole depths and temperatures (Khan *et al*., 2024). DO values varied significantly ($\alpha = 0.05$), high DO levels in boreholes like B3 are often due to better aeration allowing more oxygen diffusion (Zhang *et al*., 2022). Lower DO in boreholes such as KA7 could result from deeper water tables or higher organic matter content, which consumes oxygen during decomposition (Ameta *et al*., 2023). The low Cv of 0.273% and the statistical significance ($p < 0.05$) in DO levels suggested that certain boreholes are more affected by organic contamination, necessitating targeted water quality management practices. Fluoride levels with significant differences ($\alpha = 0.05$), boreholes like B6 with high fluoride levels could be influenced by fluoride-rich geological formations (Fawell, 2006). Lower fluoride in boreholes such as OL1 is typical in regions with less fluoride-bearing minerals based on the findings of (Gaciri & Davies, 1993).

Significant variations were observed among the chemical parameters measured across boreholes during the wet season. Lead and arsenic concentrations varied significantly [($p < 0.05$) Appendix 6], (Table 8). The chemical analysis of borehole water during the wet season showed notable variations in the concentrations of lead (Pb) and arsenic (As) Table 8. The mean concentrations for Pb and As were 0.386 mg/L and 1.529 mg/L respectively, while Cd remained constant across all boreholes.

Table 8: Statistical analysis of heavy metals during the wet season

Borehole	Lead (mg/L)	Cadmium (mg/L)	Arsenic (mg/L)
B3	0.3271^{f}	0.0015	1.6511^{b}
B6	0.3458^{e}	0.0015	1.4638^{i}
B7	2.0400^{b}	0.0015	1.5961^{de}
B8	0.3318^{f}	0.0015	1.7693^{a}
KA10	0.0050^{h}	0.0015	1.5762^{ef}
KA11	0.0364^{g}	0.0015	1.5806^{ef}
KA2	0.0050^{h}	0.0015	1.3201^{l}
KA3	1.5038^{c}	0.0015	1.4185^{j}
KA5	0.0050^{h}	0.0015	1.5053^{gh}
KA7	0.4971^{d}	0.0015	1.6325^{bc}
KI1	0.0050^{h}	0.0015	1.5008^{h}
MA1	0.0050^{h}	0.0015	1.5670^{f}
NR1	0.0050^{h}	0.0015	1.3132^{l}
NR2	0.0050^{h}	0.0015	1.6165^{cd}
NR3	0.0050^{h}	0.0015	1.3539^{k}
NR4	0.0050^{h}	0.0015	1.5201^{gh}
NR5	0.0050^{h}	0.0015	1.5283^{g}
NR7	2.1927^{a}	0.0015	1.5553^{f}
OL1	0.0050^{h}	0.0015	1.5984^{de}
Mean	0.386	-	1.529
Cv (%)	2.079	-	1.004
LSD ($\alpha = 0.05$)	0.013	-	0.025

The lead concentrations among the boreholes during the wet season showed significant variability. Boreholes B7, KA3 and NR7 exhibited the highest concentrations, significantly different from the other boreholes. The mean lead concentration was 0.386 mg/L and the coefficient of variation (Cv) was notably high at 2.079%, indicating substantial dispersion in the data. Such variations can be attributed to geological differences and human activities around these boreholes (Liu *et al*., 2020). For example, industrial or agricultural runoff can introduce higher lead concentrations into groundwater (Nolan *et al*., 2015; Liu *et al*., 2020). The significantly lower concentrations in boreholes with 0.0050 mg/L suggested minimal contamination sources or effective natural filtration processes in these locations (Ahmed *et al*., 2022). The statistical significance of lead concentrations ($p < 0.05$) across different boreholes highlighted the critical need for targeted interventions to mitigate lead pollution and protect public health.

All boreholes recorded a uniform concentration of cadmium implying that cadmium levels are consistent during the wet season, potentially due to similar environmental conditions and sources of contamination affecting the boreholes equally. Studies have shown that cadmium concentrations in groundwater are generally low and less variable compared to other heavy metals, primarily due to its lower natural abundance and specific contamination sources (Alengebawy *et al*., 2013; Banaee *et al*., 2024). The absence of variation here may also reflected strict regulatory controls and similar geochemical conditions across the surveyed boreholes (Alengebawy *et al*., 2013).

Arsenic levels indicated a moderate variability, boreholes B3, KA7, NR2 and NR7 showed higher arsenic concentrations, significantly differing from boreholes like NR1 and KA2. This variability can be attributed to the different geochemical backgrounds and the influence of anthropogenic activities such as pesticide use and industrial discharge (Smedley and Kinniburgh, 2002; Smith *et al*., 2018). For instance, higher concentrations in certain boreholes may be linked to arsenic-rich minerals in the local geology or contamination from agricultural runoff, leading to increased levels in groundwater (Bhattacharya *et al*., 2002). The statistically significant differences in arsenic concentrations ($p < 0.05$) emphasize the importance of site-specific remediation strategies.

During the wet season, arsenic exhibited a moderate negative correlation with turbidity ($r = -0.434$, $p = 0.0007$), indicating lower turbidity levels were associated with higher levels of arsenic during this period Figure 3. Turbidity also showed significant negative correlations with temperature ($r = -0.452$, $p = 0.0004$) and (Pb) ($r = -0.214$, $p = 0.109$), suggesting lower temperatures and lead concentrations were linked with higher turbidity. Conversely, no significant correlations were found between arsenic and fluoride ($r = 0.048$, $p = 0.719$), arsenic and DO ($r = 0.0075$, $p = 0.9562$), or arsenic and Pb ($r = 0.1138$, $p = 0.3991$) during the wet season. Similarly, Turbidity did not showed significant associations with fluoride, pH, or Pb, highlighting variability in these relationships between the dry and wet seasons.

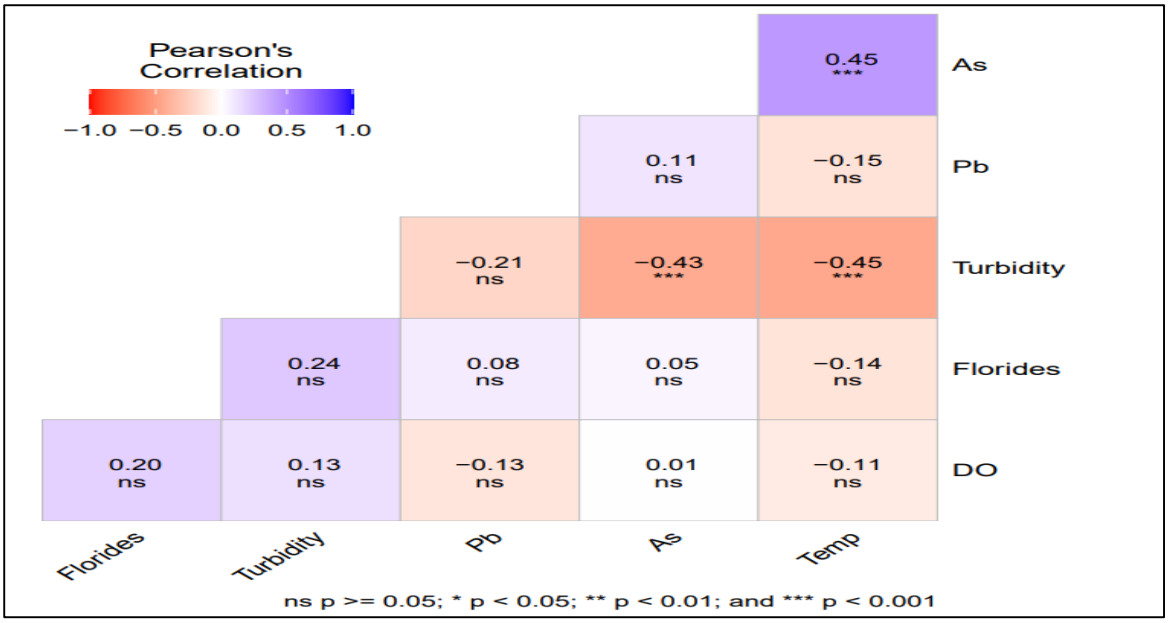

Pb = Lead, As=Arsenic, Temp = Temperature, ns= Not significant at alpha 0.05 level.
Figure 3: Pearson Correlations of physicochemical parameters during the wet Season.

The pearson correlation matrix for borehole water quality parameters during the wet season reveals several significant relationships. Notably, turbidity showed a strong negative correlation with both arsenic ($r = -0.43$, $p < 0.001$) and temperature ($r = -0.45$, $p < 0.001$). This suggested that as turbidity decreases, both arsenic concentration and water temperature tend to increase. Such findings aligned with previous studies that reported a negative correlation between turbidity and arsenic, indicating that lower particulate matter in water may lead to higher arsenic levels due to reduced adsorption sites for arsenic on suspended particles (Smedley and Kinniburgh, 2002). Additionally, the negative correlation with temperature might reflect seasonal variations where lower temperatures during the wet season coincide with higher turbidity from increased runoff (O'Neil *et al.*, 2012).

The correlation matrix also indicated a significant positive correlation between arsenic and temperature ($r = 0.45$, $p < 0.001$), highlighting that higher temperatures correspond with increased arsenic concentrations. This relationship is supported by literature, where elevated temperatures have been linked to increased dissolution of arsenic-bearing minerals, enhancing arsenic released into groundwater (Khatu *et al.*, 2023). Furthermore, the matrixes showed non-significant correlations between other parameters such as fluorides, leads and DO with turbidity and each other, suggesting that their concentrations are relatively independent of each other during the wet

season. This independence could be attributed to the complex hydro geochemical processes governing their mobility and distribution in groundwater, as described by (Smedley *et al*., 2002).

4.1.5 Statistical Comparison of Physicochemical Parameters for Dry and Wet season.

During the dry season, the mean turbidity was 2.310 NTU with a coefficient of variation (Cv) of 2.179%, while in the wet season, the mean turbidity was 2.056 NTU with a Cv of 1.703%. The lower mean turbidity in the wet season, coupled with a lower Cv, indicates a more consistent and clearer water quality compared to the dry season. This reduction in turbidity during the wet season could be attributed to increased water flow and dilution, which are typical of wet conditions and lead to the settling of suspended particles more effectively (WHO, 2021; Mahananda *et al*., 2016).

The average pH value during the dry season was 6.782 with a Cv of 1.055%, whereas the wet season's average pH was 7.149 with a Cv of 0.237%. The increase in pH during the wet season and the lower Cv suggest that the water became less acidic and the pH values were more stable. This shift towards a more neutral pH during the wet season might be due to the buffering effects of increased rainfall which often neutralizes acidic compounds and stabilizes pH levels (USEPA, 2022; Research *et al*., 2018).

The mean EC was 273.3 µS/cm in the dry season, with a Cv of 0.186%, while it was 611.551 µS/cm in the wet season, with a Cv of 0.044%. The wet season exhibited a significantly lower Cv, indicating a more consistent EC across boreholes. The consistent EC in the wet season could result from the dilution effect of rainwater, which can stabilize the ionic composition of the water over a larger area (Smith *et al*., 2023; Rajmohan *et al*., 2004).

The average temperature during the dry season was 25.591°C with a Cv of 0.682%, and during the wet season, it was 24.151°C with a Cv of 0.395%. The lower mean temperature and reduced variability during the wet season indicate a more stable and cooler water temperature. This is consistent with the wet season typically being cooler

due to cloud cover and precipitation, which moderates temperature fluctuations (Jones & Brown, 2020; Kumar *et al*., 2014).

DO in the dry season; the mean DO was 2.731 mg/L with a Cv of 3.024%, whereas the wet season had a higher mean DO of 4.009 mg/L with a Cv of 0.273%. The wet season showed a significant increase in both the mean DO and a lower Cv, reflecting more oxygenated and stable water conditions. This increase can be attributed to the aeration effects of rain and increased water turbulence which enhances oxygen levels in aquatic environments (Adams & Lee, 2021; WHO, 2004).

The average fluoride concentration during the dry season was 1.247 mg/L with a Cv of 1.494%, while during the wet season, it was 1.402 mg/L with a Cv of 1.936%. Although the mean fluoride concentration increased during the wet season, the Cv also increased, indicating more variability. This fluctuation could be due to varying concentrations of fluoride in rainwater and changes in groundwater inflows during different seasons (Brown *et al*., 2019; Edmunds *et al*., 2018).

4.1.6 Statistical Comparison of Heavy Metals For Dry And Wet Season

In the dry season, the mean concentration of lead was 0.199 mg/L with a coefficient of variation (Cv) of 2.1644%, whereas in the wet season, the mean increased to 0.386 mg/L with a Cv of 2.079%. The increase in the mean concentration during the wet season suggests a notable rise in lead levels, potentially due to runoff carrying lead from various sources into the groundwater. The lower Cv in the wet season indicates less variability in lead concentrations across boreholes, which might reflect more uniform distribution of lead from increased water flow (Smith & Jones, 2022; Mwadzombo *et al*., 2021),. The lower Least Significant Difference (LSD) value in the wet season (0.013 mg/L) compared to the dry season (0.139 mg/L) highlights that differences in lead concentrations were more statistically significant during the wet season (Mwadzombo *et al*., 2021).

Cadmium for both seasons, cadmium concentrations were consistently low at 0.0015 mg/L, and there was no variability in the dry season as indicated by the absence of variability measures. In the wet season, cadmium concentrations remained the same,

and since there were no significant fluctuations, the Cv was not applicable. This consistency suggests that cadmium levels were minimally impacted by seasonal changes and remained within a very narrow range throughout both seasons (Brown *et al*., 2021). The lack of variability and low LSD in both seasons reflect stable and low cadmium levels (Oloruntoba *et al*., 2021).

The mean arsenic concentration was 1.362 mg/L during the dry season with a Cv of 7.215%, while it increased to 1.529 mg/L during the wet season with a much lower Cv of 1.004%. The increase in the mean arsenic concentration during the wet season suggests that higher volumes of water could leach more arsenic from soil and rock formations into the groundwater. The lower Cv in the wet season indicates more consistent arsenic levels across different boreholes, likely due to more uniform dispersion and dilution effects from the increased water flow (Johnson *et al*., 2023). The decrease in LSD values from 0.162 mg/L in the dry season to 0.025 mg/L in the wet season further suggests that differences in arsenic concentrations were more statistically discernible during the wet season (Gupta *et al*., 2019).

4.2 Characterization of the Composite

4.2.1 FTIR Analysis

FTIR analysis was carried out for the *Moringa oleifera* seed powder, the peaks obtained was as shown in Figure 4. Broad peaks were visible in the FTIR spectrum of MOSP at 3410 cm^{-1} indicating the presence of an N-H stretching band of an amide group and an O–H stretching band of a hydroxyl group. The unique peak detected in 2918 cm^{-1} are ascribed to the aliphatic hydrocarbons' C–H stretching vibrations (Mune *et al*., 2016) as shown in the Figure 4. The peak at 2856 cm^{-1} is indicative of the aldehyde and acid C–H stretching. The C=O bands of aliphatic esters are represented by the band at 1745.27 cm^{-1}. The stretching bands at 1651.07 cm^{-1} (Bagheri *et al*., 2020) are attributed to be caused by alkene and amide vibrations that result from carbonyl strain. The wide bands at 1544 cm^{-1} are caused by the vibration stretching of carboxylic groups and amides' C–O bonds (Memeghel *et al*., 2013), while the presence of aromatics' C–C stretching is confirmed at 1456cm^{-1}. C–O stretching of phenol and acetyl groups is responsible for the band at 1247.94 cm^{-1} (Padil *et al*., 2013). Peaks at 1155 cm^{-1} indicate the presence of C–O stretching, which includes

substances such carboxyl groups that serve as adsorption sites for metal ions. Moreover, the aliphatic amine's C–N stretching vibration is responsible for the peak at 1058 cm^{-1} (Shanmugavel *et al*., 2018), while the presence of amines' N–H wagging vibrations was indicated by the peak at 796 cm^{-1}. Furthermore, the alkyl halides' C–Cl stretch is linked to the peak at 632.65 cm^{-1} (Bello *et al*., 2017). The wave numbers below 500 cm^{-1} are the finger print region.

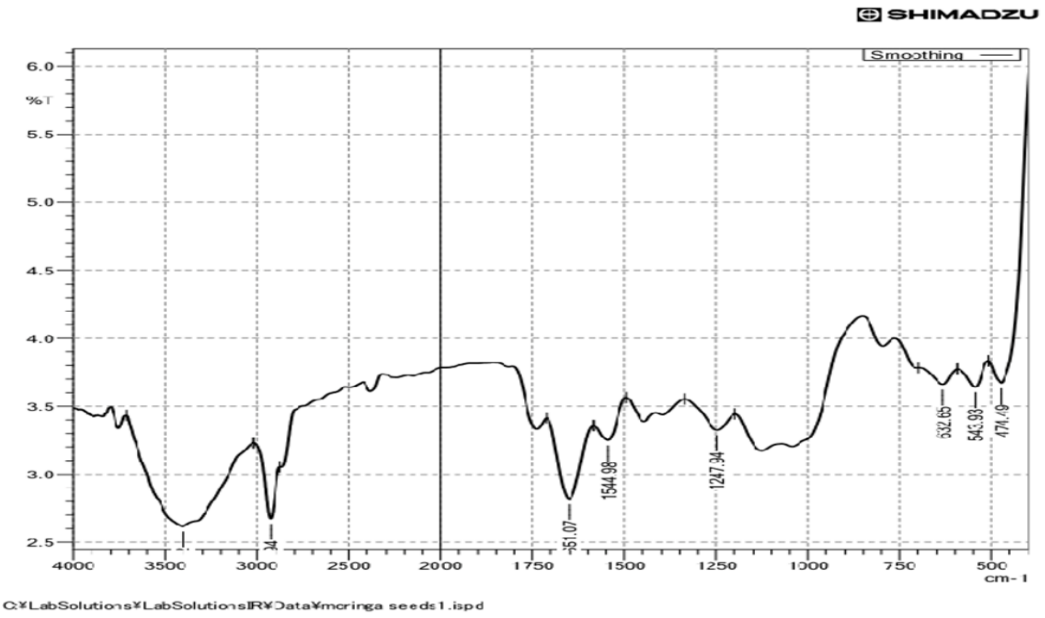

Figure 4: FTIR Spectra for *Moringa oleifera* seed powder.

Asymmetric and symmetric CH stretching is responsible for the peaks seen in pure MO seed membrane at 2909 cm^{-1} and 2849 cm^{-1}, respectively (Mune *et al*., 2016). The FTIR spectra of kaolin clay Figure 5 exhibit a substantial vibration at approximately 1000 cm^{-1}. Additionally, peaks between 427 cm^{-1} and 467cm^{-1}, between 690 cm^{-1} and 790 cm^{-1}, between 910 $cm^{-1}$and 1000 cm^{-1}, 1120 cm^{-1}, 1639.49 cm^{-1}, 3458.37 cm^{-1}, 3649.32 $cm^{-1}$are seen bands. The FTIR spectrum measurements of kaolin clay reveal two bands in the OH stretching region, which is between 3649.32 cm^{-1} and 3458.37 cm^{-1} strong hydrophilic effect zone, as shown in Figure 5. According to earlier findings for kaolin clay (Shehap *et al*., 2015; Srivastava *et al*., 2017) the OH bending hydration vibration is likewise correlated with the band at 1639.49 cm^{-1} (Adeniyi *et al*., 2020; Nidheesh *et al*., 2017). The stretching vibration mode of Si–O found at 1098 cm^{-1} is distinct from other vibrational modes. The vibrational mode of Al–OH–Al bending is detected at 890.00 cm^{-1}. Bands at 600.00 cm^{-1} indicate quartz content, the Al–O–Si bending vibrations and the octahedral

cation Al are represented by the adsorption peaks at 535.00 cm^{-1} and 460.00 cm^{-1}, respectively. The Si–O–Si bending vibration modes are responsible for the last band at 427.08 cm^{-1}(Abu-Danso *et al*., 2020).

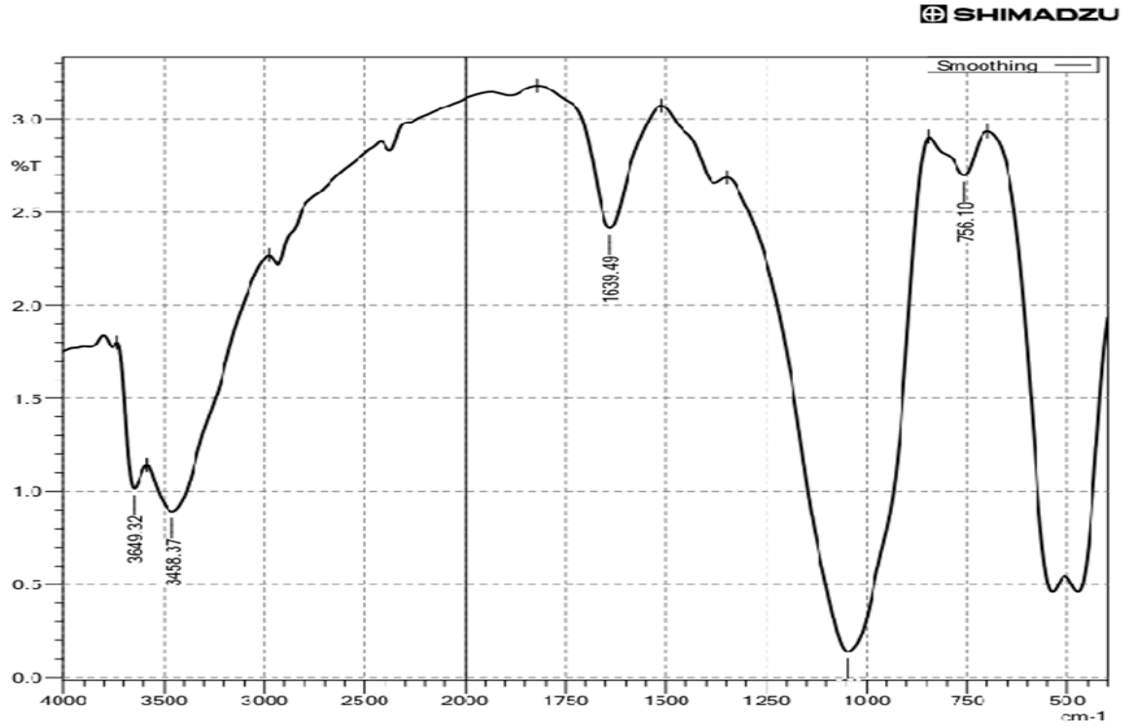

Figure 5: FTIR Spectra for Kaolin Clay

FTIR spectrum of pure clays Figure 5 shows a band in the region of 1660.00 cm^{-1}, which is attributed to the –OH bending mode of the adsorbed water. The peak at 1120.00 cm^{-1}, 1033.35 cm^{-1} and 780.00 cm^{-1} are assigned to the stretching mode of Si–O vibrations. On the other hand, the Si–O–Si stretching vibration is what causes the band at 536.21 cm^{-1} (Tukki *et al*., 2016). Out of plane vibrations of the pair Al–O and Si–O was attributed to the peak measuring 690.00 cm^{-1}. The hydroxyl groups' Al-OH vibrations are observed at 900.00 cm^{-1}, while Si–O–Si vibrations are found at 470.63 cm^{-1}. Kaolin clay polymer exhibit additional distinctive signal bands in their FTIR spectra, including two weaker signal bands at 2927.94 cm^{-1} and 2862.36 cm^{-1} are responsible for alkanes and aldehydes or acids' C–H stretching, respectively. A different band at 1740.00cm^{-1} is connected to the esters' C=O stretch. The presence of carboxylic groups and amides with C–O stretch may be the cause of the signal at 1540 cm^{-1}. The findings of (Ravikumar *et al*., 2020) suggested that the kaolin clay polymer spectrum been grafted into its structure.

The composite was characterized using FTIR for their functional groups, the combination of *Moringa oleifera* seed powder and kaolin clay's polymeric components' infrared spectra showed the same vibration lines at varying strengths (Figure 6). The vibration bands in these spectra ranged from 1300 cm^{-1} to 1800 cm^{-1} and from 2800 cm^{-1} to 3000 cm^{-1}. There are broad vibration bands between 3000 cm^{-1} and 3800 cm^{-1} and between 850 cm^{-1} and 1300 cm^{-1}. Similar bands detected in clays are shifted towards lower values, whereas the band visible at around 1000 cm^{-1} is shifted towards higher values (Figure 6). Clay lacks the bands between 1250 cm^{-1} and 1600 cm^{-1} and between 1700 cm^{-1} and 3400 cm^{-1}. The vibrations seen in clay are covered by broad bands between 3000 cm^{-1} and 3800 cm^{-1}. Clay's spectra are hidden by the vibration lines of polymeric materials (lipids, proteins and phenolic compounds), which are visible in infrared spectra. The FTIR spectrum's transmittance bands at 3600.00 cm^{-1} and 3393.51 cm^{-1} are attributed to the stretching vibrations caused by the O–H stretching of the kaolin clay's inner hydroxyl groups and inner-surface hydroxyl groups, respectively.

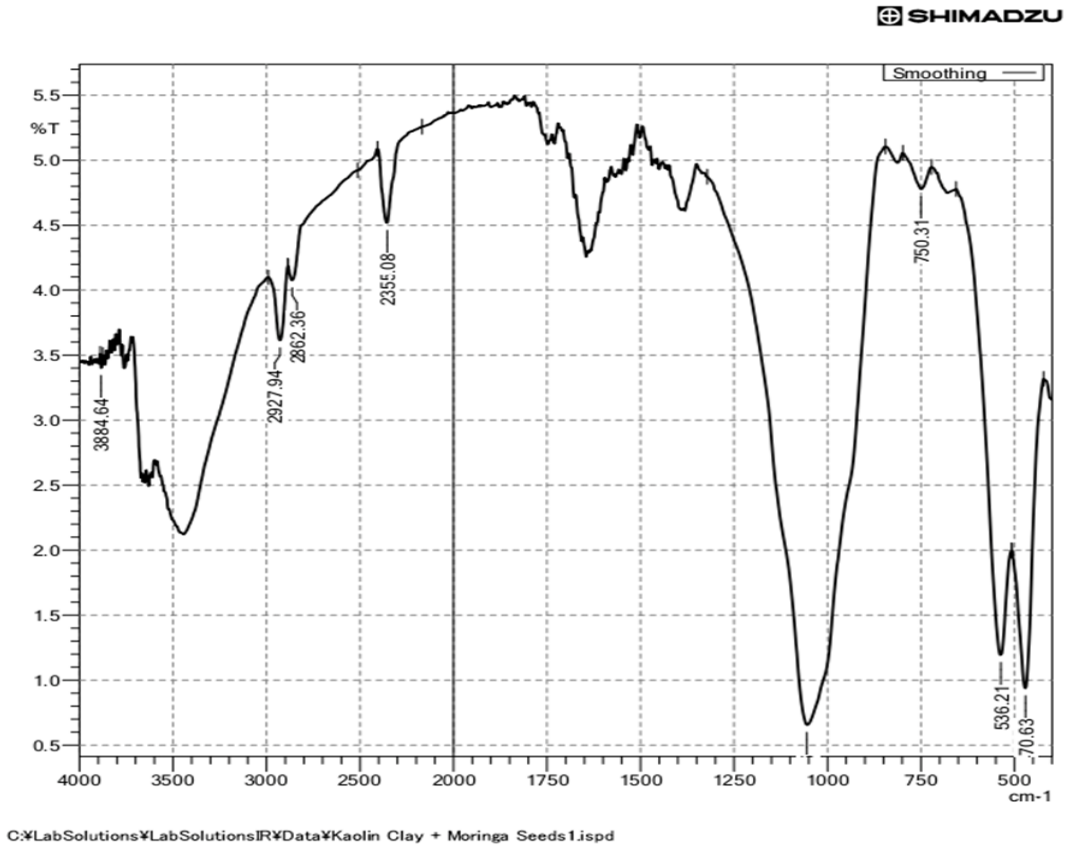

Figure 6: FTIR spectrum for a Pure Composite.

The composite formed was activated with NaOH which increases the presences of the OH group in the compound hence it easily bind with the cations presence in the water samples and H_2SO_4 increases the presence of the H^+ in the composite which will bind with the anions like F^-. The FTIR spectra base and acid activated composite (Figure 7 and 8 respectively) had a minor shift. The establishment of a chemical link between the functional groups on the composite may be the cause of this shift in peak values, similar observations have been made and reported by other researchers (Bello *et al*., 2017; Al-Ghouti *et al*., 2003). The FTIR can be used to verify the possible applicability of various pollutants' adsorption on the composite formed with adequate and satisfying removal efficiency. For acid activated composite, the FTIR spectroscopic analysis indicated broad band at 3280 cm^{-1}, representing bonded –OH groups. The band observed at 2926.06 cm^{-1} and 2856.63 cm^{-1} was assigned to the aliphatic C–H group both alkane and alkenes. The peak seen at 1460 $cm^{-1}$was attributed to C-H scissoring and bending for methylene, while the peak around 1630 cm^{-1}corresponds to C=O stretch. The symmetric bending of CH_3 is represented by the peak seen at 1370 cm^{-1}. Additionally, the peak at 1059.90 cm^{-1}relates to ether, ester, or phenol C=O bonds, whilst the peaks at 755.14 cm^{-1} were linked to AL-O and Si-O stretching, respectively. The signal measured at 564 cm^{-1} is associated with S–O.

According to FTIR research, the majority of the adsorption process will involve bonded –OH groups, C=O stretching, and secondary amine groups. Band shifts and decreases in intensity were clearly seen at 3415 cm^{-1}, 2927.94 cm^{-1}, 2355.08 cm^{-1}, 1059.90 cm^{-1}, and 477.39 cm^{-1}. The effects of acid activation on the composite were validated by the alterations in FTIR spectra. The spectra shifts indicated that the produced composite will work well as an adsorbent to remove heavy metals and dyes, the same observation was also made by the following scholars (Bekci *et al*., 2009; Al-Ghouti *et al*., 2003). FTIR spectroscopy examination for base activation revealed a wide band at 3420 cm^{-1}, which is indicative of linked -OH groups. The aliphatic C–H group was attributed to the band that was seen at 2926.06 cm^{-1} and 2857.59 cm^{-1}. The C=O stretch corresponds to the peak at approximately 1610 cm-1. The symmetric bending of CH_3 is represented by the peak detected at approximately 1375 cm^{-1}, whereas the C=O bonds of ether, ester, or phenol are represented by the peak observed at approximately 1010 cm^{-1}. While S-O was identified as the source of the

peak at 539.11 cm^{-1}, Si-O was found to be the peak at 710 cm^{-1}. The shift or displacement of peaks shows that the functional groups responsible for the peaks have reacted. These shifts revealed that the composite was likely to be useful adsorbate.

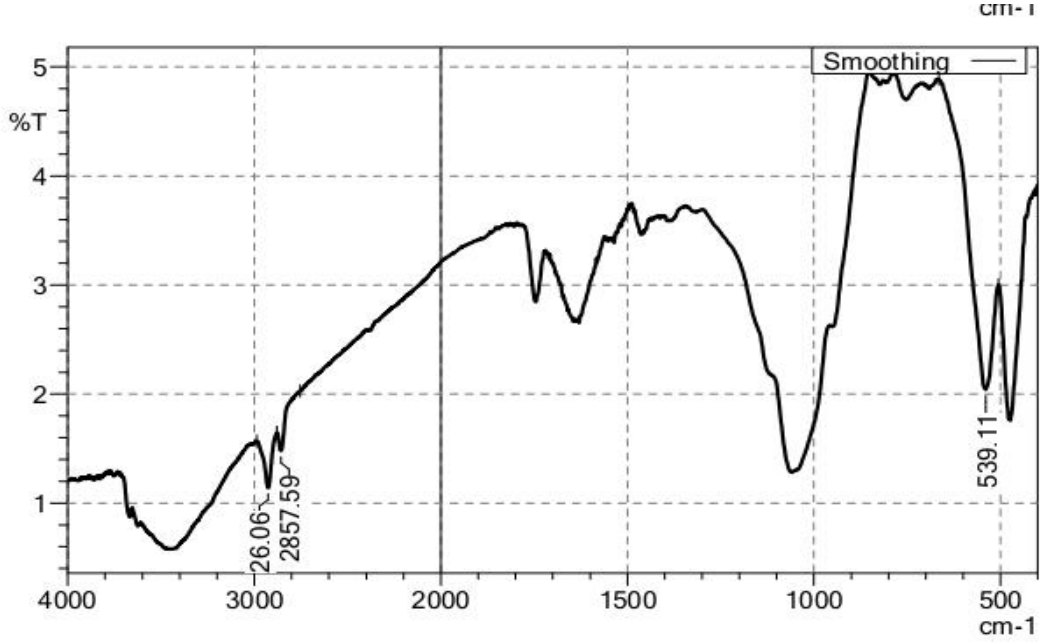

Figure 7: FTIR spectra of the composite activated with NaOH

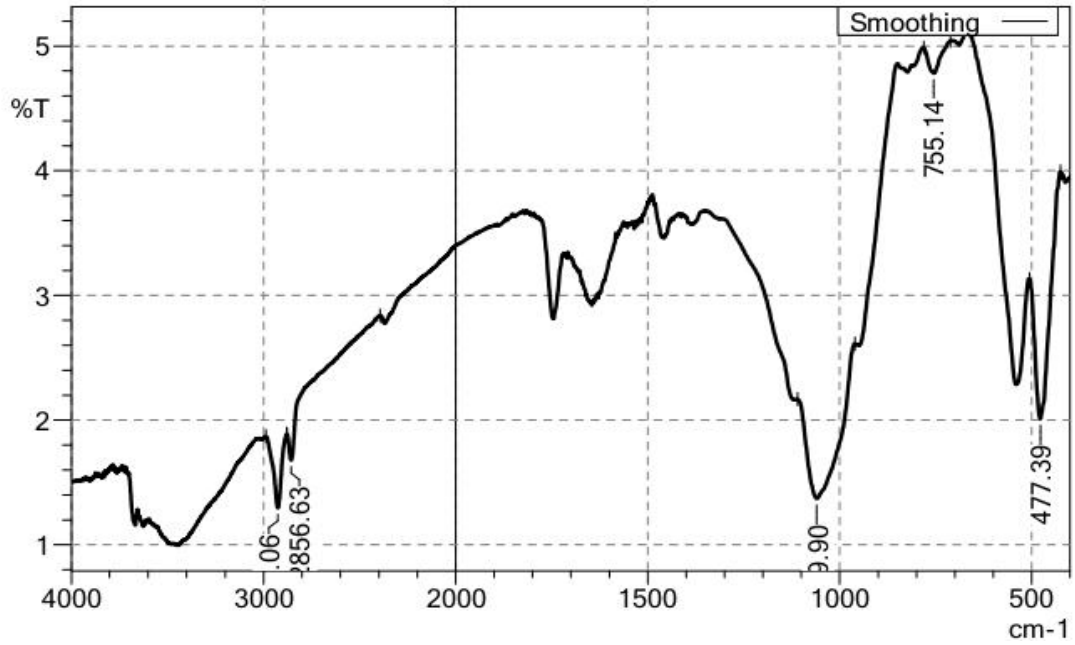

Figure 8: FTIR spectra of the composite activated with H_2SO_4

4.2.2 Powder XRD Analysis

The crystallinity was ascertained by powder XRD method. The XRD examination of kaolin clay, *Moringa oleifera* seed powder, raw composite, acid and base activated

composites yielded a pattern with narrow, sharp, and substantial peaks. The provided image Figure 9 shows an X-ray Diffraction (XRD) pattern of the samples, including pure *Moringa oleifera* seeds, pure Kaolin clay, and pure *Moringa* + kaolin clay and base activated. The sample description of the XRD patterns in Figure 9 includes; (a) Pure *moringa* + clay, which is a composite of *Moringa oleifera* and kaolin clay (b) wet residue, (c) activated with NaOH, (d) pure *Moringa*, (e) kaolin clay. The patterns indicate a combination of amorphous and crystalline phases (Adebayo *et al*., 2022). The prominent peak around 2θ: 22-23°, suggests the presence of a crystalline structure typical of certain kaolin clay (Hamadeen *et al*., 2021).

Acid activated indicated by Figure 9 (b) showed multiple sharp peaks. This pattern suggests that the wet residue contains several crystalline phases. The peaks are more defined compared to the pure *Moringa oleifera*, indicating higher crystallinity (Ngulube *et al*., 2024). Figure 9 (c) shows the pattern for NaOH activated reflecting the sample treated with sodium hydroxide (NaOH). Treatment with NaOH may alter the crystalline structure, evident from the new or shifted peaks compared to pure *Moringa oleifera*. This activation might introduce or highlight specific crystalline phases (Roy *et al*., 2022). The purple pattern for Kaolin clay shown in Figure 9 (d) is that of pure clay, showing distinct sharp peaks. The sharpness and positions of these peaks can be matched with known clay minerals. The reference at the bottom indicates the presence of muscovite, a common clay mineral, along with other possible components (Yang *et al*., 2004). The XRD patterns reveal significant differences in the crystallinity and composition of the samples. The treatment and combination of materials like *Moringa oleifera* and kaolin clay produce distinct changes in their crystalline structure, which can be essential for understanding their properties and potential applications (Abatal *et al*., 2021).

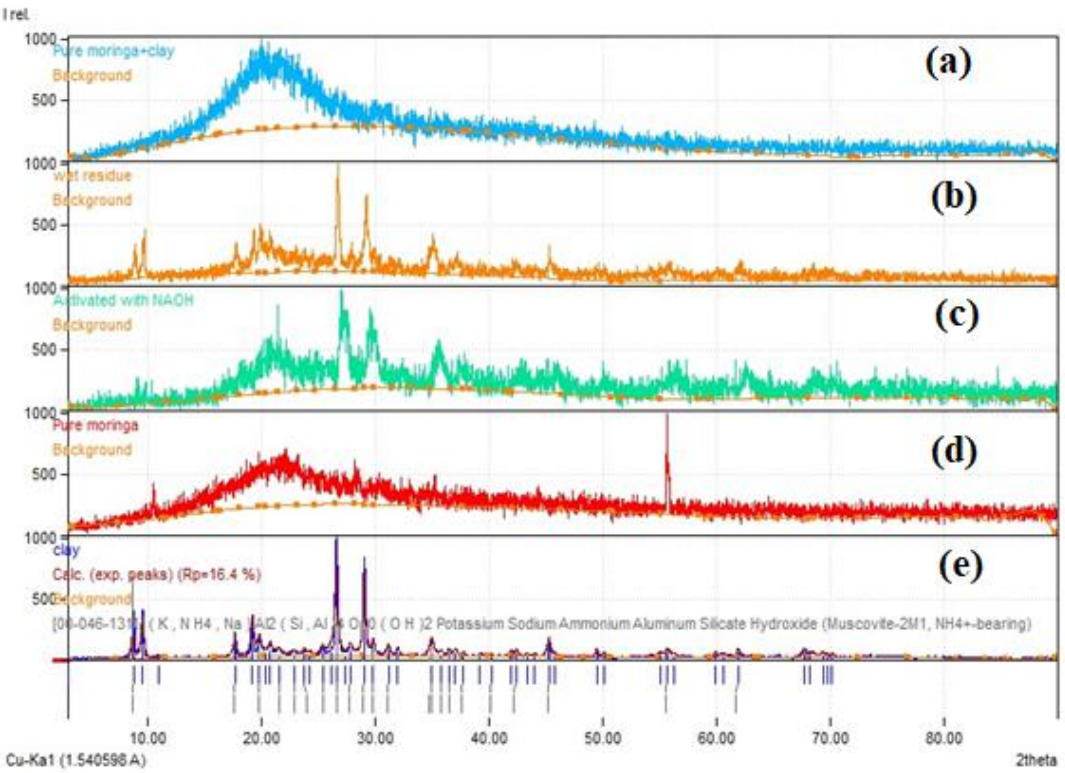

Figure 9: XRD results for Different Composites (a) Pure moringa + clay, (b) activated with HCl (c) activated with NaOH, (d) pure *Moringa*, (e) kaolin clay.

The XRD patterns shown in Figures 10 and 11 are for a composite that has been activated with NaOH. The pattern includes experimental peaks (in blue), calculated peaks (in red), and a background correction (in orange). The reference compound indicated at the top is Cu0.81Fe0.48Pb8.14Bi12.59S28, which is an Eclarite (a copper-lead-bismuth-iron sulfide). There are several prominent peaks between 2θ: 10° and 50°, with the highest peak appearing around 2θ: 27°. Peaks at approximately 2θ: 12°, 19°, 23°, 27°, 31°, and 44° show high intensities. This suggests the presence of highly crystalline phases in the sample (Roy *et al*., 2022). The calculated peaks match closely with the experimental peaks, indicating a good fit. This is confirmed by the Rp (residual percentage) value of 30.7%, indicating a reasonable agreement between the calculated and experimental data (Hamadeen *et al*., 2021). Comparing the major peaks with the JCPDS values, it showed that, 2θ: 12° possible match with sulphide compounds such as PbS (Galena) or Bi_2S_3 (Bismuthinite), 19° 2θ possible match sulphide minerals like CuS (Covellite) or mixed metal sulphides, 2θ: 23° possible match could indicate complex sulphides or sulphate, 2θ: 27° strong peak, likely indicative of a primary component Eclarite (Ngulube *et al*., 2024), 2θ: 31° possible

match secondary sulphide phases or oxides/hydroxides formed during NaOH treatment, 2θ: 44° possible match metallic phases or intermetallic compounds (Adebayo *et al*., 2022). The XRD analysis shows that the sample activated with NaOH contains multiple crystalline phases, predominantly sulphide minerals (Abatal *et al*., 2021). The comparison with JCPDS cards suggests the presence of complex sulphides such as Eclarite and possibly other sulphide minerals like Galena, Bismuthinite, and Covellite. The good match between calculated and experimental peaks supports the identification of these phases (Yang *et al*., 2004).

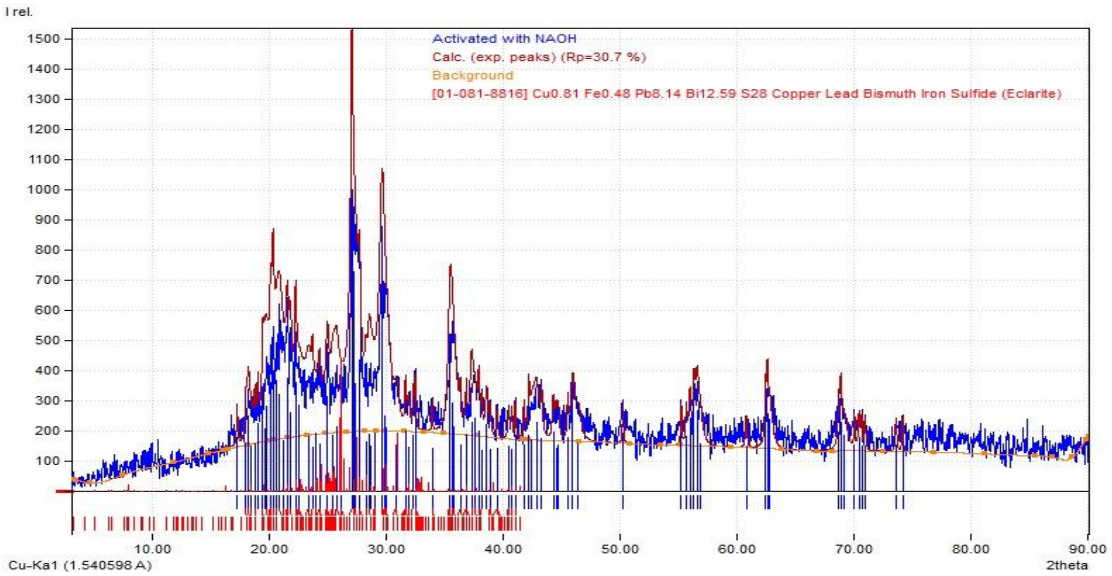

Figure 10: XRD for the base activated composite.

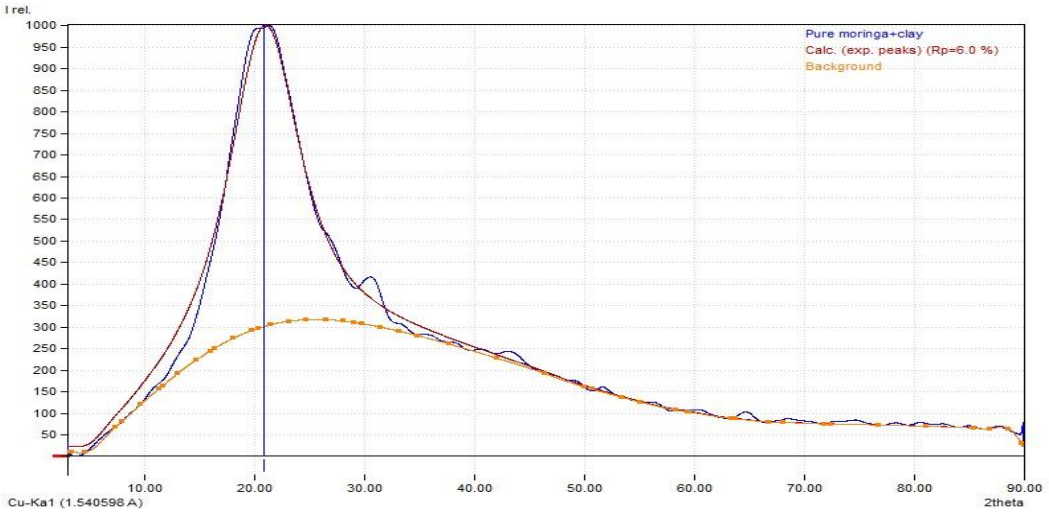

Figure 11: XRD for pure Composite.

Figure 11 shows a broad peak between 2θ: 10-30°. Smaller crystallites are associated with larger half-widths, and larger crystallites are associated with narrower half-widths. Lattice distortions and structural flaws may be the cause of the diffraction peaks' widening. By comparing the integrated intensity of the background pattern to that of the sharp peaks, powder XRD was utilized to assess the crystallinity of the samples.

4.3 Adsorption Studies

4.3.1 Adsorption Efficiency of Lead Using Various Composites and Dosages

The adsorption efficiency of lead (Pb (II)) using different composites and dosages revealed distinct trends, with each composite demonstrating optimal performance at specific dosages. For the raw composite, the Pb adsorption efficiency remained high and consistent across all tested dosages, with percentages of 96.97% at 0.5g, 97.44% at 1.0g, and 96.49% at 1.5g as shown in Figure 12. The highest adsorption efficiency for the raw composite was observed at 1.0g, with an optimal adsorption of 97.44%, indicating stable and effective performance across various dosages.

In contrast, the composite activated with NaOH showed the highest adsorption efficiency at the lowest dosage of 0.5g, achieving a complete Pb (II) removal of 100%. However, as the dosage increased, the efficiency decreased to 94.10% at 1.0 g and 90.75% at 1.5 g. This trend suggests that the NaOH-activated composite is most effective at the lower dosage of 0.5g, where it achieved optimal adsorption. The composite activated with H_2SO_4 exhibited significantly lower adsorption efficiency compared to the other two composites. The Pb (II) adsorption percentages were 19.95% at 0.5g, 14.92% at 1.0g, and 6.39% at 1.5g, with the highest adsorption efficiency at the lowest dosage of 0.5 g as per Figure 12.

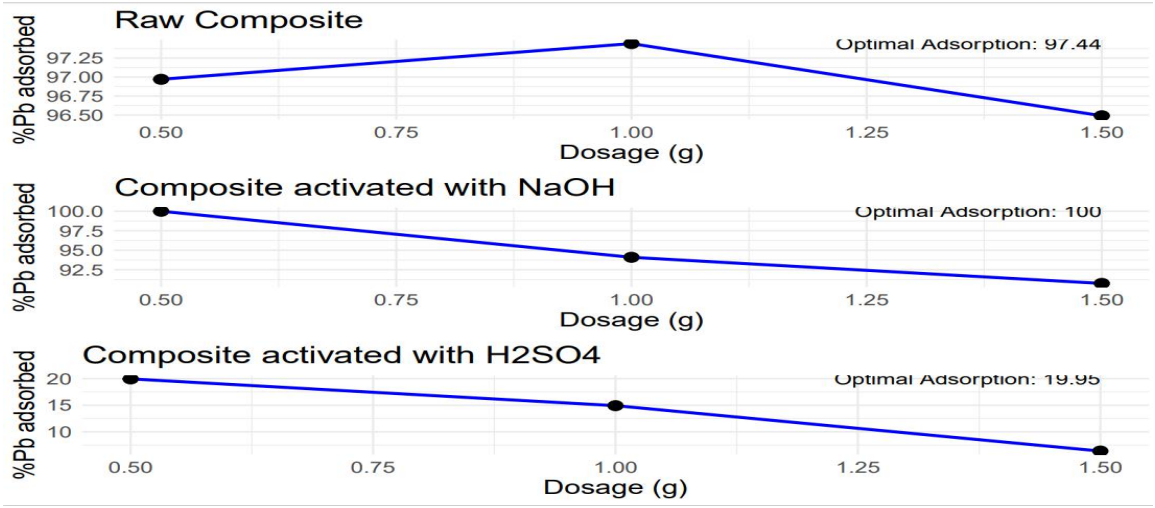

Figure 12: Concentration of Pb (II) basing on the Type and Dosage of the Adsorbate

The study compared the Pb (II) adsorption efficiencies of raw composite and composites activated with NaOH and H_2SO_4 at varying dosages as shown in Figure 12. Raw composite demonstrated high adsorption efficiency, with an optimal dosage of 1.0 g resulting in 97.44% Pb (II) removal. This suggested that the raw composite was inherently effective for Pb (II) adsorption. NaOH activated Composite showed superior adsorption efficiency, achieving 100% Pb (II) removal at a lower dosage of 0.5 g. However, efficiency declined at higher dosages, indicating potential aggregation issues. H_2SO_4 activated composite exhibited significantly lower adsorption efficiency, with the highest adsorption of only 19.9%. This indicated that H_2SO_4 activation was not suitable for enhancing the composite's Pb (II) adsorption capacity (Alengebawy *et al*., 2023). Overall, NaOH activation enhanced the Pb (II) adsorption capacity of the composite compared to the raw composite, while H_2SO_4 activation is detrimental (Yameogo *et al*., 2011). These findings provided a valuable insight for optimizing composite materials for effective lead removal from aqueous solutions (Alengebawy *et al*., 2023).

4.3.2 Concentration

The effect of lead concentration on adsorption efficiency was investigated. The data exhibited a notable trend wherein adsorption efficiency initially increased from 41.26% at 2 ppm to 81.42% at 6 ppm. Subsequently, a slight increase was observed at 8 ppm (96.57%) followed by a consistent high efficiency at 10 ppm (95.50%). A

Pearson correlation test indicated a strong positive relationship between Pb (II) concentration and adsorption efficiency, r(3) = 0.9516, p = 0.0127 Figure 13.

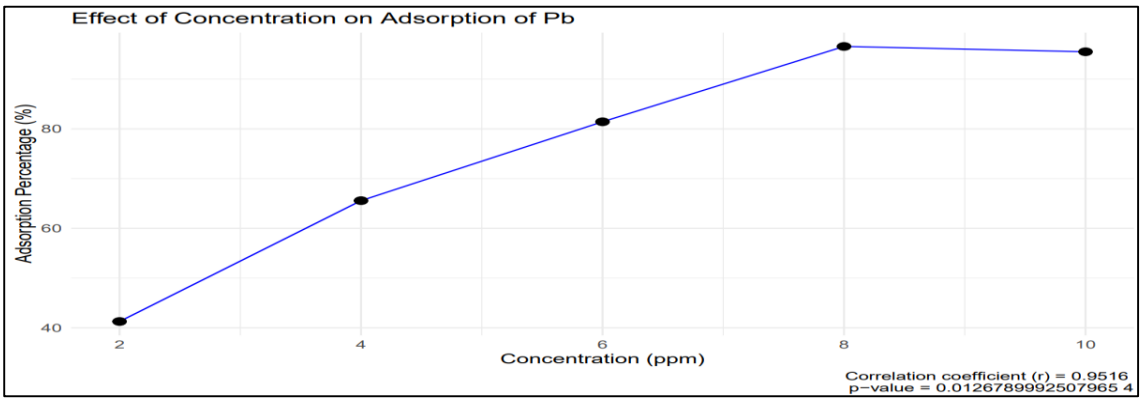

Figure 13: Effect of Concentration of on adsorption of Pb (II) (0.5g base activated composite)

The adsorption percentage increased with Pb concentration up to a point as shown in Figure 13, indicating that the adsorption sites were becoming saturated. After reaching the saturation point at 8 ppm, additional increases in Pb (II) concentration did not result in higher adsorption, and might have even led to a slight decrease. The trend suggested an optimal Pb (II) concentration for maximum adsorption, which appeared at 8 ppm. Beyond this concentration, the adsorption process became less efficient (Dwivedi *et al*., 2015). The diagram in Figure 13 demonstrated that the adsorption of Pb was highly efficient up to a certain concentration, beyond which the efficiency declined (Dwivedi *et al*., 2015).

4.3.3 pH

The effect of pH on Pb (II) adsorption efficiency was investigated. The results showed that Pb (II) adsorption efficiency increased significantly at a pH of 7, reaching 78.49%, which was the highest adsorption observed. The adsorption efficiencies at pH 8 and pH 12 were 60.09% and 67.30% respectively, while at lower pH values of 3 and 6, the adsorption efficiencies were 8.03% and 16.24% as per Figure 14. A Pearson correlation test indicated a moderate positive correlation between pH and adsorption efficiency, r(3) = 0.7168, p = 0.173.

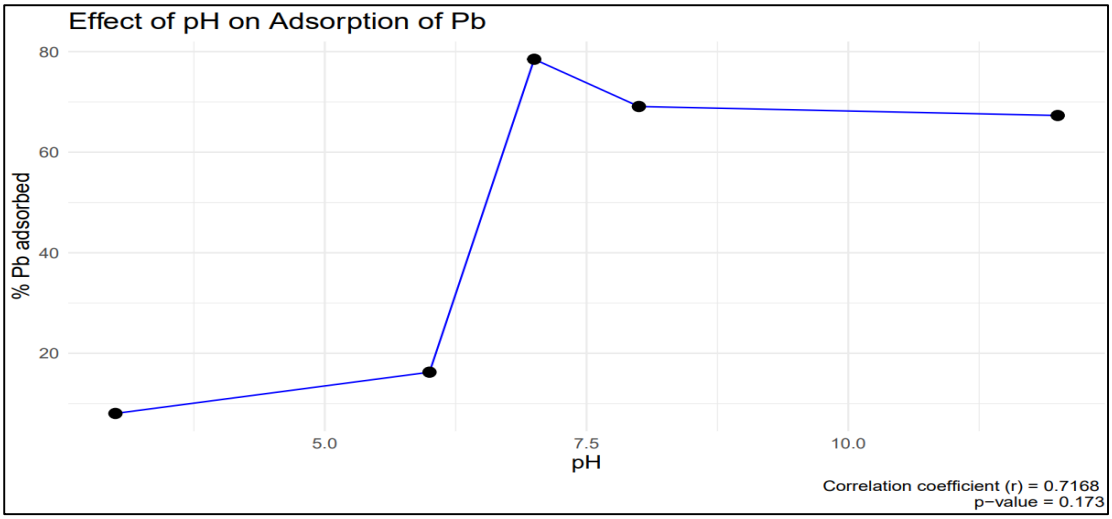

Figure 14: Effect of pH during the Adsorption of Pb (II) (0.5g base activated composite, 10 ppm of Pb (II))

Different pH values were chosen for these study, pH 3, pH 6, pH 7, pH 8 and pH 12 to represent the strong acidic, weakly acidic, neutral, weakly basic and strong basic respectively. The adsorption of Pb (II) was highly dependent on pH, with optimal adsorption occurring around pH 7 as shown in Figure 14. Within this range, the adsorption process was most efficient. At lower pH values the adsorption efficiency was significantly lower. This may be due to increased competition between H^+ ions and Pb (II) for adsorption sites. At higher pH values the adsorption efficiency decreased slightly from the peak at pH 7. This could be due to the formation of $Pb(OH)_2$ precipitates, reducing the availability of Pb (II) for adsorption. This observation concurs with the work of (Dwivedi *et al*., 2015), who demonstrated that acidic conditions hinder Pb (II) adsorption due to the protonation of active adsorption sites and increased competition from hydrogen ions. They reported Pb (II) adsorption efficiencies of 10% and 15% at pH values of 3 and 5, respectively, further supporting the current findings.

The study indicated that pH significantly affects the adsorption of Pb (II), with the highest adsorption percentage observed at pH 7. Despite the moderate correlation, the lack of statistical significance (p-value > 0.05) suggested that additional factors might influence the adsorption process (Zvinownda *et al*., 2011). In practical applications, such as water treatment, maintaining the pH around neutral maximizes the adsorption

efficiency of Pb (II), ensuring more effective removal from contaminated water sources (Zvinownda *et al*., 2011).

The Pearson correlation test indicated a moderate positive correlation between pH and Pb adsorption efficiency, with an r value of 0.7168 and a p-value of 0.173. Although the correlation was not statistically significant, the positive trend suggests that pH plays a crucial role in the adsorption process. This is in line with the conclusions drawn by other researchers, such as (Alengebawy *et al*., 2022), who found a similar moderate positive correlation between pH and Pb adsorption efficiency (r = 0.684, p = 0.210).

4.3.4 Temperature

The effect of temperature on Pb (II) adsorption efficiency was analyzed across different temperature levels. The results indicated that adsorption efficiency was highest at 75°C (99.33%), followed by 125°C (97.78%) and 25°C (97.26%). However, a significant decrease in adsorption efficiency was observed at 175°C (6.43%) and further at 225°C (1.45%). A Pearson correlation test revealed a significant negative relationship between temperature and adsorption efficiency, r(3) = -0.8715 , p = 0.05424 as shown in Figure 15.

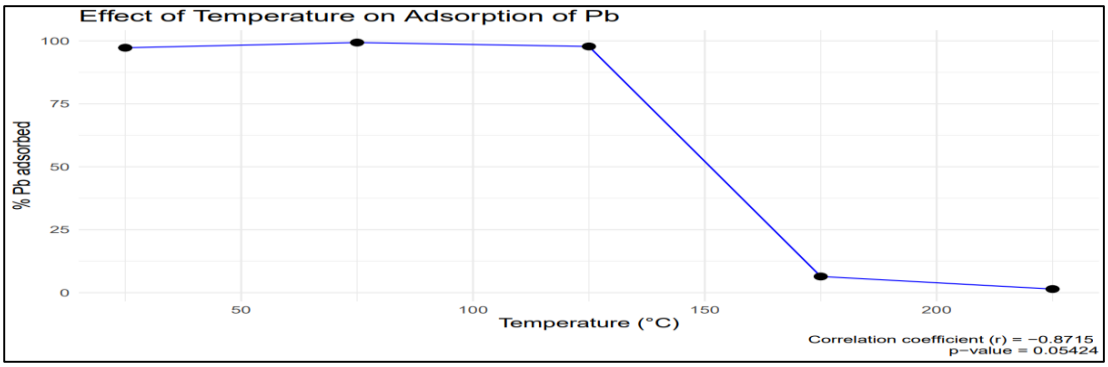

Figure 15: Effect of Temperature on Adsorption of Pb (II) (0.5g base activated composite, 10 ppm of Pb (II) and pH 7)

The adsorption of Pb (II) was relatively unaffected by temperature up to 125 °C. A significant decrease in adsorption efficiency was observed at temperatures above 125 °C, indicating that higher temperatures negatively impacted the adsorption process. This trend may be due to the increased kinetic energy at higher temperatures, which can disrupt the adsorbent's structure or reduce the interactions between Pb (II) and

adsorption sites (Apau *et al*., 2023). The data suggested that temperatures up to 75 °C were optimal for maintaining high Pb (II) adsorption efficiency. Beyond this temperature, the adsorption efficiency declined sharply, making it less effective for practical applications at higher temperatures (Jabeen *et al*., 2015). The study demonstrated that temperature had a significant impact on the adsorption of Pb. While the adsorption efficiency remained high up to 75 °C, it decreases sharply at temperatures above this threshold. The strong negative correlation (r = -0.8715) highlighted the inverse relationship between temperature and adsorption efficiency (Apau *et al*., 2023).

4.3.5 Rotation

The effect of rotation speed on Pb (II) adsorption efficiency was examined. The results showed that Pb (II) adsorption efficiency increased with rotation speed, reaching the highest efficiency at 500 rpm (98.62%). The adsorption efficiencies at 400 rpm, 300 rpm, 200 rpm, and 100 rpm were 93.75%, 73.94%, 66.46%, and 60.30% respectively. A Pearson correlation test indicated a strong positive correlation between rotation speed and adsorption efficiency, r(3) = 0.9758, p = 0.004493 Figure 16.

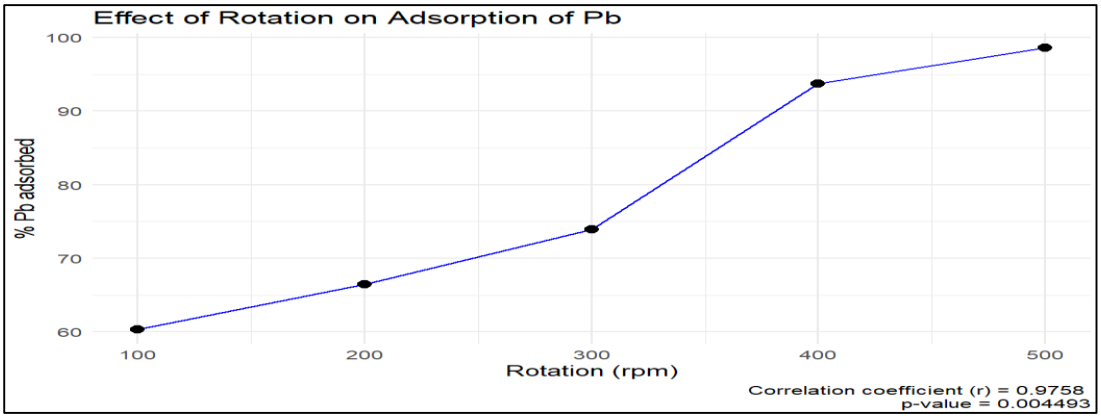

Figure 16: Effect of Rotation on the Adsorption of Pb (II) (0.5g base activated composite, 10 ppm of Pb (II), pH 7 and 348K)

Various rotations were done in order to obtain the optimum rotation for these adsorption studies. Rotation of 100 rpm, 200 rpm, 300 rpm, 400 rpm and 500 rpm were used for these studies. The data indicated that increasing the rotation speed enhanced the adsorption of Pb (II). Higher rotation speeds likely increased the

interaction between Pb (II) and the adsorbent, leading to more efficient adsorption (Placet *et al*., 2012). The adsorption efficiency improved consistently with increased rotation speed up to 500 rpm. This suggested that higher rotation speeds facilitated better mixing and contact between the adsorbate and adsorbent (Placet *et al*., 2012). The study demonstrated a clear positive relationship between rotation speed and the adsorption efficiency of Pb (Arismendi *et al*., 2023). The very strong correlation (r = 0.9758) and statistically significant p-value (0.004493) reinforced the reliability of this observation. Maintaining higher rotation speeds can ensure more effective mixing and contact, thereby maximizing the removal of Pb (II) from contaminated water (Arismendi *et al*., 2023).

4.3.6 Contact time

The effect of contact time on Pb (II) adsorption was examined over varying durations. The percentage of Pb (II) adsorbed ranged from 69.70% to 74.12% across different time intervals (10 to 50 minutes). A loess smoothing trend line was applied to illustrate the relationship, indicating negative significant correlation between contact time and Pb (II) adsorption efficiency, r(3) = -0.5248, p = 0.3639 as shown in Figure 17.

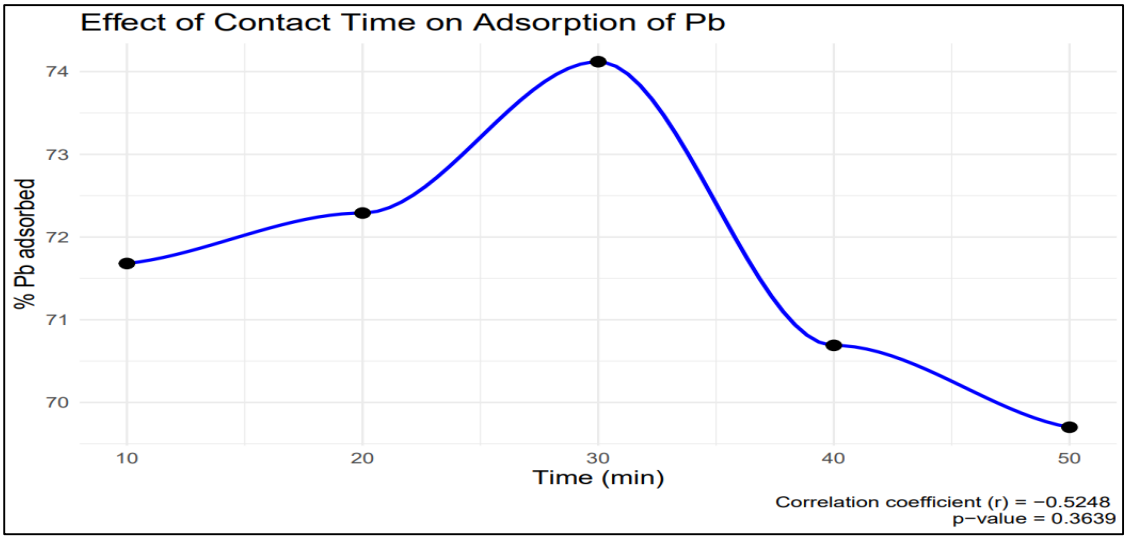

Figure 17: Effect of Contact Time on Adsorption of Pb (II) (0.5g base activated composite, 10 ppm of Pb (II), pH 7, 348K and 500 rpm)

The trend illustrated the effect of contact time on the adsorption percentage of Pb (II). The adsorption process was monitored over a period of 50 minutes. Initially, there was a gradual increase in the percentage of Pb (II) adsorbed. This suggested that the adsorption sites were readily available and the Pb (II) were actively interacting with these sites (Smith *et al*, 2007). The highest adsorption of Pb (II) (74.12 %) occured at 30 minutes. After reaching the peak at 30 minutes, there was a noticeable decline in the percentage of Pb (II) adsorbed. This reduction continues until the 50 minute mark, where the adsorption percentage dropped to approximately 70%. The correlation coefficient (r) is -0.5248, indicated a moderate inverse relationship between contact time and Pb (II) adsorption after the peak at 30 minutes. However, the p-value was 0.3639, which was greater than the conventional alpha level of 0.05 (Fan *et al*., 2013). This suggested that the observed changes in adsorption percentage with contact time were not statistically significant. The study revealed a non-linear relationship between contact time and the percentage of Pb (II) adsorbed. The adsorption process was most effective at 30 minutes, beyond which the efficiency declined. This trend may be attributed to the saturation of adsorption sites or possible desorption processes occurring after prolonged contact time (Fan *et al*., 2013). These findings contributed valuable insights into optimizing the adsorption process for effective lead removal from aqueous solutions (Smith *et al*, 2007).

4.3.7 Interference of As (III) on adsorption of Pb (II)

The effect of interference by As (III) on Pb (II) adsorption was investigated across varying concentrations of As (III) (2 to 10 ppm). Results indicated a fluctuating trend in Pb (II) adsorption percentages, ranging from 77.68% to 86.46% nonetheless, negative significant correlation was observed, $r(3) = -0.5524$, $p = 0.3343$ between concentration and Pb (II) adsorption efficiency as shown in Figure 18.

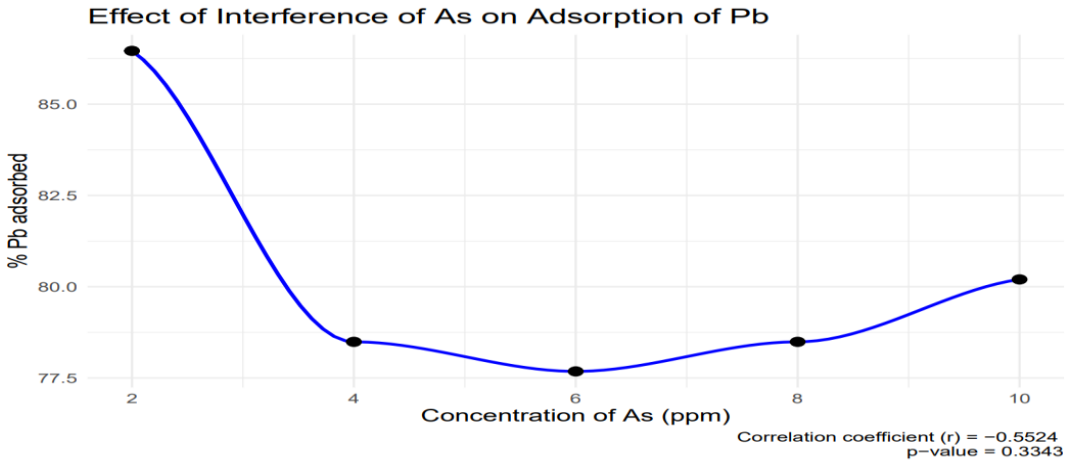

Figure 18: Effect of Interference of As during the Adsorption of Pb (II) (II) (0.5g base activated composite, 10 ppm of Pb (II), pH 7, 348K, 500 rpm and 30 min).

Real water samples contain multi heavy metals and organic chemicals and the presence of one heavy metal and an organic substance may hinder the adsorption of other heavy metals and organic chemicals (Nguyen *et al*., 2013). To examine the interference of As (III) during the adsorption of Pb (II), 2 ppm, 4 ppm, 6 ppm, 8 ppm and 10 ppm of As (III) was introduced to constant solution of 8 ppm Pb (II) and other optimum conditions obtained. The results obtained indicated a lower interference for the concentration of 2 ppm which showed 86.46% adsorption of Pb (II). Therefore, the concentration of 2 ppm was used for this since there was less interference during the adsorption of Pb (II). Interference of Cd (II) was not carried since it concentration was below the detection limit (Ramesh *et al*, 2007).

4.3.8 Adsorption Studies on Standard Solution of Pb and NR7 Sample

The identified optimum conditions were then applied to adsorption of standard solution of 10 ppm Pb (II), to investigate the effectiveness of the adsorbate. The results obtained indicated that the concentration of Pb (II) was lowered till below the detection limit, indicating the adsorbate and the chosen optimum condition was effective for the adsorption of Pb (II) from the standard solution, this leads to a suggestion that the parameters applied to the standard will be effective when it comes to the adsorption of Pb (II) on the actual samples. The same conditions were then applied to one of the sample NR7 which had the highest concentration of Pb (II) where the concentration of Pb (II) which was 1.7496 was lowered up to 0.284 mg/l which equates to 83.77%, according to the following calculations;

% removal = (1.7496 – 0.284)/ 1.7496 × 100% = 83.77%.

4.3.9 Adsorption Isotherms

The adsorption data was analyzed using Langmuir, Freundlich, and Temkin isotherm models to understand the adsorption behavior of Pb (II) onto the composite of *Moringa oleifera* and Kaolin clay. The Langmuir model estimated a maximum adsorption capacity (Q_{max}) of 14.98 mg/g with a Langmuir constant (b) of 0.20 L/mg. The goodness of fit (R^2) for the Langmuir model was 0.98676, indicating a strong correlation between the model predictions and the experimental data as shown in Figure 19. Similarly, the Freundlich model yielded a constant (K_F) of 3.21 and an exponent (1/n) of 2.00, with an R^2 value of 0.98253, suggesting a satisfactory fit of the model to the experimental data Figure 20. The Temkin model parameters, A and B, were determined to be 1.58 L/g and 3.61, respectively, with an R^2 value of 0.98, indicating a good agreement between the model and experimental data shown in Figure 20.

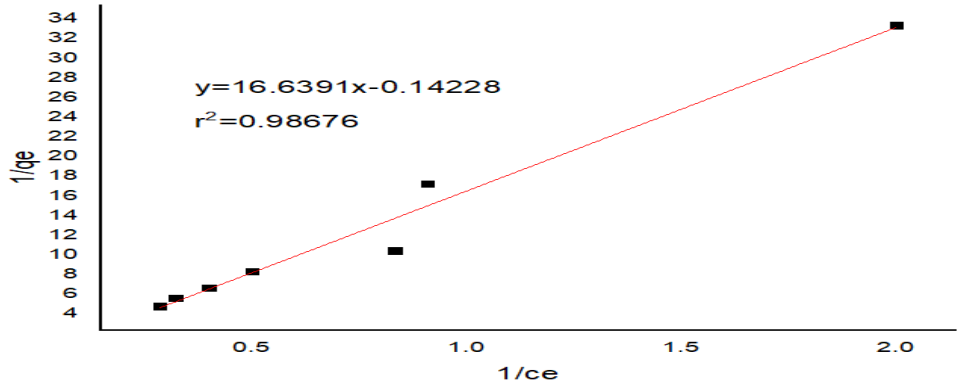

Figure 19: Langmuir isotherm graph fit model

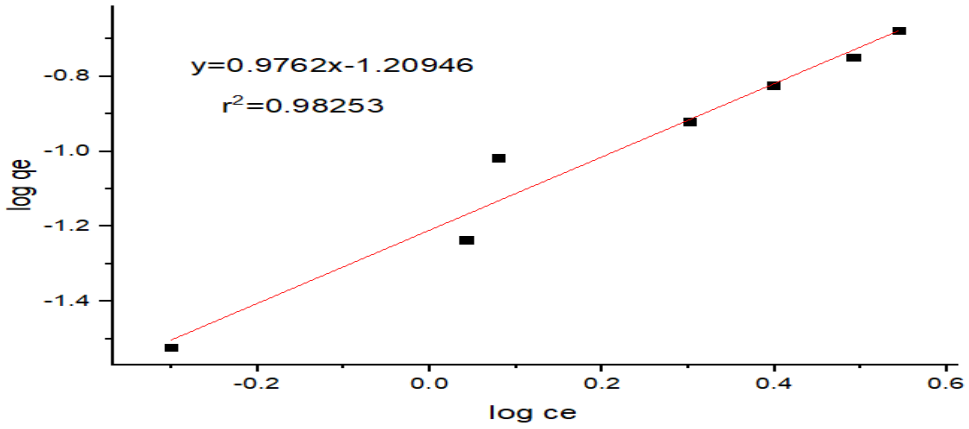

Figure 20: Freundlich isotherm graph fit

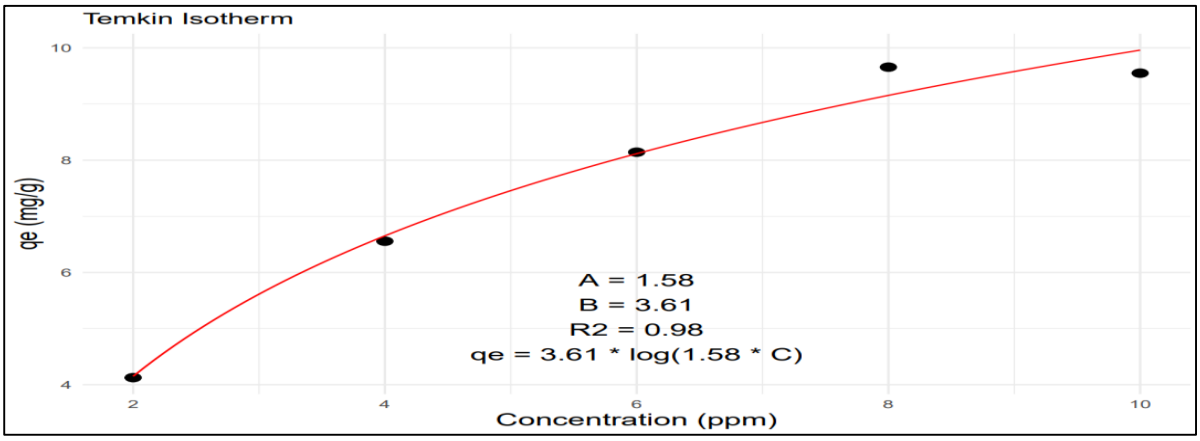

Figure 21: Temkin Isotherm graph fit model

The Langmuir model assumes monolayer adsorption on a surface with a finite number of identical sites, which implied that all adsorption sites had equal affinity for the adsorbate and that there was no interaction between adsorbed molecules. The high goodness of fit R^2 in Figure 19 and 20 indicated that this assumption holds true for the studied adsorption process, making the Langmuir model suitable for describing the adsorption behavior (Das *et al*., 2022). A constant was related to the maximum binding energy. A higher value of A indicated a stronger interaction between the adsorbate and the adsorbent. In this case, A=1.58 L/g suggested a moderate affinity between the adsorbate and the adsorbent. B parameter was directly proportional to the heat of adsorption and gives insight into the adsorption energy distribution. A value of B=3.61 indicated that the adsorption process was a moderate heat of adsorption, suggested that the adsorbate-adsorbent interactions were neither too weak nor too strong (Das *et al*., 2022).

4.3.10 Adsorption Kinetics

A kinetic analysis was conducted using pseudo-first-order and pseudo-second-order kinetic models. For the pseudo-first-order kinetic model, the logarithm of the difference between the equilibrium adsorption capacity (qe) and the adsorption at time t (qt) was calculated and regressed against time. The resulting equation for the pseudo-first-order kinetics was $\log(qe-qt) = -0.0001 \times \text{time} + 4$, with an R^2 value of 0.7859 shown in Table 9, indicating a moderate fit to the data shown in Figure 21.

The pseudo-second-order kinetic model was evaluated by plotting t/qt against 1/qe. The equation obtained was t/qt=100.0226×1/qe−99.9972 with an R^2 value of 1.0000, indicating an excellent fit to the data. These results suggest that the pseudo-second-order kinetic model better describes the adsorption process of Pb (II), as evidenced by the higher R^2 value Table 9.

Table 9: Pseudo-First-Order and Pseudo-Second-Order Values

Model	Parameter	Value
Pseudo-First-Order	K_1 (1/min)	-0.0001
	R^2	0.7859
Pseudo-Second-Order	K_2 (g/mg·min)	99.9972
	R^2	1

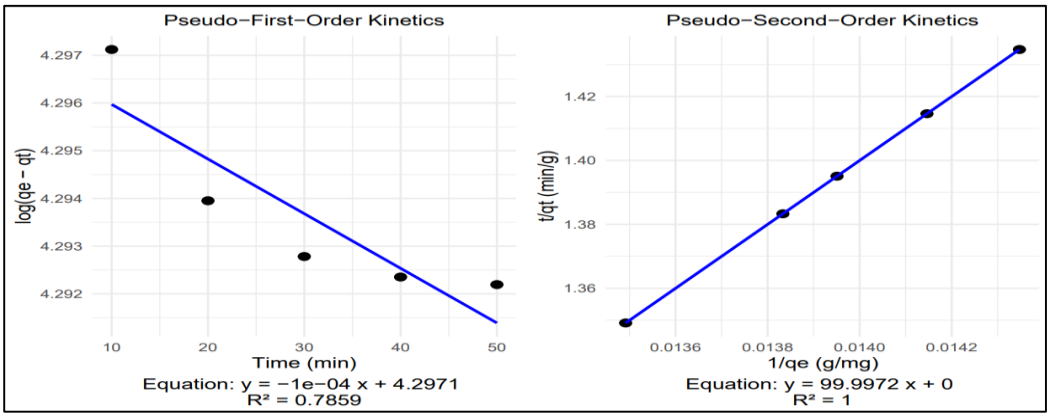

Figure 22: Pseudo-First-Order and Pseudo-Second-Order Models Fit

In conclusion, the kinetic analysis suggested that the pseudo-second-order model provided a much better fit for the experimental data compared to the pseudo-first-order model as shown in Figure 22. The negative rate constant K_1 and lower R^2 value for the pseudo-first-order model indicated its unsuitability for this system (Meneghel *et al*., 2013). In contrast, the high K_2 and perfect R^2 value for the pseudo-second-order model demonstrated its effectiveness in describing the kinetics of the adsorption process (Das *et al*., 2022). Similar results for the adsorption kinetics models who obtained related work on a solid adsorbate are (Das *et al*., 2022; Roy *et al*., 2022; Meneghel *et al*., 2013).

4.3.11 Thermodynamic Analysis on the Effect of Temperature on Adsorption of Pb (II) by the Composite

Adsorption data was collected at five different temperatures (25 °C to 225 °C), with the percentage of Pb adsorbed ranging from 1.45% to 99.33. The total Pb concentration in the solution was maintained at 10 ppm. The adsorption data was converted to adsorption capacity (qe) in mg/g, and the temperatures were converted to Kelvin (K) for analysis. Using the Van't Hoff equation in the form ln(qe)=A−TB, a nonlinear least squares fitting was performed to estimate the thermodynamic parameters ΔH (enthalpy change) and ΔS (entropy change). The fitting process yielded values for ΔH and ΔS, which were found to be 25,340.57 J/mol and 58.32 J/mol/K, respectively Figure 22. The Gibbs free energy change (ΔG) was calculated at various temperatures, showing a decrease from 7.95 kJ/mol at 25 °C to -3.71 kJ/mol at 225 °C Table 10, indicating an increasingly favorable adsorption process at higher temperatures. The calculated ΔG at 298 K (25 °C) was 7,952.01 J/mol (7.95 kJ/mol). The fit of the Van't Hoff model was evaluated by computing the R-squared value, which was found to be 0.6792, suggesting a reasonably good fit to the experimental data.

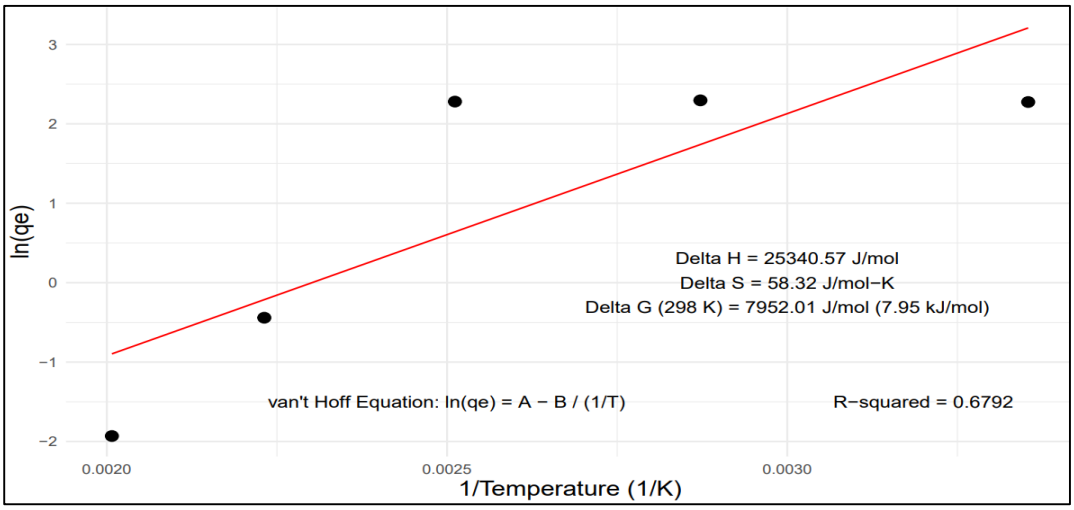

Figure 23: Thermodynamics ΔG, ΔS and ΔH.

Table 10: Thermodynamic Parameters and Gibbs Free Energy Changes

Temperature (°C)	ΔG (J/mol)	ΔG (kJ/mol)
25	7952.01	7.95
75	5035.94	5.04
125	2119.86	2.12
175	-796.21	-0.8
225	-3712.29	-3.71
298 (25°C)	7952.01	7.95

The given data presents Gibbs free energy (ΔG) values at different temperatures as shown in Table 10, both in J/mol and kJ/mol. These values were crucial for understanding the thermodynamics of a reaction process. ΔG was a thermodynamic potential that measures the maximum reversible work obtainable from a thermodynamic system at constant temperature and pressure (Das *et al*., 2022). It was a critical parameter in determining the spontaneity of a reaction. A negative ΔG indicated a spontaneous reaction, while a positive ΔG indicated non-spontaneity as illustrated in Figure 23. The data demonstrated a clear trend in the behavior of ΔG with increasing temperature. At 25°C, ΔG was positive (7.95 kJ/mol), indicated that the reaction was non-spontaneous under these conditions. The system required an input of energy to proceed. As the temperature increased from 25 °C to 125 °C, ΔG decreased significantly, becoming less positive. This suggested that the system required less energy to proceed with the reaction at higher temperatures, making it more favorable (Das *et al*., 2022). At 175 °C, ΔG became negative (-0.8 kJ/mol), indicating a transition to spontaneity. At this temperature, the reaction or process became thermodynamically favorable without the need for additional energy input. Beyond 175 °C, the ΔG values continued to decrease, became more negative at 225°C (-3.71 kJ/mol). The enthalpy change (ΔH) of 25,340.57 J/mol indicated that the reaction was endothermic. However, the positive entropy change (ΔS) of 58.32 J/mol/K implies that the disorder of the system increased during the reaction. As temperature increased, the TΔS term grows larger, leading to a decrease in ΔG, eventually making it negative and indicating spontaneity (Das *et al*., 2022). This trend showed that the reaction became increasingly spontaneous at higher temperatures. The observed trend suggested that temperature played a significant role in the spontaneity of the reaction (Roy *et al*., 2022). At lower temperatures, the reaction was non-spontaneous and required energy input. However, as the temperature rose, the reaction transitions to a spontaneous process indicated that heat acted as a driving force for the reaction. The data indicated that the reaction in question became more thermodynamically favorable as temperature increased (Roy *et al*., 2022).

CHAPTER FIVE
SUMMARY, CONCLUSION AND RECOMMENDATIONS

5.1 Summary

The study aimed to assess the levels of physicochemical parameters and investigate the remediation of lead (Pb II) in borehole water in Nakuru East Sub County, which is contaminated primarily by heavy metals and non-metals from both natural and anthropogenic sources. It involved the collection of water samples from various borehole locations during both dry and wet seasons. The analysis focused on several parameters, including temperature, pH, turbidity, electrical conductivity, dissolved oxygen, fluoride and concentrations of lead, cadmium and arsenic. Key objectives included determining the extent of contamination and evaluating the efficacy of a composite made from *Moringa oleifera* seed powder and kaolin clay as an adsorbent for lead remediation.

The findings revealed significant health risks associated with the borehole water, with Pb (II) levels exceeding WHO limits in over 31% of samples during the dry season and 42% during the wet season. Additionally, arsenic concentrations were also above the acceptable limits in both seasons. The physicochemical parameters indicated various degrees of contamination, including turbidity levels exceeding WHO guidelines in the wet season and electrical conductivity levels surpassing thresholds in the dry season. The composite adsorbent demonstrated effective Pb (II) removal, achieving an adsorption efficiency of 83.77% under optimal conditions, and the adsorption data conformed to Langmuir isotherm and Pseudo-Second-Order models. The study highlighted an urgent need for water treatment solutions due to the elevated levels of arsenic and lead and recommended further research into the composite's effectiveness for other heavy metals and in different contexts.

5.2 Conclusion

The turbidity of all the boreholes sampled during the dry and wet seasons were within the WHO and KEBS recommended limit except for only two boreholes NR1 and OL1 during the wet season. The entire pH of the boreholes was within the WHO and KEBS limit, while temperature had minor significant variation but with no effect to human consumptions. DO was higher during the wet season but with less variations,

resulting on less effect on human health. Fluoride was higher in dry season, although the levels were above the WHO and KEBS limit it has no advance effect of causing skeletal fluorosis. The levels of Pb (II) concentration showed that, 36.8 % of the samples were above the WHO and KEBS recommended level, while the cadmium concentrations were below the detections limits in all the collected samples. The concentration of arsenic in both the dry and wet seasons was above the WHO and KEBS set limits. The composite showed an effectiveness of 83.71 % basing on the adsorption done. The adsorptions mechanism demonstrated in the research was chemisorption and well described by Langmuir and pseudo second order models.

Residents of Nakuru East, particularly children, are at a high risk of experiencing negative health effects from high As (III) and Pb (II) consumption because water from these sources is used for drinking, cooking and other household tasks, causing people to directly consume high levels of As (III) and Pb (II), if water is supplied to customers directly without any sort of treatment, it is advised that some sort of low-cost treatment be used to lower the levels of trace metal as the one used as an adsorbent in this study.

5.2 Recommendations of the study

i. It is advised that all of the NAWASSCO boreholes have their water quality analyzed at least every year. This will guarantee that instances of contamination are identified sooner so that corrective action can be implemented.
ii. Water quality needs to be monitored in order to find long-term solutions to health issues related to the use and drinking of low-quality waters. This will protect public health and minimize unpleasant experiences associated with drinking or using low-quality waters.
iii. People should be informed about the importance of doing farming activities far from potential sources of contamination to boreholes in order to maintain the state of boreholes.
iv. Further research to be done on the applicability and efficiency of the composite of *Moringa oleifera* seeds and kaolin clay on other metals and non-metals remediation.

REFERENCES

Abatal, M., Olguin, M. T., Anastopoulos, I., Giannakoudakis, D. A., Lima, E. C., Vargas, J., & Aguilar, C. (2021). Comparison of heavy metals removal from aqueous solution by *Moringa oleifera* leaves and seeds. *Coatings*, *11*(5), 508.

Abdul Maulud, K. N., Fitri, A., Wan Mohtar, W. H. M., Wan Mohd Jaafar, W. S., Zuhairi, N. Z., & Kamarudin, M. K. A. (2021). A study of spatial and water quality index during dry and rainy seasons at Kelantan River Basin, Peninsular Malaysia. *Arabian Journal of Geosciences*, *14*, 1-19.

Abu-Danso, E., Peräniemi, S., Leiviskä, T., Kim, T., Tripathi, K. M., & Bhatnagar, A. (2020). Synthesis of clay-cellulose biocomposite for the removal of toxic metal ions from aqueous medium. *Journal of Hazardous Materials, 381,* 120-871.

Abu-Dief, A., & Zikry, M. (2018). Adsorption of the heavy metal ions onto bio sorbents: a review. *International Journal of Nanomaterials and Chemistry*, *4*(3), 27-39.

Adams, R., & Lee, S. (2021). Effects of precipitation on dissolved oxygen levels in freshwater lakes. *Journal of Environmental Quality, 50*(1).

Adebayo, M. A., Jabar, J. M., Amoko, J. S., Openiyi, E. O., & Shodiya, O. O. (2022). Coconut husk-raw clay-Fe composite: preparation, characteristics and mechanisms of Congo red adsorption. *Scientific Reports*, *12*(1), 14370.

Adefemi, S., & Awokunmi, E. (2021). Determination of physico-chemical parameters and heavy metals in water samples from Itaogbolu area of Ondo-State, Nigeria. *African Journal of Environmental Science and Technology*, *4*(3), 5-10.

Adekola, O., Bashir, A., & Kasimu, A. M. (2015). Physico-chemical characteristics of borehole water quality in Gassol Taraba State, Nigeria. *African Journal of Environmental Science and Technology*, *9*(2), 143-154.

Adeniyi, F. I., Ogundiran, M. B., Hemalatha, T., & Hanumantrai, B. B. (2020). Characterization of raw and thermally treated Nigerian kaolinite-containing clays using instrumental techniques. *Applied Sciences, 2*(5), 8-21.

Aderemi, A. V., Ayeleso, A. O., Oyedapo, O. O., & Mukwevho, E. (2021). Metabolomics: A scoping review of its role as a tool for disease biomarker discovery in selected non-communicable diseases. *Metabolites*, *11*(7), 4-18.

Adeyemo, O. K., Adedokun, O. A., Yusuf, R. K., & Abeleye, E. A. (2008). Seasonal changes in physico-chemical parameters and nutrient load of river sediments in Ibadan city, Nigeria. *Global nest. The International Journal*, *10*(3), 326-336.

Afonne, O. J., Chukwuka, J. U., & Ifediba, E. C. (2020). Evaluation of drinking water quality using heavy metal pollution indexing models in an agrarian, non-industrialised area of South-East Nigeria. *Journal of Environmental Science and Health, Part A*, *55*(12), 1406-1414.

Aga, B., & Brhane, G. (2014). Determination the level of some heavy metals (Mn and Cu) in drinking water using wet digestion method of Adigrat Town. *International Journal of Technology Enhancements and Emerging Engineering Research*, *2*(10), 32-36.

Agbasi, J., Egbueri, J., Ayejoto, D., Unigwe, C., Omeka, M., Nwazelibe, V., & Fakoya, A. A. (2023). The impact of seasonal changes on the trends of physicochemical, heavy metal and microbial loads in water resources. *Environment and Sustainable Development*, 20, 505-539.

Ahmed, A., Khan, S., & Malik, M. (2019). Sources and distribution of heavy metals in urban groundwater. *Journal of Environmental Management*, 231, 146-157.

Ahmed, S., Jamali, M. Z., Khoso, S., Azeem, F., & Ansari, A. A. (2022). Assessment of groundwater quality in rural areas of taluka dokri, sindh, pakistan, through physicochemical parameters. *International Journal of Energy, Environment and Economics*, *30*(3), 211-226.

Akhtar, N., Syakir Ishak, M. I., Bhawani, S. A., & Umar, K. (2021). Various natural and anthropogenic factors responsible for water quality degradation: A review. *Water*, *13*(19), 26-60.

Akkoyunlu, A., & Akiner, M. E. (2012). Pollution evaluation in streams using water quality indices: A case study from Turkey's Sapanca Lake Basin. *Ecological Indicators*, *18*, 501-511.

Alengebawy, A., Abdelkhalek, S. T., Qureshi, S. R., & Wang, M. Q. (2021). Heavy metals and pesticides toxicity in agricultural soil and plants: Ecological risks and human health implications. *Toxics*, *9*(3), 42-25.

Al-Ghouti, M. A., Khraisheh, M. A. M., Allen, S. J., & Ahmad, M. N. (2003). The removal of dyes from textile wastewater: a study of the physical characteristics and adsorption mechanisms of diatomaceous earth. *Journal of Environmental Management*, *69*(3), 229-238.

Al-Ghouti, M., Da'ana, D., Abu-Dieyeh, M., & Khraisheh, M. (2019). Adsorptive removal of mercury from water by adsorbents derived from date pits. *Scientific Reports*, *9*(1), 15-327.

Ali, H., Khan, E., & Sajad, M. (2013). Phytoremediation of heavy metals-concepts and applications. *Chemosphere*, *91*(7), 869-881.

Ali, R., Hamad, H., Hussein, M., & Malash, G. (2016). Potential of using green adsorbent of heavy metal removal from aqueous solutions: adsorption kinetics, isotherm, thermodynamic, mechanism and economic analysis. *Ecological Engineering*, *91*, 317-332.

Ali, W., Mushtaq, N., Javed, T., Zhang, H., Ali, K., Rasool, A., & Farooqi, A. (2019). Vertical mixing with return irrigation water the cause of arsenic enrichment in groundwater of district Larkana Sindh, Pakistan. *Environmental Pollution*, *245*, 77-88.

Alnashiri, H. M. (2021). Assessment of physicochemical parameters and heavy metal concentration in the effuents of sewage treatment plants in Jazan Region, Saudi Arabia. *Journal of King Saud University-Science*, *33*(8), 101-600.

Alrumman, S. A., El-kott, A. F., & Kehsk, M. A. (2016). Water pollution: Source & treatment. *American Journal of Environmental Engineering and Science*, 3(1), 42-54.

Alum, O. L., Okoye, C. O., & Abugu, H. O. (2021). Quality assessment of groundwater in an agricultural belt in eastern Nigeria using a Water Quality Index. *African Journal of Aquatic Science*, *46*(3), 304-318.

Ameta, S. K., Kamaal, M., & Ahamad, F. (2023). Impact of domestic and industrial effluent disposal on physicochemical characteristics of River Malin at Najibabad City, India. *Agricultural Environmental Sustainability*, *1*(3), 246-256.

Apau, J., Coffie, D., Akoto, O., Osei-Owusu, J., Gyamfi, O., & Boateng, G. (2023). Seasonal variation in water quality of river Subin in Kumasi. *Chemistry Africa*, *6*(4), 2175-2185.

Appolonia, K., & Juliet, M. (2013). Water analysis for heavy metals content in selected boreholes in Port Harcourt metropolis (a case study during 2010-2011). *Journal of Environmental Science and Engineering. A*, *2*(7A), 418-420.

Areerachakul, S., Sophatsathit, P., & Lursinsap, C. (2013). Integration of unsupervised and supervised neural networks to predict dissolved oxygen concentration in canals. *Ecological Modelling*, *261*, 1-7.

Arismendi, D., Vera, I., Ahumada, I., & Richter, P. (2023). A thin biofilm of chitosan as a sorptive phase in the rotating disk sorptive extraction of triclosan and methyl triclosan from water samples. *Analytica Chimica Acta*, *1252*, 34-1053.

Asowata, T. I., & Olatunji, A. S. (2019). Tracking lead in environmental media in the City of Onitsha, Southeast Nigeria. *Journal of Health and Pollution*, *9*(24), 191-202.

Awual, Md. R. (2019). An efficient composite material for selective lead (II) monitoring and removal from wastewater. *Journal of Environmental Chemical Engineering*, 7(3), 103087-103090.

Ayoob, S., & Gupta, A. K. (2006). Fluoride in drinking water: A review on the status and stress effects. *Critical Reviews in Environmental Science and Technology*, 36(6), 433-487.

Azizian, S. (2011). Derivation of a simple equation for close to equilibrium adsorption dynamics of surfactants at air/liquid interface using statistical rate theory. *Colloids and Surfaces A: Physicochemical and Engineering Aspects, 380*(1-3), 107-110.

Bagheri, A., Abu-Danso, E., Iqbal, J., & Bhatnagar, A. (2020). Modified biochar from *Moringa seed* powder for the removal of diclofenac from aqueous solution. *Environmental Science and Pollution Research, 27*(7), 7318-7327.

Banaee, M., Zeidi, A., Mikušková, N., & Faggio, C. (2024). Assessing metal toxicity on crustaceans in aquatic ecosystems: a comprehensive review. *Biological Trace Element Research*, 1-19.

Barringer, J. L. and Reilly, P.A. (2013). Arsenic in Groundwater: A Summary of Sources and the Biogeochemical and Hydrogeologic Factors Affecting Arsenic Occurrence and Mobility. *In*: P. M. Bradley (Ed.). *Current Perspectives in Contaminant Hydrology and Water Resources Sustainability, 27*(7), 7318-7327.

Bastia, A., Tiwari, P., Yadav, M., Pandey, G. C., & Rath, C. (2016). Structural transformation, magnetization reversal and magnetic switching in Cr doped GdMnO3_33 perovskite. *New Journal of Chemistry*, 45(47), 22396-22405.

Bastías, J. M., & Beldarrain, T. (2016). Arsenic translocation in rice cultivation and its implication for human health. *Chilean Journal of Agricultural Research, 76*(1), 114-122.

Bekçi, Z., Seki, Y., & Cavas, L. (2009). Removal of malachite green by using an invasive marine alga *Caulerpa racemosa var. cylindracea*. *Journal of Hazardous Materials, 161*(2-3), 1454-1460.

Bello, O. S., Adegoke, K. A., & Akinyunni, O. O. (2017). Preparation and characterization of a novel adsorbent from *Moringa oleifera* leaf. *Applied Water Science, 7*, 1295-1305.

Bello, O. S., Lasisi, B. M., Adigun, O. J., & Ephraim, V. (2017). Scavenging Rhodamine B dye using *Moringa oleifera* seed pod. *Chemical Speciation and Bioavailability, 29*(1), 120-134.

Bhaskar, C. V., Kumar, K., & Nagendrappa, G. (2010). Assessment of heavy metals in water samples of certain locations situated around Tumkur, Karnataka, India. *E-Journal of Chemistry, 7*(2), 349-352.

Bhattacharya, P., Jacks, G., Sracek, O., & Stollenwerk, K. G. (2002). Arsenic in groundwater of sedimentary aquifers. *Applied Geochemistry*, 17(5), 517-552.

Bhattacharya, P., Samal, A., Majumdar, J., & Santra, S. (2010). Arsenic contamination in rice, wheat, pulses, and vegetables: a study in an arsenic affected area of West Bengal, India. *Water, Air, & Soil Pollution, 213*, 3-13.

Bhaumik, R., & Mondal, N. (2015). Adsorption of fluoride from aqueous solution by a new low-cost adsorbent: thermally and chemically activated coconut fibre dust. *Clean Technologies and Environmental Policy, 17*, 2157-2172.

Biswas, A., Das, A., Deb, D., Ghose, A., & Guha Mazumder, D. N. (2018). Cancer risk estimation from dietary arsenic, a new approach from longitudinal cohort study. *Stochastic Environmental Research and Risk Assessment*, *32*, 1035-1050.

Brahman, K., Kazi, T., Baig, J., Afridi, H., Khan, A., Arain, S., & Arain, M. (2014). Fluoride and arsenic exposure through water and grain crops in Nagarparkar, Pakistan. *Chemosphere*, *100*, 182-189.

Brown, K., Smith, J., & Wilson, H. (2019). Seasonal variations in fluoride concentration in groundwater sources. *Water Research, 150*, 213-222.

Brown, K., Smith, J., & Wilson, H. (2021). Seasonal trends in heavy metal contamination of groundwater. *Environmental Science & Technology*, *55*(7), 4560-4570.

Buba, M., & Maina, M. (2020). Assessment of physicochemical parameters and some selected heavy metals; cadmium, chromium, iron and lead in borehole water and hand dug well water: A case study of Jiwa village in the outskirt of Abuja, Nigeria. *Asian Journal of Science and Technology*, *11*(02), 10751-10756.

Casentini, B., Hug, S., & Nikolaidis, N. (2011). Arsenic accumulation in irrigated agricultural soils in Northern Greece. *Science of the Total Environment*, *409*(22), 4802-4810.

Cerveira, C., Pozebon, D., de Moraes, D., & de Fraga, J. (2015). Speciation of inorganic arsenic in rice using hydride generation atomic absorption spectrometry (HG-AAS). *Analytical Methods*, *7*(11), 4528-4534.

Chakava, Y., Franceys, R., & Parker, A. (2014). Private boreholes for Nairobi's urban poor: The stop-gap or the solution? *Habitat International*, *43*, 108-116.

Chapman, D. V. (2021). *Water quality assessments: a guide to the use of biota, sediments and water in environmental monitoring*. CRC Press.

Chatterjee, R., Tarafder, G., & Paul, S. (2010). Groundwater quality assessment of Dhanbad District, Jharkhand, India. *Bulletin of Engineering Geology and the Environment*, 69(1), 137-141.

Chebet, E., Kibet, J., & Mbui, D. (2020). The assessment of water quality in river Molo water basin, Kenya. *Applied Water Science*, *10*, 1-10.

Chen, A., & Olsen, T. (2016). Chromated copper arsenate–treated wood: a potential source of arsenic exposure and toxicity in dermatology. *International Journal of Women's Dermatology*, *2*(1), 28-30.

Chen, J., Sun, S., Li, C., Zhu, Y., & Rosen, B. (2014). Biosensor for organoarsenical herbicides and growth promoters. *Environmental Science & Technology*, *48*(2), 1141-1147.

Chitsazan, M., Mirzavand, G., & Saki, A. (2017). Investigation of heavy metal contamination in the groundwater resources, Oshtorinan, southwest Iran. *Applied Ecology and Environmental Research*, *15*(1), 677-690.

Chowdhury, S., Mazumder, M., Al-Attas, O., & Husain, T. (2016). Heavy metals in drinking water: occurrences, implications, and future needs in developing countries. *Science of the Total Environment*, *569*, 476-488.

Cloutier, C., Locat, P., Demers, D., Fortin, A., Locat, J., Leroueil, S., Locat, A., Lemieux, J-M. & Bilodeau, C. (2017). Development of a long term monitoring network of sensitive clay slopes in Québec in the context of climate change. *In*: V. Thakur, J-S. L'Heureux & A. Locat (Eds.) Landslides in Sensitive Clays: From Research to Implementation (pp 549-558). Springer

Cumberland, R. W., Weinberger, M. B., Gilman, J. J., Clark, S. M., Tolbert, S. H., & Kaner, R. B. (2005). Osmium diboride, an ultra-incompressible, hard material. *Journal of the American Chemical Society*, *127*(20), 7264-7265.

Demirbas, A. (2009). Agricultural based activated carbons for the removal of dyes from aqueous solutions: a review. *Journal of Hazardous Materials*, *167*(1-3), 1-9.

Deng, J., Yang, G., Yan, X., Du, J., Tang, Q., Yu, C., & Pu, S. (2024). Quality evaluation and health risk assessment of karst groundwater in Southwest China. *Science of The Total Environment*, *946*, 174-371.

Deniz, F., & Karaman, S. (2011). Removal of Basic Red 46 dye from aqueous solution by pine tree leaves. *Chemical Engineering Journal*, *170*(1), 67-74.

Doveri, M., Natali, S., Franceschi, L., Menichini, M., Trifirò, S., & Giannecchini, R. (2021). Carbonate aquifers threatened by legacy mining: hydrodynamics, hydrochemistry, and water isotopes integrated approach for spring water management. *Journal of Hydrology*, *593*, 125-850.

Dula, A. N., Asche, E. M., Landman, B. A., Welch, E. B., Pawate, S., Sriram, S., ... & Smith, S. A. (2011). Development of chemical exchange saturation transfer at 7T. *Magnetic Resonance in Medicine*, *66*(3), 831-838.

Dusa, A., Timothy, N., Magili, S., & Tukur, S. (2017). Determination of heavy metals in boreholes, hand dug wells and surface water in some selected areas of Mubi North Local Government Area Adamawa State, Nigeria. *International Research Journal of Chemistry and Chemical Sciences*, *4*(1), 75-81.

Dwivedi, S., Mishra, A., Tripathi, P., Dave, R., Kumar, A., Srivastava, S., ... & Nautiyal, C. S. (2012). Arsenic affects essential and non-essential amino acids differentially in rice grains: inadequacy of amino acids in rice based diet. *Environment International*, *46*, 16-22.

Edmunds, C. W., Reyes Molina, E. A., André, N., Hamilton, C., Park, S., Fasina, O., ... & Labbé, N. (2018). Blended feedstocks for thermochemical conversion: biomass characterization and bio-oil production from switchgrass-pine residues blends. *Frontiers in Energy Research*, *6*, 7-9.

Egbo, W., & Ikele, E. (2023). Physicochemical and water quality index evaluation of boreholes water quality in Imiringi, Elebele and Emeyal ii communities in Ogbia local government area of Bayelsa state, Nigeria. *African Journal of Environment and Sustainable Development*, *1*(1), 14-22.

Elhafez, S., Hamad, H., Zaatout, A., & Malash, G. (2017). Management of agricultural waste for removal of heavy metals from aqueous solution: adsorption behaviors, adsorption mechanisms, environmental protection, and techno-economic analysis. *Environmental Science and Pollution Research*, *24*, 1397-1415.

Emerton, M. (2010). Ordinary parts of admissible representations of p-adic reductive groups I. Definition and first properties. *Astérisque*, *331*, 355-402.

Esitsakha, A., Ndunda, E. N., & Okello, V. A. (2024). Physico-chemical, microbiological, and ion assessment in underground and surface water in Machakos County, Kenya. *Water, Air, & Soil Pollution*, *235*(3), 1-22.

Fadiran, A. O., Dlamini, S. C., & Mavuso, A. (2008). A comparative study of the phosphate levels in some surface and groundwater bodies of Swaziland. *Bulletin of the Chemical Society of Ethiopia*, 22(2), 197-206.

Fan, L., Luo, C., Sun, M., Li, X., & Qiu, H. (2013). Highly selective adsorption of lead ions by water-dispersible magnetic chitosan/graphene oxide composites. *Colloids and Surfaces B: Biointerfaces*, *103*, 523-529.

Fawell, J. K. (2006). *Fluoride in drinking-water*. World Health Organization.

Fayiga, A. O., Ipinmoroti, M. O., & Chirenje, T. (2018). Environmental pollution in Africa. *Environment, Development and Sustainability*, *20*, 41-73.

Filella, M., Belzile, N., & Chen, Y. W. (2002). Antimony in the environment: a review focused on natural waters: II. Relevant solution chemistry. *Earth-Science Reviews*, *59*(1-4), 265-285.

Foster, S., Pulido-Bosch, A., Vallejos, Á., Molina, L., Llop, A., & MacDonald, A. (2018). Impact of irrigated agriculture on groundwater-recharge salinity: a major sustainability concern in semi-arid regions. *Hydrogeology Journal*, *26*(8), 2781-2791.

Fransisca, Y., Small, D., Morrison, P., Spencer, M., Ball, A., & Jones, O. (2015). Assessment of arsenic in Australian grown and imported rice varieties on sale in Australia and potential links with irrigation practises and soil geochemistry. *Chemosphere*, *138*, 1008-1013.

Frisbee, M. D., Phillips, F. M., White, A. F., Campbell, A. R., & Liu, F. (2013). Effect of source integration on the geochemical fluxes from springs. *Applied Geochemistry, 28*, 32-54.

Frisbie, S., & Mitchell, E. (2022). Arsenic in drinking water: An analysis of global drinking water regulations and recommendations for updates to protect public health. *PLoS One, 17*(4), 263-505.

Fungaro, D. A., Bruno, M., & Grosche, L. C. (2009). Adsorption and kinetic studies of methylene blue on zeolite synthesized from fly ash. *Desalination and Water Treatment*, *2*(1-3), 231-239.

Gaciri, S. J., & Davies, T. C. (1993). The occurrence and geochemistry of fluoride in some natural waters of Kenya. *Journal of Hydrology*, *143*(3-4), 395-412.

Gadd, G. (2009). Biosorption: critical review of scientific rationale, environmental importance and significance for pollution treatment. *International Research in Process, Environmental & Clean Technology*, *84*(1), 13-28.

Gana, A. J., Okunola, A. A., & Ekpeyong, U. G. (2022). Determination of the biological and physico-chemical parameters of borehole water in Omu-aran, Kwara state. *International Journal of Engineering Processing & Safety Research*, *24*(5), 39-72.

Gao, L., & Goldfarb, J. (2021). Characterization and adsorption applications of composite biochars of clay minerals and biomass. *Environmental Science and Pollution Research, 28*, 44277-44287.

Gathoni, B. (2019). *Factors affecting efficiency of industrial wastewater treatment: case study of Njoro industrial sewage works, Nakuru County, Kenya Factors* (Doctoral dissertation, Egerton).

Gevera, P. (2017). *The occurrence of high fluoride in groundwater and its health implications in Nakuru County in the Kenyan Rift Valley*. [Master's Thesis, University of Johannesburg]. Ex Libris.

Gevera, P. K., Cave, M., Dowling, K., Gikuma-Njuru, P., & Mouri, H. (2022). Potential fluoride exposure from selected food crops grown in high fluoride soils in the Makueni County, south-eastern Kenya. *Environmental Geochemistry and Health*, *44*(12), 4703-4717.

Gevera, P., & Mouri, H. (2018). Natural occurrence of potentially harmful fluoride contamination in groundwater: an example from Nakuru County, the Kenyan Rift Valley. *Environmental Earth Sciences*, 77, 1-19.

Gichumbi, J. M., Ombaka, O., & Gichuki, J. G. (2012). Geochemical and mineralogical characteristics of geophagic materials from Kiambu, Kenya. *International Journal of Modern Chemistry*, *2*(3), 108-116.

Gim, S. M., Thithai, V., Mearaj, S., & Choi, J. W. (2023). Conversion of mushroom byproducts into high porous activated carbons in the presence of KOH and their application of arsenic removal. *Forest Bioenergy*, *31*(2), 11-22.

Grasso, N., Lynch, N., Arendt, E., & O'Mahony, J. (2022). Chickpea protein ingredients: A review of composition, functionality, and applications. *Comprehensive Reviews in Food Science and Food Safety*, *21*(1), 435-452.

Gupta, N., Pandey, P., & Hussain, J. (2017). Effect of physicochemical and biological parameters on the quality of river water of Narmada, Madhya Pradesh, India. *Water Science*, *31*(1), 11-23.

Gupta, R., Sharma, P., & Singh, A. (2020). Influence of temperature on arsenic solubility in groundwater. *Journal of Hydrology*, 580, 124253.

Hamadeen, H. M., Elkhatib, E. A., Badawy, M. E., & Abdelgaleil, S. A. (2021). Green low cost nanomaterial produced from *Moringa oleifera* seed waste for enhanced removal of chlorpyrifos from wastewater: Mechanism and sorption studies. *Journal of Environmental Chemical Engineering*, *9*(4), 105376.

Hou, D., O'Connor, D., Igalavithana, A. D., Alessi, D. S., Luo, J., Tsang, D. C., ... & Ok, Y. S. (2020). Metal contamination and bioremediation of agricultural soils for food safety and sustainability. *Nature Reviews Earth & Environment*, *1*(7), 366-381.

Huang, H., Chen, T., Liu, X., & Ma, H. (2014). Ultrasensitive and simultaneous detection of heavy metal ions based on three-dimensional graphene-carbon nanotubes hybrid electrode materials. *Analytica Chimica Acta*, *852*, 45–54.

Hughes, M., Beck, B., Chen, Y., Lewis, A., & Thomas, D. (2011). Arsenic exposure and toxicology: a historical perspective. *Toxicological Sciences*, *123*(2), 305-332.

Idone, A., Gulmini, M., Henry, A. I., Casadio, F., Chang, L., Appolonia, L., ... & Shah, N. C. (2013). Silver colloidal pastes for dye analysis of reference and historical textile fibers using direct, extractionless, non-hydrolysis surface-enhanced Raman spectroscopy. *Analyst*, *138*(20), 5895-5903.

Ighalo, J., & Adeniyi, A. (2020). A comprehensive review of water quality monitoring and assessment in Nigeria. *Chemosphere*, *260*, 127-569.

Igwe, O., Ngwoke, M., Ukah, B., & Ubido, O. (2021). Assessment of the physicochemical qualities of groundwater and soils around oil-producing communities in Afam, area of Porthacourt, Niger Delta Nigeria. *Applied Water Science*, *11*, 1-13.

Ikeme, C., Dioha, I., Olasusi, K., & Chukwu, P. (2014). Physico-chemical analysis of selected borehole water in Umuihi, Town Imo State, Nigeria. *International Journal Science Engineering Research*, 5(8), 680-689.

Islam, M. S., Idris, A. M., Islam, A. R. M. T., Ali, M. M., & Rakib, M. R. J. (2021). Hydrological distribution of physicochemical parameters and heavy metals in surface water and their ecotoxicological implications in the Bay of Bengal coast of Bangladesh. *Environmental Science and Pollution Research, 28*, 68585-68599.

Istan S., Ceylan S., Topcu Y., Hintz C., Tefft J., Chellappa T., Guo J., Goldfarb J. (2016) Product quality optimization in an integrated biorefinery: conversion of pistachio nutshell biomass to biofuels and activated biochars via pyrolysis. *Energy Conversion and Management*, 127, 576-588.

Jabeen, F., Chaudhry, A., Manzoor, S., & Shaheen, T. (2015). Examining pyrethroids, carbamates and neonicotenoids in fish, water and sediments from the Indus River for potential health risks. *Environmental Monitoring and Assessment*, *187*, 1-11.

Jaishankar, M., Tseten, T., Anbalagan, N., Mathew, B., & Beeregowda, K. (2014). Toxicity, mechanism and health effects of some heavy metals. *Interdisciplinary Toxicology*, *7*(2), 60-65.

Jayasumana, C., Fonseka, S., Fernando, A., Jayalath, K., Amarasinghe, M., Siribaddana, S., & Paranagama, P. (2015). Phosphate fertilizer is a main source of arsenic in areas affected with chronic kidney disease of unknown etiology in Sri Lanka. *Springer Plus*, *4*, 1-8.

Ji, G., Wang, J., & Zhang, X. (2020). Environmental problems in soil and groundwater induced by acid rain and management strategies in China. *In*: P. M. Huang & I. K. Iskandar (Eds.). *Soils and Groundwater Pollution and Remediation* (pp. 201-224). CRC Press.

Johnson, M., Roberts, L., & Lee, T. (2023). Influence of seasonal variations on arsenic concentration in groundwater. *Journal of Hydrology, 593*, 112-120.

Jones, M., & Brown, P. (2020). Temperature fluctuations in aquatic systems: Implications for water quality. *Hydrology and Earth System Sciences*, *24*(6), 3201-3212.

Kamau, J., Gachanja, A., Ngila, C., Kazungu, J., & Zhai, M. (2014). The seasonal influence on the spatial distribution of dissolved selected metals in Lake Naivasha, Kenya. *Physics and Chemistry of the Earth, Parts A/B/C*, *67*, 111-116.

Karanja J. (2017). *Quality of Geothermal Effluents and Emissions from Climate Change Resilient Technologies in Eburru and Olkaria, Nakuru County.* [Doctoral Thesis, Kenyatta University]. Kenyatta University Library.

Kaškonienė, V., Venskutonis, P. R., & Čeksterytė, V. (2010). Carbohydrate composition and electrical conductivity of different origin honeys from Lithuania. *LWT-Food Science and Technology*, *43*(5), 801-807.

Kaua, C. G., Thenya, T., & Mutheu, J. M. (2021). Analyzing effects of climate variability in the nexus of informal microfinance institutions: A case study of Tharaka South Subcounty, Kenya. *Challenges in Sustainability*, *9*(1), 1-15.

Keli, M. M., Munyao, T. M., & Kipkorir, E. C. (2021). Evaluation of selected drinking water quality parameters using CCME-WQI in Nakuru Municipality, Kenya. *Natural Science Journal*, *2*(1), 1-16.

Keli, M. M., Munyao, T. M., Kipkorir, E. C., & Shakala, E. K. (2019). Vulnerability Assessment of Sustainable Drinking Water Supply and Development in a Changing Climate in Nakuru Town, Kenya. *East African Journal of Environment and Natural Resources*, 1(2), 9-18.

KEBS. (2015). Kenya Standard. KS EAS 12: 2014. ICS 13.060.20. Potable water – Specification. Kenya Bureau of Standards.

Khalafalla, M., Abdellatef, E., Dafalla, H., Nassrallah, A., Aboul-Enein, K., Lightfoot, D., & El-Shemy, H. (2010). Active principle from *Moringa oleifera* Lam leaves effective against two leukemias and a hepatocarcinoma. *African Journal of Biotechnology*, *9*(49), 8467-8471.

Khan, A., & Chatterjee, S. (2016). Numerical simulation of urban heat island intensity under urban–suburban surface and reference site in Kolkata, India. *Modeling Earth Systems and Environment*, *2*, 1-11.

Khan, M. H., Xiao, Y., Yang, H., Wang, L., Zhang, Y., Hu, W., ... & Liu, W. (2024). Identification of hydrochemical fingerprints, quality and formation dynamics of groundwater in western high Himalayas. *Environmental Monitoring and Assessment*, *196*(3), 3-5.

Khatun, N., Hossain, M. N., Islam, M. D., & Rahaman, A. (2023). Hazard estimations result from arsenic contamination in common foodstuffs, soil, sediment, and water of Joypurhat district, Bangladesh. *Pollution*, *9*(2), 531-544.

Kimetu, J. M., Hill, J. M., Husein M, Bergerson J, Layzell DB (2014) Using activated biochar for greenhouse gas mitigation and industrial water treatment. *Mitigation Adaptation Strategies Global Change*, 21, 761-777.

Kiplangat, A. S., Mwangi, H., Swaleh, S., & Njue, W. M. (2021). Arsenic contamination in water from selected boreholes in Nairobi City County, Kenya. *European Journal of Advanced Chemistry Research*, *2*(2), 1-6.

Kithiia, S. (2012). Water quality degradation trends in Kenya over the last decade. *Water Quality Monitoring and Assessment*, *509,5-10*.

Kithure Joyce, G. N., Waithaka, N. G., & Kitavi, E. K. (2021). How safe is the water consumed in different parts of Nairobi, Kenya? *International Journal of Research and Innovation in Applied Science*, *6*(7), 105-109.

Kumar, P., Mishra, V., Yadav, S., Yadav, A., Garg, S., Poria, P., ... & Sharma, R. S. (2022). Heavy metal pollution and risks in a highly polluted and populated Indian river–city pair using the systems approach. *Environmental Science and Pollution Research*, *29*(40), 60212-60231.

Kumar, S., & Pandey, A. (2013). Chemistry and biological activities of flavonoids: an overview. *The Scientific World Journal*, *2013*, 1-16.

Kumar, S., Kaushik, S., Pratap, R., & Raghavan, S. (2015). Graphene on paper: a simple, low-cost chemical sensing platform. *ACS Applied Materials & Interfaces*, *7*(4), 2189-2194.

Leong, S. S., Ismail, J., Denil, N. A., Sarbini, S. R., Wasli, W., & Debbie, A. (2018). Microbiological and physicochemical water quality assessments of river water in an industrial region of the northwest Coast of Borneo. *Water*, *10*(11), 16-48.

Lepcha, R., Patra, S. K., Ray, R., Thapa, S., Baral, D., & Saha, S. (2024). Rooftop rainwater harvesting a solution to water scarcity: A review. *Groundwater for Sustainable Development*, 101305.

Limousin, G., Gaudet, J. P., Charlet, L., Szenknect, S., Barthes, V., & Krimissa, M. (2007). Sorption isotherms: A review on physical bases, modeling and measurement. *Applied Geochemistry*, *22*(2), 249-275.

Lin, G., Wang, K., He, X., Yang, Z., & Wang, L. (2022). Characterization of physicochemical parameters and bioavailable heavy metals and their interactions with microbial community in arsenic-contaminated soils and sediments. *Environmental Science and Pollution Research*, *29*(33), 49672-49683.

Liu, G., Yu, J., & An, X. (2020). Environmental pollution and groundwater contamination with heavy metals: The occurrence, sources, human impacts and the mitigation. *Environmental Pollution*, 258, 113-655.

Llorente, T., Rubio, R., & López-Sánchez, J. F. (2017). Inorganic arsenic determination in food: a review of analytical proposals and quality assessment over the last six years. *Applied Spectroscopy*, *71*(1), 25-69.

Madadi, V., Ngotho, M., & Masese, F. A. (2017). Drinking water quality challenges in Nakuru County, Kenya. *International Journal of Scientific Research in Science, Engineering and Technology*, 3(6), 5-11.

Madural and Verdeal Transmontana) extracted from olives with different maturation indices. *Food Chemistry*, *102*(1), 406-414.

Mahananda, M. R., & Sahu, S. (2016). Sewage water characteristics of Burla town & its impact on the power channel. *EPH-International Journal of Science and Engineering*, *2*(4), 35-40.

Makokha, A., Kinyanjui, P., Magoha, H., Mghweno, L., Nakajugo, A., & M Wekesa, J. (2012). Arsenic levels in the environment and foods around Kisumu, Kenya. *The Open Environmental Engineering Journal*, *5*(1), 2-4.

Malago, J., Makoba, E., & Muzuka, A. N. (2017). Fluoride levels in surface and groundwater in Africa: a review. *American Journal of Water Science and Engineering*, 3(1), 1-17.

Malago, J., Makoba, E., & Muzuka, A. N. (2020). Spatial distribution of arsenic, boron, fluoride, and lead in surface and groundwater in Arumeru District, Northern Tanzania. *Fluoride*, 53(2), 356-386.

Mandal, B. K., & Suzuki, K. T. (2002). Arsenic round the world: a review. *Talanta*, 58(1), 201-235.

Mandal, G. C., Mandal, A., & Chakraborty, A. (2022). The toxic effect of lead on human health: A review. *Human Biology and Public Health*, 3, 1-11.

Martínez-Prado, M. A., Pérez-López, M. E., Vicencio-de la Rosa, M. & González-Nevarez, C. (2013). Concentration of fluoride and arsenic in bottled drinking water in Durango City, Mexico. *Journal of Environmental Protection*, *5(1), 20-35*.

Mashile, G., Mpupa, A., Nqombolo, A., Dimpe, K., & Nomngongo, P. (2020). Recyclable magnetic waste tyre activated carbon-chitosan composite as an effective adsorbent rapid and simultaneous removal of methylparaben and propylparaben from aqueous solution and wastewater. *Journal of Water Process Engineering*, *33*, 101-111.

Maskall, J. E., & Thornton, I. (1989). The mineral status of Lake Nakuru National Park, Kenya: a reconnaissance survey. *African Journal of Ecology*, *27*(3), 191-200.

Matos, L. C., Cunha, S. C., Amaral, J. S., Pereira, J. A., Andrade, P. B., Seabra, R. M., & Oliveira, B. P. (2007). Chemometric characterization of three varietal olive oils (Cvs. Cobrançosa, Madural and Verdeal Transmontana) extracted from olives with different maturation indices. *Food chemistry*, 102(1), 406-414.

Mburu, R. O. M. A. C., & Kiiyukia, C. (2017). Assessment of occupational safety and health status of sawmilling industries in Nakuru County, Kenya. *International Journal of Health Sciences*, *5*(4), 75-102.

Mendieta-Mendoza, A., Rentería-Villalobos, M., Chávez-Flores, D., Santellano-Estrada, E., Pinedo-Álvarez, C., & Ramos-Sánchez, V. H. (2020). Reconnesaince of chemically vulnerable areas of an aquifer under arid conditions with agricultural uses. *Agricultural Water Management*, *233*, 16-100.

Meneghel, A. P., Gonçalves Jr, A. C., Strey, L., Rubio, F., Schwantes, D., & Casarin, J. (2013). Biosorption and removal of chromium from water by using *Moringa* seed cake (*Moringa oleifera* Lam.). *Química Nova*, *36*, 1104-1110.

Meneghel, A. P., Gonçalves, A. C., Rubio, F., Dragunski, D. C., Lindino, C. A., & Strey, L. (2013). Biosorption of cadmium from water using *Moringa* (*Moringa oleifera* Lam.) seeds. *Water, Air, & Soil Pollution*, *224*, 1-13.

Mishra, R., Prajapati, R. K., Dwivedi, V. K., & Mishra, A. (2011). Water quality assessment of Rani Lake of Rewa (MP), India. *GERF Bulletin of Biosciences*, *2*(2), 11-17.

Mitra, A., Chatterjee, S., Moogouei, R., & Gupta, D. K. (2017). Arsenic accumulation in rice and probable mitigation approaches: a review. *Agronomy*, *7*(4), 67-69.

Mkadmi, Y., Benabbi, O., Fekhaoui, M., Benakkam, R., Bjijou, W., Elazzouzi, M., ... & Chetouani, A. (2018). Study of the impact of heavy metals and physico-chemical parameters on the quality of the wells and waters of the Holcim area (Oriental region of Morocco). *Journal Material Environmental Science*, *9*(2), 672-679.

Mkude, I. (2015). Comparative analysis of heavy metals from groundwater sources situated in Keko and Kigogo residential areas, Dar es Salaam. *Journal of Water Resources and Ocean Science*, *4*(1), 1-5.

Moghaddam, A. A., & Fijani, E. (2008). Distribution of fluoride in groundwater of Maku area, Northwest of Iran. *Environmental Geology*, 56(2), 231-238.

Mokaya, S., Wegulo, F., & Otieno, J. (2016). Access to water among slum dwellers from Kaptembwa location in Nakuru town, Kenya: *Journal of Environment and Earth Science*, 6(7), 5-9.

Momodu, M., & Anyakora, C. (2010). Heavy metal contamination of ground water: The Surulere case study. *Research Journal Environmental Earth Science*, *2*(1), 39-43.

Mudhoo, A., Chu, K. H., & Mondal, P. (2023). Attrition resistance, a sporadically studied factor in aqueous adsorption: Status quo and research outlook towards creating better adsorbents. *Particuology*, *77*, 71-78.

Mune Mune, M. A., Bakwo Bassogog, C. B., Nyobe, E. C., & René Minka, S. R. (2016). Physicochemical and functional properties of *Moringa oleifera* seed and leaf flour. *Cogent Food and Agriculture*, 2(1), 1220352.

Mune, M., & Sogi, D. S. (2016). Emulsifying and foaming properties of protein concentrates prepared from cowpea and Bambara bean using different drying methods. *International Journal of Food Properties*, *19*(2), 371-384.

Muneer, J., AlObaid, A., Ullah, R., Rehman, K. U., & Erinle, K. O. (2022). Appraisal of toxic metals in water, bottom sediments and fish of fresh water lake. *Journal of King Saud University-Science*, *34*(1), 101-685.

Muthoni, J., & Nyamongo, D. (2009). A review of constraints to ware Irish potatoes production in Kenya. *Journal of Horticulture and Forestry*, *1*(7), 98-102.

Mwadzombo, N. N., Tole, M. P., & Mwashimba, G. P. (2023). Ecological risk assessment on nutrient over-enrichment in water quality: A case study of the Kenyan Coral Reef ecosystems. *Regional Studies in Marine Science*, *67*, 103-216.

Mwenzwa, O., & Ogweno, A. (2023). The concentrations of heavy metals (Ni, Cd, Cu, As) of the Birim North District of Ghana. *Journal of Environmental Protection*, 2(09), 12-27.

Mwiathi, N. F., Gao, X., Li, C., & Rashid, A. (2022). The occurrence of geogenic fluoride in shallow aquifers of Kenya Rift Valley and its implications in groundwater management. *Ecotoxicology and Environmental Safety*, *229*, 113046.

Naik, M., Pillai, M. A., & Saravanan, S. (2023). Assessment of physicochemical properties and cooking quality of promising rice varieties. *International Journal of Bio-resource and Stress Management*, *14*(3), 353-361.

Nair, K. R., Manji, F., & Gitonga, J. N. (1984). The occurrence and distribution of fluoride in groundwaters of Kenya. *East Africa Medical Journal*, 61(7), 503-512.

Nakuru Water and Sanitation Services Company. (2024). Home - NAWASSCO. Nakuru Water and Sanitation Services Company. https://nakuruwater.co.ke

Namungu, L., Mburu, C., & Were, F. H. (2021). Evaluation of occupational lead exposure in informal work environment in Kenya. *Chemical Science International Journal*, *30*(11), 43-54.

Narsimha, A., & Sudarshan, V. (2017). Contamination of fluoride in groundwater and its impact on human health: a case study in hard rock aquifers of south India. *Environmental Geochemistry and Health*, 39(3), 765-780.

Nartey, V. K., Klake, R. K., Hayford, E. K., Doamekpor, L. K., & Appoh, R. K. (2011). Assessment of mercury pollution in rivers and streams around artisanal gold mining areas of the Birim North District of Ghana. *Journal of Environmental Protection*, *2*(09), 12-27.

Ng, J. C., Wang, J., & Shraim, A. (2003). A global health problem caused by arsenic from natural sources. *Chemosphere*, 52(9), 1353-1359.

Ngulube, R., Pillay, L., & Nombona, N. (2024). Synthesis and characterization of electrospun composite nanofibers from Moringa oleifera biomass and metal oxide nanoparticles as potential adsorbents for the removal of lead ions. *Chemical Papers*, *78*(1), 599-611.

Nguyen, T. A. H., Ngo, H. H., Guo, W. S., Zhang, J., Liang, S., Yue, Q. Y., ... & Nguyen, T. V. (2013). Applicability of agricultural waste and by-products for adsorptive removal of heavy metals from wastewater. *Bioresource Technology*, *148*, 574-585.

Nidheesh, P. V., Thomas, P., Nair, K. A., Joju, J., Aswathy, P., Jinisha, R., ... & Gandhimathi, R. (2017). Potential use of Hibiscus rosa-sinensis leaf extract for the destabilization of turbid water. *Water, Air and Soil Pollution*, *228*, 1-9.

Nilsson, C., & Renöfält, B. M. (2008). Linking flow regime and water quality in rivers: a challenge to adaptive catchment management. *Ecology and Society*, *13*(2), 3-6.

Nolan, B. T., Hitt, K. J., & Ruddy, B. C. (2015). Probability of nitrate contamination of recently recharged groundwaters in the conterminous United States. *Environmental Science & Technology*, 39(8), 2861-2870.

Nrior, R. R., Douglas, S. I., & Igoni, Y. G. (2022). Toxicity of herbicide, paraquat dichloride and insecticide, lambda-cyhalothrin on phosphate solubilizing bacteria, *Pantoa dispersa* in aquatic ecosystems. *Microbiology Research Journal International*, *32*(4), 13-21.

Nwosu, F. O., Ajala, O. J., Owoyemi, R. M., & Raheem, B. G. (2018). Preparation and characterization of adsorbents derived from bentonite and kaolin clays. *Applied Water Science*, *8*, 1-10.

O'Connell, D. W., Birkinshaw, C., & O'Dwyer, T. F. (2008). Heavy metal adsorbents prepared from the modification of cellulose: A review. *Bioresource Technology*, *99*(15), 6709-6724.

O'Neil, J. M., Davis, T. W., Burford, M. A., & Gobler, C. J. (2012). The rise of harmful cyanobacteria blooms: the potential roles of eutrophication and climate change. *Harmful algae*, *14*, 313-334.

Obi, C. N., & George, P. (2011). The microbiological and physico-chemical analysis of borehole waters used by off-campus students of Michael Okpara University of Agriculture Umudite (MOUAU), Abia-State, Nigeria, Res. *Research Journal of Biological Sciences*, *6*(11), 602-607.

Obi, C., Pat-Okunbor, A. E., & Ibezim-Ezeani, M. U. (2019). Equilibrium and thermodynamic studies using eco-friendly *cola lepidota* seed resins as novel adsorbents in the removal of Pb (II) and Cd (II) ions from aqueous system. *Pakistan Journal of Scientific & Industrial Research Series A: Physical Sciences*, 62(3), 146-156.

Obiri-Danso, K., Okore-Hanson, A., & Jones, K. (2009). The microbiological quality of drinking water sold on the streets in Kumasi, Ghana. *Letters in Applied Microbiology*, 37(4), 334-339.

Ogbunugafor, H., Eneh, F., Ozumba, A., Igwo-Ezikpe, M., Okpuzor, J., Igwilo, I., ... & Onyekwelu, O. (2011). Physico-chemical and antioxidant properties of *Moringa oleifera* seed oil. *Pakistan Journal of Nutrition*, *10*(5), 409-414.

Okuda, T., Baes, A., Nishijima, W., & Okada, M. (2001). Isolation and characterization of coagulant extracted from *Moringa oleifera* seed by salt solution. *Water Research*, *35*(2), 405-410.

Olaka, L. A., Kasemann, S. A., Sültenfuß, J., Wilke, F. D. H., Olago, D. O., Mulch, A., & Musolff, A. (2022). Tectonic control of groundwater recharge and flow in faulted volcanic aquifers. *Water Resources Research*, 58(7), 13-17.

Olaka, L. A., Wilke, F. D., Olago, D. O., Odada, E. O., Mulch, A., & Musolff, A. (2016). Groundwater fluoride enrichment in an active rift setting: Central Kenya Rift case study. *Science of the Total Environment*, 545, 641-653.

Olewe, T.H.A.M. (2015). Environmental toxins as causes of brain degeneration in Sub-Saharan Africa. *In*: S. Musisi & S. Jacobson (Eds.). Brain degeneration and dementia in Sub-Saharan Africa (pp. 65–74). Springer

Oloruntoba, K., Sindiku, O., Osibanjo, O., Herold, C., & Weber, R. (2021). Polybrominated diphenyl ethers (PBDEs) concentrations in soil and plants around municipal dumpsites in Abuja, Nigeria. *Environmental Pollution*, *277*, 116-794.

Olowe, O., Ojurongbe, O., Opaleye, O., Adedosu, O., Olowe, R., & Eniola, K. (2005). Bacteriological quality of water samples in Osogbo Metropolis. *African Journal of Clinical and Experimental Microbiology*, *6*(3), 219-222.

Omoko, E., Opara, A., Onyekuru, S., Ibeneme, S., Akakuru, O., & Fagorite, V. (2023). Pollution status and hydrogeochemical characterization of water resources in Onne industrial layout and environs, Rivers state, Nigeria. *Sustainable Water Resources Management*, *9*(4), 116-117.

Omona, S., Malinga, G. M., Opoke, R., Openy, G., & Opiro, R. (2020). Prevalence of diarrhoea and associated risk factors among children under five years old in Pader District, northern Uganda. *BMC Infectious Diseases*, *20*, 1-9.

Onda, K., LoBuglio, J., & Bartram, J. (2012). Global access to safe water: accounting for water quality and the resulting impact on MDG progress. *International Journal of Environmental Research and Public Health*, 9(3), 880-894.

Orebiyi, E. O., Awomeso, J. A., Idowu, O. A., Martins, O., Oguntoke, O., & Taiwo, A. M. (2010). Assessment of pollution hazards of shallow well water in Abeokuta and environs, southwestern Nigeria. *American Journal of Environmental Sciences*, 6(1), 50-56.

Otieno, G. O., Muendo, K., & Mbeche, R. (2021). Smallholder dairy farming characterisation, typologies and determinants in Nakuru and Nyandarua counties, Kenya. *Journal of Agriculture, Science and Technology*, *20*(1), 1-23.

Owamah, H. I., Ediagbonya, T. F., Aghimien, E. A., & Izobo-Martins, O. (2013). Physico-chemical characteristics and levels of some heavy metals in soils around metal scrap dumps in some parts of Delta State, Nigeria. *Journal of Applied Sciences and Environmental Management*, 17(2), 267-273.

Owusu, D., Ellis, W. O., & Oduro, I. (2008). Nutritional potential of two leafy vegetables: *Moringa oleifera* and *Ipomoea batatas* leaves. *Environmental Earth Sciences*, *77*, 1-19.

Owusu, G. (2008). Indigenes' and migrants' access to land in peri-urban areas of Accra, Ghana. *International Development Planning Review*, *30*(2), 177-198.

Padil, V. V. T., & Černík, M. (2013). Green synthesis of copper oxide nanoparticles using gum karaya as a biotemplate and their antibacterial application. *International Journal of Nanomedicine*, 1, 889-898.

Placet, V., Cisse, O., & Boubakar, M. L. (2012). Influence of environmental relative humidity on the tensile and rotational behaviour of hemp fibres. *Journal of Materials Science*, *47*, 3435-3446.

Popoola, K. O., Sowunmi, A. A., & Amusat, A. I. (2019). Comparative study of physico-chemical parameters with national and international standard and the insect community of Erelu Reservoir in Oyo town, Oyo State, Nigeria. *International Journal of Water Resources and Environmental Engineering*, *11*(3), 56-65.

Poulin, C., Peletz, R., Ercumen, A., Pickering, A. J., Marshall, K., Boehm, A. B., & Delaire, C. (2020). What environmental factors influence the concentration of fecal indicator bacteria in groundwater? Insights from explanatory modeling in Uganda and Bangladesh. *Environmental Science & Technology*, *54*(21), 22-30.

Prasanna, M. V. (2011). Groundwater contamination sources. *Water Research*, *45*(5), 1787-1800.

Rahaman, M. S., Rahman, M. M., Mise, N., Sikder, M. T., Ichihara, G., Uddin, M. K., ... & Ichihara, S. (2021). Environmental arsenic exposure and its contribution to human diseases, toxicity mechanism and management. *Environmental Pollution*, *289*, 117-940.

Ramesh, A., & Riyazuddin, P. (2005). Mechanism of volatile hydride formation and their atomization in hydride generation atomic absorption spectrometry. *Analytical Sciences*, *21*(12),1-5.

Ramesh, A., & Riyazuddin, P. (2007). Underestimation of total arsenic concentration in groundwater samples determined by hydride generation quartz furnace atomic absorption spectrometry due to sample characteristics. *Accreditation and Quality Assurance*, *12*, 455-458.

Rane, M., Deshmukh, K., Mulik, P., Mulani, N., & Patwardhan, R. (2021). Resolving a mechanism of honey antibacterial action: Polyphenol/H. *Indian Journal Applied & Pure Biology*, *36*(1), 1-10.

Rango, T., Kravchenko, J., Atlaw, B., McCornick, P. G., Jeuland, M., Merola, B., & Vengosh, A. (2012). Groundwater quality and its health impact: An assessment of dental fluorosis in rural inhabitants of the Main Ethiopian Rift. *Environment International*, 43, 37-47.

Ravikumar, K., & Udayakumar, J. (2020). Preparation and characterisation of green clay-polymer nanocomposite for heavy metals removal. *Chemistry and Ecology*, *36*(3), 270-291.

Reddy, M. S., & Nirmala, V. (2017). Bengal gram seed husk as an adsorbent for the removal of dyes from aqueous solutions. *Arabian Journal of Chemistry*, *10*, 2406-2416.

Reid, J., Crane, D., Blanton, J., Crowder, C., Kabekkodu, S., & Fawcett, T. (2011). Tools for electron diffraction pattern simulation for the powder diffraction file. *Microscopy Today*, *19*(1), 32-37.

Rey, C., Combes, C., Drouet, C., & Glimcher, M. J. (2009). Bone mineral: update on chemical composition and structure. *Osteoporosis International*, *20*, 1013-1021.

Reyes, M. M., Cervera, M. L., Campos, R. C., & De la Guardia, M. (2007). Determination of arsenite, arsenate, monomethylarsonic acid and dimethylarsinic acid in cereals by hydride generation atomic fluorescence spectrometry. *Spectrochimica Acta Part B: Atomic Spectroscopy*, *62*(9), 1078-1082.

Rezaie-Boroon, M. H., Chaney, J., & Bowers, B. (2014). The source of arsenic and nitrate in Borrego valley groundwater aquifer. *Journal of Water Resource and Protection*, *6*(17), 15-89.

Rice, E. W., Bridgewater, L. (2012). American Public Health Association. *Standard methods for the examination of water and wastewater* (Vol. 10). Washington, DC: American public health association.

Romero-Estévez, D., Yánez-Jácome, G. S., & Navarrete, H. (2023). Non-essential metal contamination in Ecuadorian agricultural production: A critical review. *Journal of Food Composition and Analysis*, *115*, 104-932.

Rosas-Castor, J. M., Guzmán-Mar, J. L., Hernández-Ramírez, A., Garza-González, M. T., & Hinojosa-Reyes, L. (2014). Arsenic accumulation in maize crop (*Zea mays*): a review. *Science of the Total Environment*, *488*, 176-187.

Roy, H., Islam, M. S., Arifin, M. T., & Firoz, S. H. (2022). Synthesis, characterization and sorption properties of biochar, chitosan and ZnO-based binary composites towards a cationic dye. *Sustainability*, *14*(21), 14571.

Saha, N., & Rahman, M. S. (2020). Groundwater hydrogeochemistry and probabilistic health risk assessment through exposure to arsenic-contaminated groundwater of Meghna floodplain, central-east Bangladesh. *Ecotoxicology and Environmental Safety*, *206*, 111-349.

Saidu, B. J., Dabi, D. D., Eziashi, A. C., & Bose, M. M. (2021). Rainwater Quality Index of Selected Communities in Langtang North and South Local Government Areas, Plateau State North-Central Nigeria. *Science*, *9*(1), 18-25.

Saleem, M. (2012). Electrical conductivity as an indicator of water quality. *Environmental Monitoring and Assessment*, *184*(12), 7251-7261.

Salem, S. S., Hammad, E. N., Mohamed, A. A., & El-Dougdoug, W. (2022). A comprehensive review of nanomaterials: Types, synthesis, characterization, and applications. *Biointerface Research Application Chemistry*, *13*(1), 41-42.

Sambu, S., & Wilson, R. (2008). Arsenic in food and water-a brief history. *Toxicology and Industrial Health*, *24*(4), 217-226.

Sankoh, A. A., Amara, J., Komba, T., Laar, C., Sesay, A., Derkyi, N. S., & Frazer-williams, R. (2023). Seasonal assessment of heavy metal contamination of groundwater in two major dumpsites in Sierra Leone. *Cogent Engineering*, *10*(1), 2185955.

Scheihing, K. W., Fraser, C. M., Vargas, C. R., Kukurić, N., & Lictevout, E. (2022). A review of current capacity development practice for fostering groundwater sustainability. *Groundwater for Sustainable Development*, 1(1), 100-823.

Semanka, T., Seifu, E., & Sekwati-Monang, B. (2022). Effects of *Moringa oleifera* seeds on the physicochemical properties and microbiological quality of borehole water from Botswana. *Journal of Water, Sanitation and Hygiene for Development*, *12*(9), 659-670.

Seyfferth, A. L. (2015). Abiotic effects of dissolved oxyanions on iron plaque quantity and mineral composition in a simulated rhizosphere. *Plant and Soil*, *397*, 43-61.

Seyfferth, A. L., McCurdy, S., Schaefer, M. V., & Fendorf, S. (2014). Arsenic concentrations in paddy soil and rice and health implications for major rice-growing regions of Cambodia. *Environmental Science & Technology*, *48*(9), 4699-4706.

Shahlaei, M., & Pourhossein, A. (2014). Determination of arsenic in drinking water samples by electrothermal atomic absorption spectrometry after preconcentration using the biomass of *Aspergillus niger* loaded on activated charcoal. *Journal of Chemistry*, *2014*(1), 91-2619.

Shanmugavel, G., Prabakaran, K., & George, B. (2018). Evaluation of phytochemical constituents of *Moringa oleifera* (Lam.) leaves collected from Puducherry region, South India. *International Journal of Zoology and Applied Biosciences*, *3*(1), 1-8.

Shehap, A., Bakr, A., & Hussein, O. T. (2015). Characterization of clay/chitosan nanocomposites and their use for adsorption on Mn (II) from aqueous solution. *International Journal of Science and Engineering Applications*, *4*, 174-185.

Shields, K. F., Bain, R. E., Cronk, R., Wright, J. A., & Bartram, J. (2015). Association of supply type with fecal contamination of source water and household stored drinking water in developing countries: a bivariate meta-analysis. *Environmental health Perspectives*, *123*(12), 1222-1231.

Shigut, D. A., Liknew, G., Irge, D. D., & Ahmad, T. (2017). Assessment of physico-chemical quality of borehole and spring water sources supplied to Robe Town, Oromia region, Ethiopia. *Applied Water Science*, 7, 155-164.

Shin, E., & Koo, J. S. (2021). Glucose metabolism and glucose transporters in breast cancer. *Frontiers in Cell and Developmental Biology*, *9*, 728759.

Shrivastava, A., Ghosh, D., Dash, A., & Bose, S. (2015). Arsenic contamination in soil and sediment in India: sources, effects, and remediation. *Current Pollution Reports*, *1*, 35-46.

Shrivastava, M., Easter, R. C., Liu, X., Zelenyuk, A., Singh, B., Zhang, K., .. & Tiitta, P. (2015). Global transformation and fate of SOA: Implications of low-volatility SOA and gas-phase fragmentation reactions. *Journal of Geophysical Research: Atmospheres*, *120*(9), 4169-4195.

Singh, A. L., & Sarma, P. N. (2010). Removal of arsenic (III) from waste water using *Lactobacillus acidophilus*. *Bioremediation Journal*, *14*(2), 92-97.

Smedley, P. L., & Kinniburgh, D. G. (2002). A review of the source, behaviour and distribution of arsenic in natural waters. *Applied Geochemistry*, *17*(5), 517-568.

Smith, A. H., Lingas, E. O., & Rahman, M. (2018). Contamination of drinking-water by arsenic in Bangladesh: a public health emergency. *Bulletin of the World Health Organization*, 78(9), 1093-1103.

Smith, A. H., Marshall, G., Roh, T., Ferreccio, C., Liaw, J., & Steinmaus, C. (2018). Lung, bladder, and kidney cancer mortality 40 years after arsenic exposure reduction. *Journal of the National Cancer Institute*, *110*(3), 241-249.

Smith, A., & Jones, L. (2022). Impact of seasonal runoff on lead levels in groundwater. *Water Quality Research Journal*, *57*(4), 238-247.

Smith, A., Johnson, L., & Roberts, R. (2023). Electrical conductivity as an indicator of water quality and seasonal changes. *Environmental Monitoring and Assessment*, *195*(5), 340-352.

Smith, J., Brown, L., & Wilson, K. (2018). Geochemical behavior of cadmium in groundwater: A regional study. *Environmental Geology*, 73(5), 2109-2121.

Smoke, T., & Smoking, I. (2004). IARC monographs on the evaluation of carcinogenic risks to humans. *IARC: Journal of Molecular Liquid*, *1*, 1-1452.

Šolomek, T., Mercier, S., Bally, T., & Bochet, C. G. (2012). Photolysis of ortho-nitrobenzylic derivatives: the importance of the leaving group. *Photochemical & Photobiological Sciences*, *11*, 548-555.

Sreedevi, P. D., Sreekanth, P. D., Ahmed, S., & Reddy, D. V. (2019). Evaluation of groundwater quality for irrigation in a semi-arid region of South India. *Sustainable Water Resources Management*, *5*, 1043-1056.

Srivastava, N., Srivastava, M., Manikanta, A., Singh, P., Ramteke, P. W., Mishra, P. K., & Malhotra, B. D. (2017). Production and optimization of physicochemical parameters of cellulase using untreated orange waste by newly isolated *Emericella variecolor* NS3. *Applied Biochemistry and Biotechnology*, *183*, 601-612.

Srivastava, S., Agrawal, S. B., & Mondal, M. K. (2015). A review on progress of heavy metal removal using adsorbents of microbial and plant origin. *Environmental Science and Pollution Research*, *22*, 15386-15415.

Srivastava, V., & Sillanpää, M. (2017). Synthesis of malachite@ clay nanocomposite for rapid scavenging of cationic and anionic dyes from synthetic wastewater. *Journal of Environmental Sciences*, *51*, 97-110.

Steinmaus, C. M., Yuan, Y., & Smith, A. H. (2005). The temporal stability of arsenic concentrations in well water in western Nevada. *Environmental Research*, *99*(2), 164-168.

Struthers, C., Harwood, J., de Beyer, J. A., Dhiman, P., Logullo, P., & Schlüssel, M. (2021). GoodReports: developing a website to help health researchers find and use reporting guidelines. *BMC Medical Research Methodology*, *21*, 1-14.

Sudhakar, M., Velmurugan, P., Ramesh, K., & Manohar, D. (2011). Hydrochemical analysis of groundwater in the Thirupparankundram area, Madurai District, Tamil Nadu, India. *Environmental Monitoring and Assessment*, 182(1-4), 291-298.

Tamasi, G., & Cini, R. (2004). Heavy metals in drinking waters from Mount Amiata (Tuscany, Italy). Possible risks from arsenic for public health in the Province of Siena. *Science of the Total Environment*, *327*(1-3), 41-51.

Thundiyil, J. G., Yuan, Y., Smith, A. H., & Steinmaus, C. (2007). Seasonal variation of arsenic concentration in wells in Nevada. *Environmental Research*, *104*(3), 367-373.

Tiwari, A. K., Suozzi, E., Fiorucci, A., & Lo Russo, S. (2021). Assessment of groundwater geochemistry and human health risk of an intensively cropped alluvial plain, NW Italy. *Human and Ecological Risk Assessment: An International Journal*, *27*(3), 825-845.

Tran, H. N., & Chao, H. P. (2018). Adsorption and desorption of potentially toxic metals on modified biosorbents through new green grafting process. *Environmental Science and Pollution Research*, *25*, 12808-12820.

Tufa, R. A. et al. (2020). Seasonal variations in water quality. *Water Research, 184*, 115-130.

Tukki, O. H., Barminas, J. T., Osemeahon, S. A., Onwuka, J. C., & Donatus, R. A. (2016). Adsorption of colloidal particles of Moringa oleifera seeds on clay for water treatment applications. *Journal of Water Supply: Research and Technology—AQUA*, *65*(1), 75-86.

Tyagi, S., Singh, P., Sharma, B., & Singh, R. (2014). Assessment of water quality for drinking purpose in district Pauri of Uttarakhand, India. *Applied Ecology and Environmental Sciences*, *2*(4), 94-99.

USEPA. (2022). *Drinking Water Standards and Regulations*. United States Environmental Protection Agency. https://www.epa.gov/dwstandards regulations

Verma, S., Verma, P. K., Meher, A. K., Bansiwal, A. K., Tripathi, R. D., & Chakrabarty, D. (2018). A novel fungal arsenic methyltransferase, WaarsM reduces grain arsenic accumulation in transgenic rice (*Oryza sativa* L.). *Journal of Hazardous Materials*, *344*, 626-634.

Vimercati, L., Baldassarre, A., Gatti, M. F., Gagliardi, T., Serinelli, M., De Maria, L., ...& Assennato, G. (2016). Non-occupational exposure to heavy metals of the residents of an industrial area and biomonitoring. *Environmental Monitoring and Assessment*, *188*, 1-13.

Wang, J. & Chen, C. (2006). Biosorption of heavy metals by *Saccharomyces cerevisiae*: a review. *Biotechnology Advances*, *24*(5), 427-451.

Wang, L. P., Titov, A., McGibbon, R., Liu, F., Pande, V. S., & Martínez, T. J. (2014). Discovering chemistry with an ab initio nanoreactor. *Nature chemistry*, *6*(12), 1044-1048.

Wang, Z., Li, Y., Wang, Z., & Zhou, L. (2023). Factors influencing the methane adsorption capacity of coal and adsorption heat variations. *Energy & Fuels*, *37*(17), 13080-13092.

Wesley, Y. A., Njewa, J. B., Makawa, K., Maurice, S., Moteni, E., Majamanda, J., ... & Chimphepo, L. (2023). Fluoride levels in borehole water: The case of Chiradzulu District in Malawi. *Asian Journal of Applied Chemistry Research*, *14*(3), 17-22.

WHO. (2021). *Guidelines for drinking-water quality: Fourth edition incorporating the first addendum*. World Health Organization.https://www. who.int/publications/i/item/9789241549950

WHO. (2004). Fluoride in Drinking-water: Background document for development of WHO Guidelines for Drinking-water Quality. World Health Organization.

Wilschefski, S. C., & Baxter, M. R. (2019). Inductively coupled plasma mass spectrometry: introduction to analytical aspects. *The Clinical Biochemist Reviews*, *40*(3), 1-15.

WHO (2017). Guidelines for drinking-water quality: first addendum to the fourth edition.

WHO (2022). *Standards of physicochemical parameters*. Kenya Bureau of Standards. https://www.who.int/publications/standards/physico chemical_parameters.

Yaméogo, C. W., Bengaly, M. D., Savadogo, A., Nikiema, P. A., & Traore, S. A. (2011). Determination of chemical composition and nutritional values of *Moringa oleifera* leaves. *Pakistan Journal of Nutrition*, *10*(3), 264-268.

Yameogo, J. T., Sanon, Z., Moussa, B. M., Somda, I., Lykke, A. M., & Axelsen, J. A. (2019). Physicochemical indicators of land degradation in Burkina Faso. *International Journal of Biological and Chemical Sciences*, *13*(4), 2421-2432.

Yang, C. C. (2004). Chemical composition and XRD analyses for alkaline composite PVA polymer electrolyte. *Materials Letters*, *58*(1-2), 33-38.

Zeitoun, M., Goulden, M., & Tickner, D. (2013). Current and future challenges facing transboundary river basin management. *Wiley Interdisciplinary Reviews: Climate Change*, *4*(5), 331-349.

Zhang, D., Wang, P., Cui, R., Yang, H., Li, G., Chen, A., & Wang, H. (2022). Electrical conductivity and dissolved oxygen as predictors of nitrate concentrations in shallow groundwater in Erhai Lake region. *Science of the Total Environment*, *233*, 16-100.

Zhang, R. X., Li, M. X., & Jia, Z. P. (2008). Rehmannia glutinosa: review of botany, chemistry and pharmacology. *Journal of Ethnopharmacology*, *117*(2), 199-214.

Zhu, Y. G., Yoshinaga, M., Zhao, F. J., & Rosen, B. P. (2014). Earth abides arsenic biotransformation. *Annual Review of Earth and Planetary Sciences*, *42*, 443-467.

Zvinowanda, C. M., Okonkwo, J. O., Sekhula, M. M., Agyei, N. M., & Sadiku, R. (2009). Application of maize tassel for the removal of Pb, Se, Sr, U and V from borehole water contaminated with mine wastewater in the presence of alkaline metals. *Journal of Hazardous Materials*, *164*(2-3), 884-891.

APPENDICES

Appendix 1: Physicochemical parameters for dry season.

BH	Turbidity (NTU)	pH	EC (µs/cm)	Temp (ºC)	DO (mg/L)	Fluoride (mg/L)
$B3_1$	0.716667	7.142	663.3333	24.2	3.713333	2.00
$B3_2$	0.416667	7.033333	652	24.2	4.61	2.01
$B3_3$	0.566667	6.96	661.6667	24.2	9.83	2.01
$B6_1$	0.92	7.09	719.3333	23.9	4.216667	2.01
$B6_2$	0.64	7.051667	717.6667	24	4.216667	2.02
$B6_3$	0.846667	7.017667	705.3333	24	3.543333	2.03
$B7_1$	0.836667	6.959333	666.3333	24.4	3.78	1.97
$B7_2$	3.216667	7.004667	717.6667	24.3	2.423333	1.98
$B7_3$	1.01	7.099667	660.6667	24.3	3.703333	1.98
$B8_1$	0.513333	7.020333	680.6667	24.2	3.35	1.88
$B8_2$	0.146667	7.046333	676.3333	24.2	4.06	1.83
$B8_3$	0.42	7.018	671.6667	24.2	3.75	1.87
$KA10_1$	1.436667	6.751667	398.3333	24.2	2.443333	1.10
$KA10_2$	0.713333	7.047	404.3333	24.2	3.536667	1.11
$KA10_3$	3.173333	6.701333	400	24.2	3.486667	1.12
$KA1_1$	0.633333	6.840333	416.3333	24.1	4.19	1.40
$KA1_2$	2.416667	6.794667	413.6667	24.1	3.886667	1.43
$KA1_3$	1.313333	6.796667	419.6667	24.2	4.213333	1.45
$KA2_1$	0.946667	7.318333	471.6667	24.3	3.98	1.40
$KA2_2$	1.236667	7.003	469.3333	24.3	3.423333	1.41
$KA2_3$	1.463333	6.938	468	24.3	4.346667	1.42
$KA3_1$	0.53	7.159667	528.3333	24.33333	3.983333	0.81
$KA3_2$	1.203333	7.120667	531.3333	24.3	4.133333	0.82
$KA3_3$	0.783333	7.082667	541.3333	24.2	4.14	0.81
$KA5_1$	0.85	7.224333	406.6667	24.2	4.546667	1.21
$KA5_2$	0.793333	7.022	407	24.2	4.59	1.21
$KA5_3$	4.626667	6.780333	400.3333	24.2	0.183333	1.21
$KA7_1$	2.58	7.001	427.3333	24.2	4.166667	0.89
$KA7_2$	6.496667	6.937333	427	24.1	3.38	0.89
$KA7_3$	0.386667	6.366667	811.6667	24.1	3.786667	0.89
$KI1_1$	1.023333	7.060667	808.6667	23.8	4.643333	1.71
$KI1_2$	1.63	7.458333	811.3333	23.8	3.7	1.71
$KI1_3$	1.43	7.380667	808.3333	23.9	3.663333	1.78
$MA1_1$	1.31	6.974333	412.3333	24.2	3.703333	1.23
$MA1_2$	1.493333	7.105	407.3333	24.2	3.656667	1.23
$MA1_3$	6.346667	7.191	411.6667	24.2	3.293333	1.24
$NR1_1$	8.826667	7.664667	413.6667	23.4	4.04	1.12
$NR1_2$	9.083333	7.641	408.6667	24.2	4.606667	1.11
$NR1_3$	10	7.542667	404.3333	24.2	4.623333	1.21
$NR2_1$	1.133333	7.420333	806	24.2	4.41	0.78
$NR2_2$	0.266667	7.459333	818.3333	24.2	3.536667	0.81
$NR2_3$	0.23	7.498667	805.6667	24.2	3.593333	0.79
$NR3_1$	1.853333	7.336333	820.3333	24.3	3.446667	0.67
$NR3_2$	0.423333	7.359667	827.6667	24.3	3.753333	0.68
$NR3_3$	0.47	7.456333	819.6667	24.3	4.203333	0.70
$NR4_1$	0.796667	7.188	823	24.3	3.33	0.65
$NR4_2$	0.38	7.262	828.6667	24.2	4.02	0.64
$NR4_3$	0.88	7.376333	817.6667	24.2	4.596667	0.65
$NR5_1$	0.496667	7.063	814.3333	24.2	4.35	0.68
$NR5_2$	0.54	7.250333	818.3333	24.2	4.006667	0.68
$NR5_3$	0.13	7.344667	818.6667	24.2	3.966667	0.68
$NR7_1$	0.71	7.548	820.3333	24	4.23	1.30
$NR7_2$	0.353333	7.070333	802.6667	24.2	3.126667	1.30
$NR7_3$	0.55	7.399	811.6667	24.2	4.26	1.31
$OL1_1$	6.67	7.442333	398	24.2	4.316667	0.47
$OL1_2$	8.24	7.206667	391.6667	24.2	4.73	0.48
$OL1_3$	10.12667	7.199667	386.3333	24.2	4.77	0.49

Appendix 2: Physicochemical parameters for wet season.

BH	Turbidity (NTU)	pH	EC (µs/cm)	Temp (ºC)	DO (mg/L)	Fluoride (mg/L)
$B3_1$	1.723333	6.376667	234	25.4	3.626667	2.10
$B3_2$	2.476667	6.333333	302.6667	25.5	2.62	2.11
$B3_3$	1.743333	6.356667	326	25.56667	2.993333	2.12
$B6_1$	1.203333	6.213333	370	25.56667	3.75	2,20
$B6_2$	2.213333	6.376667	212	25.36667	3.003333	2.10
$B6_3$	1.303333	6.193333	367.3333	25.5	1.426667	2.15
$B7_1$	2.09	6.616667	204.6667	26.2	3.406667	1.98
$B7_2$	3.286667	6.603333	252	26.36667	2.706667	1.98
$B7_3$	1.723333	6.6	285.3333	26.6	2.673333	1.98
$B8_1$	1.706667	6.563333	264	26.16667	3.17	1.90
$B8_2$	1.763333	6.47	309	26	2.99	1.91
$B8_3$	1.933333	6.55	366.6667	26.33333	3.553333	1.92
$KA10_1$	2.613333	6.41	250.6667	25.6	3.513333	1.41
$KA10_2$	1.766667	6.526667	158	25.4	3.303333	1.45
$KA10_3$	2.42	6.44	187.3333	25.5	2.57	1.48
$KA1_1$	2.31	6.4	215	25.7	2.92	1.50
$KA1_2$	1.896667	6.433333	176.6667	25.36667	2.77	1.53
$KA1_3$	1.566667	6.413333	168.3333	25.5	2.996667	1.54
$KA2_1$	1.513333	6.446667	264.3333	25.6	2.98	0.90
$KA2_2$	1.143333	6.586667	170.3333	25.6	3.116667	0.92
$KA2_3$	1.966667	6.52	150	25.7	2.746667	0.94
$KA3_1$	2.26	6.406667	189	25.6	3.526667	1.32
$KA3_2$	2.013333	6.403333	181	25.5	3	1.35
$KA3_3$	0.64	6.4	216.6667	25.7	3.783333	1.33
$KA5_1$	1.443333	7.306667	175	25.5	1.643333	0.91
$KA5_2$	2.146667	7.156667	213.3333	25	3.013333	0.91
$KA5_3$	2.226667	7.133333	199.3333	25.3	3.506667	0.92
$KA7_1$	2.313333	6.403333	276.6667	26.1	2.366667	1.21
$KA7_2$	3.196667	6.55	159.3333	25.93333	2.016667	1.31
$KA7_3$	2.746667	6.47	165	25.93333	1.71	1.21
$KI1_1$	2.213333	6.42	230	25.6	0.74	1.61
$KI1_2$	3.15	6.416667	279.6667	25.6	2.053333	1.62
$KI1_3$	1.996667	6.396667	392	25.8	3.103333	1.64
$MA1_1$	3.853333	7.436667	220.3333	25	3.686667	1.81
$MA1_2$	2.17	7.306667	153	25.3	2.606667	1.81
$MA1_3$	2.396667	7.24	254	25.4	3.16	1.85
$NR1_1$	1.93	7.703333	370.3333	25.2	2.906667	2.01
$NR1_2$	1.653333	7.746667	286	25.1	3.1	2.00
$NR1_3$	2.27	7.413333	239	25	2.726667	2.11
$NR2_1$	2.946667	7.306667	338.3333	24.93333	3.383333	1.00
$NR2_2$	2.22	7.223333	381.6667	24.6	3.21	1.11
$NR2_3$	7.786667	7.23	316	24.3	0.34	1.12
$NR3_1$	2.026667	7.25	297	25.2	3.013333	0.75
$NR3_2$	0.953333	7.17	371.6667	24.83333	1.986667	0.76
$NR3_3$	2.27	7.213333	347	24.7	2.993333	0.77
$NR4_1$	1.69	6.47	314.6667	25.5	3.313333	0.71
$NR4_2$	1.766667	6.4	323.3333	25.43333	2.98	0.76
$NR4_3$	1.873333	6.643333	336.6667	25.6	3.326667	0.78
$NR5_1$	2.196667	7.206667	342.3333	25.66667	3.383333	0.78
$NR5_2$	2.49	7.176667	341.3333	24.9	3.04	0.78
$NR5_3$	2.52	7.22	330.6667	25.2	3.156667	0.80
$NR7_1$	2.98	7.763333	226	25.13333	2.88	1.20
$NR7_2$	1.746667	7.27	453.6667	24.9	2.263333	1.22
$NR7_3$	2.06	7.296667	369.3333	25	2.69	1.23
$OL1_1$	2.406667	6.496667	377	26.06667	1.25	0.57
$OL1_2$	5.873333	6.566667	358	26.2	0.176667	0.58
$OL1_3$	4.043333	6.61	316.6667	26.23333	0.37	0.59

Appendix 3: ANOVA table for physicochemical parameters dry season.

Turbidity

Source	DF	Sum of Squares	Mean Square	F Value	P-Value
Model	18	29.94043484	1.66335749	656.33	<.0001
Error	38	0.09630387	0.00253431		
Corrected Total	56	30.03673871			
Sample	18	29.94043484	1.66335749	656.33	<.0001

pH

Source	DF	Sum of Squares	Mean Square	F Value	P-Value
Model	18	10.16108879	0.56450493	110.19	<.0001
Error	37	0.18955996	0.00512324		
Corrected Total	55	10.35064875			
Sample	18	10.16108879	0.56450493	110.19	<.0001

Electrical Conductivity

Source	DF	Sum of Squares	Mean Square	F Value	P-Value
Model	18	223405.0509	12411.3917	47984.9	<.0001
Error	38	9.8288	0.2587		
Corrected Total	56	223414.8797			
Sample	18	223405.0509	12411.3917	47984.9	<.0001

Temperature

Source	DF	Sum of Squares	Mean Square	F Value	P-Value
Model	18	11.10561404	0.61697856	20.21	<.0001
Error	38	1.16000000	0.03052632		
Corrected Total	56	12.26561404			
Sample	18	11.10561404	0.61697856	20.21	<.0001

DO

Source	DF	Sum of Squares	Mean Square	F Value	P-Value
Model	18	23.17902713	1.28772373	188.77	<.0001
Error	38	0.25922425	0.00682169		
Corrected Total	56	23.43825137			
Sample	18	23.17902713	1.28772373	188.77	<.0001

Flourides

Source	DF	Sum of Squares	Mean Square	F Value	P-Value
Model	18	13.48959298	0.74942183	2157.43	<.0001
Error	38	0.01320000	0.00034737		
Corrected Total	56	13.50279298			
Sample	18	13.48959298	0.74942183	2157.43	<.0001

Appendix 4: ANOVA table for physicochemical parameters wet season

Turbidity

Source	DF	Sum of Squares	Mean Square	F Value	P-Value
Model	18	347.6572622	19.3142923	15738.9	<.0001
Error	38	0.0466323	0.0012272		
Corrected Total	56	347.7038945			
Sample	18	347.6572622	19.3142923	15738.9	<.0001

pH

Source	DF	Sum of Squares	Mean Square	F Value	P-Value
Model	18	2.84321393	0.15795633	550.20	<.0001
Error	38	0.01090933	0.00028709		
Corrected Total	56	2.85412326			
Sample	18	2.84321393	0.15795633	550.20	<.0001

Electrical Conductivity

Source	DF	Sum of Squares	Mean Square	F Value	P-Value
Model	18	1667387.655	92632.648	1243594	<.0001
Error	38	2.831	0.074		
Corrected Total	56	1667390.486			
Sample	18	1667387.655	92632.648	1243594	<.0001

Temperature

Source	DF	Sum of Squares	Mean Square	F Value	P-Value
Model	18	0.99578947	0.05532164	6.06	<.0001
Error	38	0.34666667	0.00912281		
Corrected Total	56	1.34245614			
Sample	18	0.99578947	0.05532164	6.06	<.0001

DO

Source	DF	Sum of Squares	Mean Square	F Value	P-Value
Model	18	22.77517954	1.26528775	10485.8	<.0001
Error	38	0.00458533	0.00012067		
Corrected Total	56	22.77976488			
Sample	18	22.77517954	1.26528775	10485.8	<.0001

F^-

Source	DF	Sum of Squares	Mean Square	F Value	P-Value
Model	18	14.71514737	0.81750819	1109.48	<.0001
Error	38	0.02800000	0.00073684		
Corrected Total	56	14.74314737			
Sample	18	14.71514737	0.81750819	1109.48	<.0001

Appendix 5: ANOVA table for heavy metals during the dry season.

Pb

Source	DF	Sum of Squares	Mean Square	F Value	P-Value
Model	18	0.15304664	0.00850259	72.17	<.0001
Error	38	0.00447720	0.00011782		
Corrected Total	56	0.15752385			
Sample	18	0.15304664	0.00850259	72.17	<.0001

As

Source	DF	Sum of Squares	Mean Square	F Value	P-Value
Model	18	1.90361061	0.10575614	10.94	<.0001
Error	38	0.36724333	0.00966430		
Corrected Total	56	2.27085394			
Sample	18	1.90361061	0.10575614	10.94	<.0001

Appendix 6: ANOVA table for heavy metals during the wet season.

Pb

Source	DF	Sum of Squares	Mean Square	F Value	P-Value
Model	18	26.96608298	1.49811572	23287.7	<.0001
Error	38	0.00244457	0.00006433		
Corrected Total	56	26.96852755			
Sample	18	26.96608298	1.49811572	23287.7	<.0001

As

Source	DF	Sum of Squares	Mean Square	F Value	P-Value
Model	18	0.73843842	0.04102436	173.84	<.0001
Error	38	0.00896742	0.00023598		
Corrected Total	56	0.74740584			
Sample	18	0.73843842	0.04102436	173.84	<.0001

Appendix 7: Section of Kabatini boreholes

Appendix 8: Samples loaded on FAAS

Appendix 9: Pure and carbonized *Moringa seed* powder respectively

Appendix 10: Authorization Letter from NAWASSCO

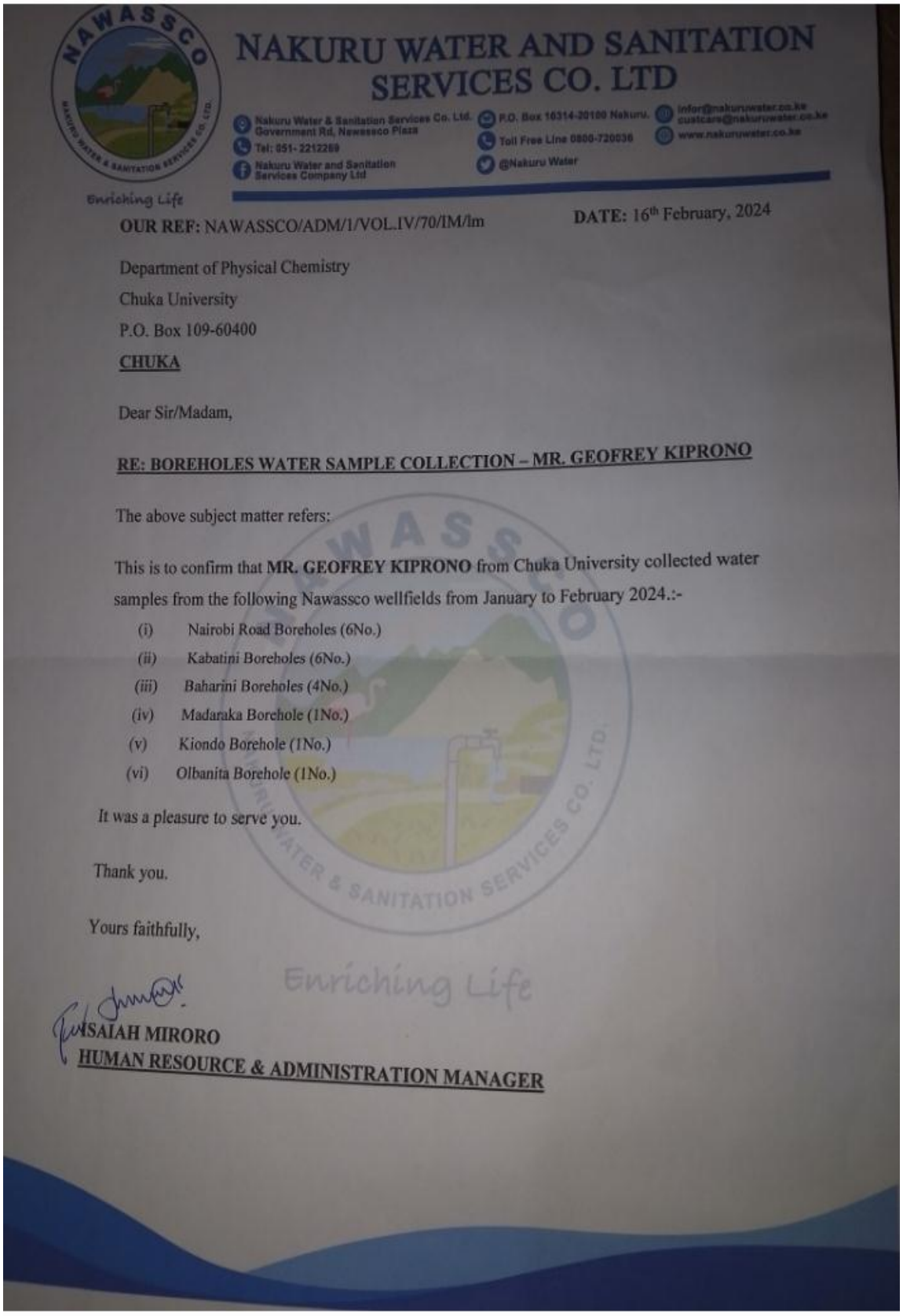

NAKURU WATER AND SANITATION SERVICES CO. LTD

Nakuru Water & Sanitation Services Co. Ltd.
Government Rd, Nawassco Plaza
Tel: 051- 2212289
Nakuru Water and Sanitation Services Company Ltd
P.O. Box 16314-20100 Nakuru.
Toll Free Line 0800-720036
@Nakuru Water
infor@nakuruwater.co.ke
custcare@nakuruwater.co.ke
www.nakuruwater.co.ke

Enriching Life

OUR REF: NAWASSCO/ADM/1/VOL.IV/70/IM/lm **DATE:** 16th February, 2024

Department of Physical Chemistry
Chuka University
P.O. Box 109-60400
CHUKA

Dear Sir/Madam,

RE: BOREHOLES WATER SAMPLE COLLECTION – MR. GEOFREY KIPRONO

The above subject matter refers:

This is to confirm that **MR. GEOFREY KIPRONO** from Chuka University collected water samples from the following Nawassco wellfields from January to February 2024.:-

(i) Nairobi Road Boreholes (6No.)
(ii) Kabatini Boreholes (6No.)
(iii) Baharini Boreholes (4No.)
(iv) Madaraka Borehole (1No.)
(v) Kiondo Borehole (1No.)
(vi) Olbanita Borehole (1No.)

It was a pleasure to serve you.

Thank you.

Yours faithfully,

ISAIAH MIRORO
HUMAN RESOURCE & ADMINISTRATION MANAGER

Appendix 11: Chuka University research authorization license

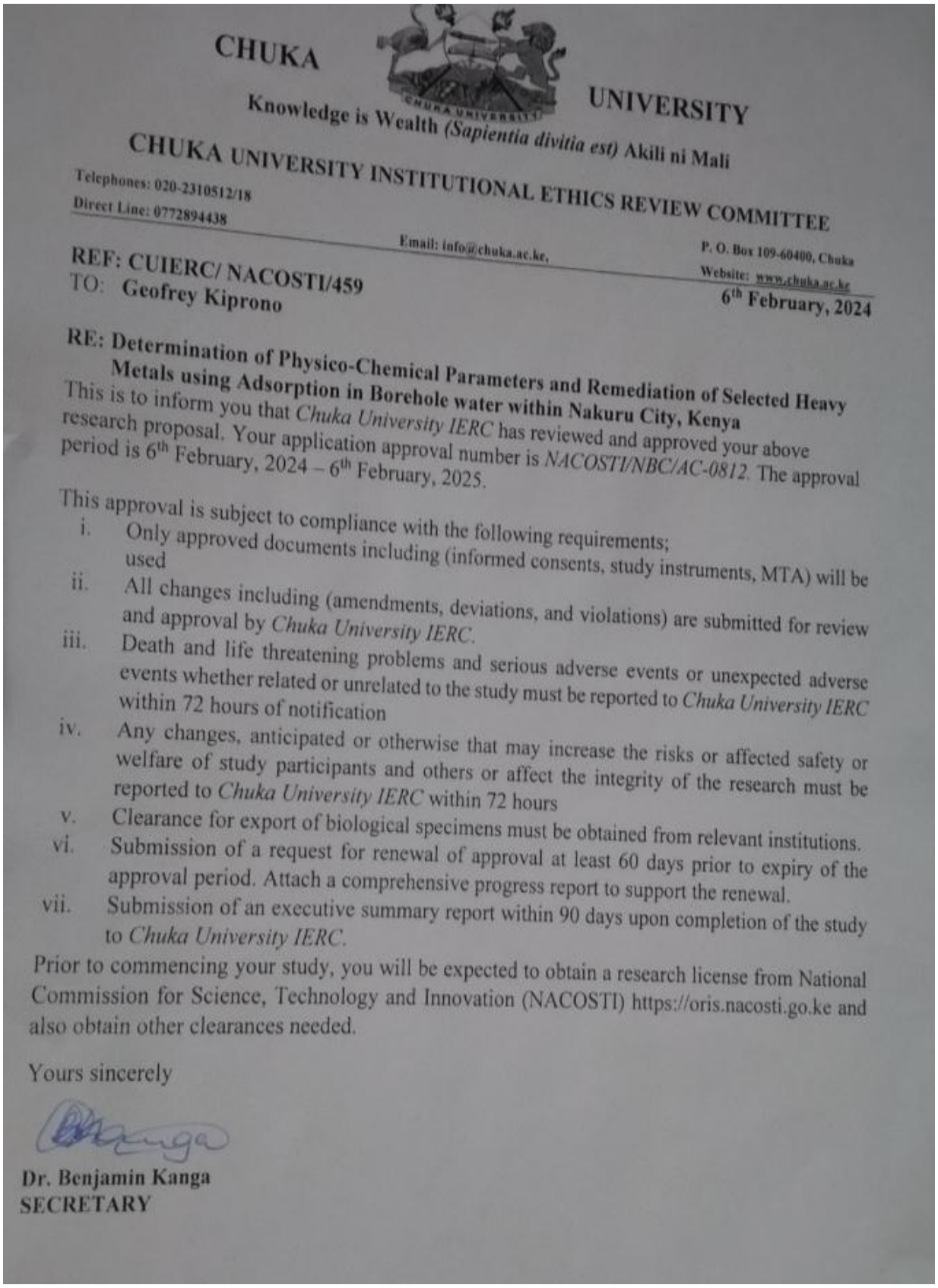

CHUKA UNIVERSITY

Knowledge is Wealth *(Sapientia divitia est)* Akili ni Mali

CHUKA UNIVERSITY INSTITUTIONAL ETHICS REVIEW COMMITTEE

Telephones: 020-2310512/18
Direct Line: 0772894438
Email: info@chuka.ac.ke,
P. O. Box 109-60400, Chuka
Website: www.chuka.ac.ke

REF: CUIERC/ NACOSTI/459
TO: **Geofrey Kiprono**

6th February, 2024

RE: Determination of Physico-Chemical Parameters and Remediation of Selected Heavy Metals using Adsorption in Borehole water within Nakuru City, Kenya

This is to inform you that *Chuka University IERC* has reviewed and approved your above research proposal. Your application approval number is *NACOSTI/NBC/AC-0812*. The approval period is 6th February, 2024 – 6th February, 2025.

This approval is subject to compliance with the following requirements;

i. Only approved documents including (informed consents, study instruments, MTA) will be used
ii. All changes including (amendments, deviations, and violations) are submitted for review and approval by *Chuka University IERC*.
iii. Death and life threatening problems and serious adverse events or unexpected adverse events whether related or unrelated to the study must be reported to *Chuka University IERC* within 72 hours of notification
iv. Any changes, anticipated or otherwise that may increase the risks or affected safety or welfare of study participants and others or affect the integrity of the research must be reported to *Chuka University IERC* within 72 hours
v. Clearance for export of biological specimens must be obtained from relevant institutions.
vi. Submission of a request for renewal of approval at least 60 days prior to expiry of the approval period. Attach a comprehensive progress report to support the renewal.
vii. Submission of an executive summary report within 90 days upon completion of the study to *Chuka University IERC*.

Prior to commencing your study, you will be expected to obtain a research license from National Commission for Science, Technology and Innovation (NACOSTI) https://oris.nacosti.go.ke and also obtain other clearances needed.

Yours sincerely

Dr. Benjamin Kanga
SECRETARY

Appendix 12: NACOSTI Research Authorization License

REPUBLIC OF KENYA

NATIONAL COMMISSION FOR SCIENCE,TECHNOLOGY & INNOVATION

Ref No: **614813**

Date of Issue: **24/February/2024**

RESEARCH LICENSE

This is to Certify that Mr.. GEOFRY KIPRONO of Chuka University, has been licensed to conduct research as per the provision of the Science, Technology and Innovation Act, 2013 (Rev.2014) in Nakuru on the topic: Determination of physico-chemical parameters and remediation of selected heavy metals using adsorption in bohole water within Nakuru City, Kenya. for the period ending : 24/February/2025.

License No: **NACOSTI/P/24/33333**

614813

Applicant Identification Number

Director General
NATIONAL COMMISSION FOR SCIENCE,TECHNOLOGY & INNOVATION

Verification QR Code

NOTE: This is a computer generated License. To verify the authenticity of this document, Scan the QR Code using QR scanner application.

See overleaf for conditions